Spring 2012

Modeling Wildfire Hazard in the Western Hindu Kush-Himalayas

David Bylow
San Jose State University

MODELING WILDFIRE HAZARD IN THE WESTERN HINDU KUSH-HIMALAYAS

A Thesis

Presented to

The Faculty of the Department of Geography

San José State University

In Partial Fulfillment

of the Requirements for the Degree

Master of Arts

by:

David Bylow

May 2012

The Designated Thesis Committee Approves the Thesis Titled

MODELING WILDFIRE HAZARD
IN THE WESTERN HINDU KUSH-HIMALAYAS

by

David Bylow

APPROVED FOR THE DEPARTMENT OF GEOGRAPHY

SAN JOSÉ STATE UNIVERSITY

May 2012

Dr. Gary Pereira	Department of Geography
Dr. Craig Clements	Department of Meteorology
Dr. Jianglong Zhang	University of North Dakota
Dr. Yong Lao	California State University Monterey Bay

ABSTRACT

MODELING WILDFIRE HAZARD
IN THE WESTERN HINDU KUSH-HIMALAYAS

by David Bylow

Wildfire regimes are a leading driver of global environmental change affecting diverse ecosystems across the planet. The objectives of this study were to model regional wildfire potential and identify environmental, topological, and sociological factors that contribute to the ignition of regional wildfire events in the Western Hindu Kush-Himalayas. The environmental, topological, and sociological factors were used to model regional wildfire potential through multi-criteria evaluation using a method of weighted linear combination. Moderate Resolution Imaging Spectroradiometer (MODIS) and geographic information systems (GIS) data were integrated to identify regional wildfire factors. Point pattern and inferential statistical analysis were used to analyze regional wildfire activity and evaluate the factors selected for the model.

ACKNOWLEDGEMENTS

First and foremost, I would like to thank my family for their limitless support of my education. I would like to thank my professors at California State University Monterey Bay and San Jose State University who patiently instructed me and encouraged my pursuit of higher education. I would also like to thank Dr. Gary Pereira, Dr. Jianglong Zhang, Dr. Yong Lao, and Dr. Craig Clements for their personal commitments to my education and this research.

Table of Contents

List of Tables

List of Figures

Introduction

Wildfire regimes are a leading driver of global environmental change affecting ecosystems and the climate at both micro and macro scales. Wildfires typically occur in wildland areas when uncontrolled fires erupt due to a combination of natural processes or human activities. This makes wildfire a particular threat to both human and animal populations and contributes to numerous casualties annually (McNamara, Stephens, & Ruminiski, 2002; Stipanicev, Bodrozic, & Vuko, 2007; Hefeeda, & Bagheri, 2007). The particulate matter and aerosols produced by wildfires are a leading cause of local and regional air pollution as well as global atmospheric CO_2 emissions (McNamara et al., 2002; Roy, 2004; Vadrevu, Badarinath, & Anuradha, 2008; Stipanicev et al., 2007; Fuller, 1991; Arno, & Allison-Bunnell, 2002; Pyne, 1984; Joshi, 2003). This makes the detection and monitoring of wildfires a crucial goal of global change research, atmospheric visibility studies, and wildfire mitigation practices (McNamara et al., 2002; Stipanicev et al., 2007; Hefeeda, & Bagheri, 2007, Frost, & Vosloo, 2006; Roy, 2004; Fuller, 1991; Arno, & Allison-

Bunnell, 2002; Pyne, 1984; Davis, Byram, & Krumm, 1959).

The objective of this study was to identify environmental, topological, and sociological factors that contribute to the ignition of regional wildfire events in the Western Hindu Kush-Himalayas. Specific questions addressed by the research included:

1. Is there a relationship between land cover type and the location of regional wildfire ignitions?
    a. Which land cover type has the greatest influence over regional wildfire ignitions?
2. Is there a relationship between vegetation health and the location of regional wildfire ignitions?
3. Is there a relationship between elevation and the location of regional wildfire ignitions?
4. Does a relationship exist between aspect and the location of regional wildfire ignitions?
5. Is there a relationship between slope and the location of regional wildfire ignitions?

6. Is there a relationship between distance to road networks and the location of regional wildfire ignitions?

7. Does a relationship between distance to water features and the location of regional wildfire ignitions?

8. Does a relationship exist between distance to settlements and the location of regional wildfire ignitions?

A combination of near-real time Moderate Resolution Imaging Spectroradiometer (MODIS) and geographic information systems (GIS) data was integrated to identify regional factors that contribute to the ignition of wildfire events. In the study, a risk neutral model of regional wildfire potential based on multi-criteria evaluation using a method of weighted linear combination was produced.

The multi-criteria evaluation was performed using IDRISI Taiga (Eastman, 2009) to execute the modeling. IBM SPSS Statistics (SPSS Inc., 2010), the R software environment for statistical computing (R Development Core Team, 2008), and ArcGIS Desktop (ESRI Inc., 2010) were used to perform statistical and point pattern analysis. Images of the

study scene were produced using ArcGIS Desktop and ERDAS ViewFinder (ERDAS Inc., 2002). The results of the multi-criteria evaluation were imported into ArcGIS Desktop to facilitate the publication of maps.

Literature Review

In the following literature review, the researcher discusses wildfires from the perspective of the Western Hindu Kush-Himalayas region. The literature review includes a general overview of wildfires, satellite detection methods, and the MODIS sensor and platforms. The Western Hindu Kush-Himalayas region is also presented.

Wildfires

Wildfires are destructive combustion events that occur in wildland areas when a fuel complex is exposed to an intense heat source and an adequate oxygen supply (Figure 1) (Hardy, 2005; Princeton University, 2006; Fuller, 1991; Arno, & Allison-Bunnell, 2002; Davis et al., 1959; Pyne, 1984). A wildfire occurs when the cellulose and carbohydrates of plant matter chemically react with oxygen and a heat source sufficient to cause ignition (Fuller, 1991; Arno, & Allison-Bunnell, 2002; Pyne, 1984; Davis et al., 1959). Once ignition occurs and the exothermic reaction process of combustion has begun, the fuel source begins to dry out. The heat generated during the process boils off the moisture and volatile

organic substances contained in the fuel source (Fuller, 1991; Arno, & Allison-Bunnell, 2002; Pyne, 1984; Davis et al., 1959).

Once the heat has completely broken down the fuel source's chemical structure, byproducts including hydrocarbons, tars, ash, and charcoal are produced (Fuller, 1991; Arno, & Allison-Bunnell, 2002; Pyne, 1984; Davis et al., 1959). As the combustion process continues, the hydrocarbons begin to flame, producing water vapor, carbon dioxide, and additional heat. Trace amounts of nitrogen, ammonia, phosphate, sulfate, and nitrate are also generated and released during the combustion process (Fuller, 1991; Arno, & Allison-Bunnell, 2002; Pyne, 1984; Davis et al., 1959).

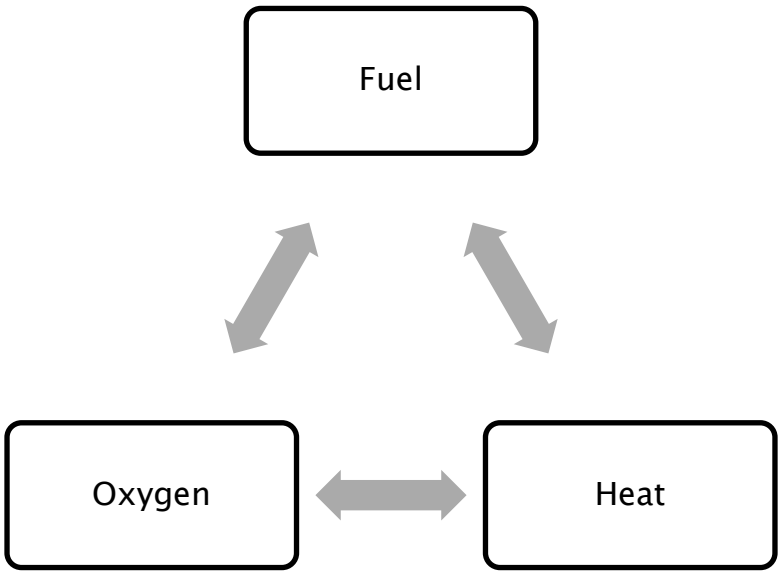

Figure 1: Combustion Triangle
(Source: Arno, & Allison-Bunnell, 2002)

The majority of global wildfires are typically ignited by human activities within or near forested areas. Slash and burn agriculture, grazing practices, logging, the collection of minor forest produce, arson, and the careless disposal of cigarette butts are human activities attributed to the ignition of wildfires (Hefeeda, & Bagheri, 2007; Sastry, Jadhav, & Thakker, 2002; Jaiswal, Mukherjee, Raju, & Saxena, 2002; Roy, 2004; Joshi, 2003; Hussin, Matakala, & Zagdaa, 2008; Vadrevu et al., 2008). Wildfires are also commonly ignited by natural processes such as the exposure of fuel to high heat and humidity, lighting strikes, and

rolling rocks (Hefeeda, & Bagheri, 2007; Sastry et al., 2002; Jaiswal et al., 2002; Roy, 2004; Fuller, 1991; Arno, & Allison-Bunnell, 2002; Davis et al., 1959; Pyne, 1984; Joshi, 2003; Hussin et al., 2008; Vadrevu et al., 2008).

There are three prevailing types of wildfires that occur globally on an annual basis. These wildfire types include ground fires, surface fires, and crown fires (Roy, 2004; Fuller, 1991; Arno, & Allison-Bunnell, 2002; Davis et al., 1959; Pyne, 1984). Ground fires occur below the undecomposed litter layer found on the forest floor. They ignite in the peat and humus layers, burning tree roots and buried branches and logs. These fires produce little to no visible flame, but intense levels of heat (Figure 2) (Roy, 2004; Fuller, 1991; Arno, & Allison-Bunnell, 2002; Davis et al., 1959; Pyne, 1984). Ground fires are quite rare and are only known to occur at high elevations levels. The ground fire regime has an average return interval of every 1 to 30 years (Fuller, 1991, Arno, & Allison-Bunnell, 2002; Davis et al., 1959; Pyne, 1984). This uncommon type of wildfire event has been documented in the mountains of the Himalayan

range (Roy, 2004; Davis et al., 1959).

Figure 2: Ground Fire
(Source: Roy, 2004)

Surface fires are the most prevalent type of wildfire that occurs in wildfire prone environments throughout the world. They produce considerable heat and visible flames that can be seen traveling along the forest floor (Figure 3). Surface fires ignite within the litter, scrub, ground cover, and regeneration layers found on or near the forest floor (Roy, 2004; Fuller, 1991, Arno, & Allison-Bunnell, 2002; Davis et al., 1959; Pyne, 1984). They consume fuels that are no taller than 4 to 6 ft above the surface. Surface fire regimes occur on average in 1 to 25 year return

intervals (Fuller, 1991, Arno, & Allison-Bunnell, 2002; Davis et al., 1959; Pyne, 1984). These types of wildfires are common and have been documented in wildfire prone forests, including those of the Himalayan mountain range (Roy, 2004; Davis et al., 1959).

Figure 3: Surface Fire
(Source: Roy, 2004)

Crown or stand replacement fires occur relatively infrequently throughout the forested regions of the world. These types of wildfires occur in the crown layer of forests, consuming foliage and shrubs taller than 6 ft as fuel. Crown fires produce intense levels of heat and large

flames that are visible at great distances from the event (Figure 4) (Roy, 2004; Fuller, 1991; Arno, & Allison-Bunnell, 2002; Davis et al., 1959; Pyne, 1984). A crown fire is incredibly destructive and usually results in complete fuel combustion and death of trees involved. These types of wildfires are rare, having a regime with return intervals that occur on average every 100 to 400 years (Fuller, 1991; Arno, & Allison-Bunnell, 2002; Davis et al., 1959; Pyne, 1984). Crown fires have been documented in the coniferous forests of the Siwalik Mountains and throughout the Himalayan mountain range (Roy, 2004; Davis et al., 1959).

Figure 4: Crown Fire
(Source: Roy, 2004)

Wildfires have varied impacts on wildland systems at different spatial and temporal scales. Wildland systems frequently impacted by wildfires include ecosystems, geosystems, the atmosphere, as well as fire management practices, and societies as a whole (Hardy, 2005; Arno, & Allison-Bunnell, 2002).

Ecosystems are affected by wildfire ignitions in a multitude of ways with both spatial and temporal implications. The extent of a wildfire can impact an ecosystem at varying spatial scales ranging from small individual spots measuring only meters in size, to large areas covering

multiple kilometers (Hardy, 2005). The duration of a wildfire event can vary greatly, resulting in short term effects lasting only days to long term effects which can persist for several years (Hardy, 2005). The ecological consequences of wildfires include such diverse effects as the loss of wildlife habitat, biodiversity, regeneration, and timber resources (Roy, 2004; Arno, & Allison-Bunnell, 2002).

Geosystems are impacted spatially by wildfire at scales ranging from individual sites such as a field or hillside, to large areas which can encompass entire watersheds and forested regions (Hardy, 2005). A wildfire ignition can have effects on a geosystem which occur concurrently with the event and can last for as little as a day. Wildfire duration can also have long term effects on a geosystem which can endure for multiple years to centuries (Hardy, 2005). Consequences to geosystems can include increased soil erosion, soil impermeability, landslide potential, and damage to water resources such as rivers and streams (Roy, 2004; Vadrevu et al, 2008).

Wildfires can affect the atmosphere at scales ranging from individual sites, to extents which can result in influences that span entire continents (Hardy, 2005). The duration of wildfire events can result in short term consequences to the atmosphere which can last for only brief periods of time (Hardy, 2005). The short term effects of wildfire ignitions can include decreased solar insolation and air temperatures (Hardy, 2005; Joshi, 2003; Vadrevu et al, 2008). Midterm consequences can also develop with consequences which can last for weeks at a time (Hardy, 2005). These effects comprise climatic alterations which include increased atmospheric carbon dioxide and aerosols concentrations (Hardy, 2005; Joshi, 2003; Vadrevu et al, 2008).

The impact of wildfire events can have numerous impacts on fire management practices. These impacts can be brief such as local level prevention activities, aerial surveys, law and code enforcement, and suppression actions taken at initial ignition identification in individual wildfire locations (Hardy, 2005; Prestemon, Pye, Butry, Holmes, & Mercer, 2002; Pyne, 1984; Fuller, 1991; Davis et al., 1959). Wildfire ignitions also

result in impacts that effect fire management practices over many seasons. Multi-season planning such as the allocation of national wildfire mitigation resources, wildfire prevention education, fire road creation and maintenance, fuel surveys, prescribed burning location determination and execution, and the distribution of wildfire fighting personnel over broad regions are common impacts of wildfire potential (Hardy, 2005; Prestemon et al., 2002; Pyne, 1984; Fuller, 1991; Davis et al., 1959). The duration of a wildfire can affect fire management practices for only brief periods of time, or result in influences which can last for many seasons (Hardy, 2005; Prestemon et al., 2002; Pyne, 1984; Fuller, 1991; Davis et al., 1959).

The ignition of a wildfire can also have significant impacts on entire societies. Effects can encompass individual spots such as a stretch of road, or can result in impacts that can span entire continents (Hardy, 2005). The smoke released from a wildfire contains significant levels of carbon monoxide, hydrocarbons, and ash and charcoal particulates which can spread over entire continents (Figure 5) (Hardy, 2005; Joshi, 2003;

Roy, 2004; Fuller, 1991; Vadrevu et al, 2008). All of these emissions can have negative impacts on human and animal health through decreased air quality resulting from wide-area aerosol emissions and dispersion (Hardy, 2005; Joshi, 2003; Roy, 2004; Fuller, 1991; Vadrevu et al, 2008). Sociological impacts from wildfires can result in brief consequences such as the short term closure of a road and eye irritation, to influences on air quality and breathing which can persist for entire seasons (Hardy, 2005; Joshi, 2003; Roy, 2004; Fuller, 1991; Vadrevu et al, 2008).

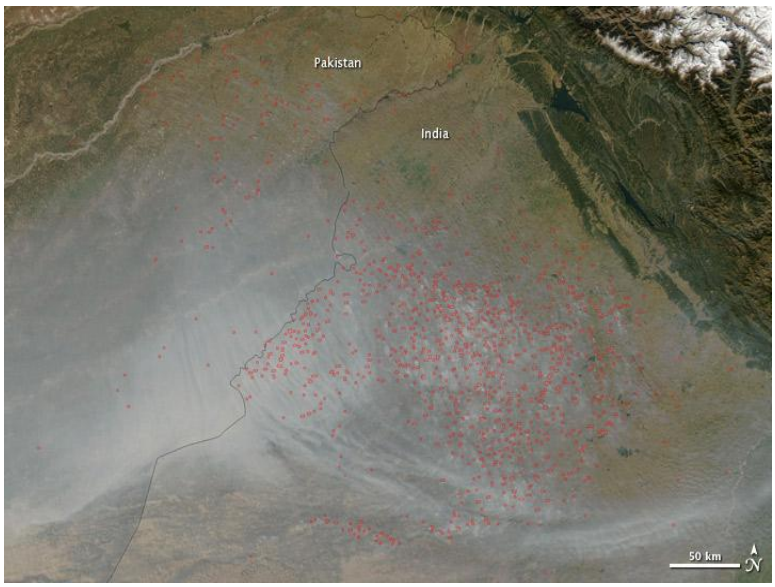

Figure 5: Wildfire Smoke over Region
(Source: NASA Earth Observatory)

Wildfires depend on a combination of mitigating factors coalescing at a single point in space and time to result in an ignition. The predominant factors attributed to wildfire ignitions include a combination of climatic, floristic, physiographic, edaphic, sociological, and environmental sources (Sastry et al., 2002; Jaiswal et al., 2002; Fuller, 1991; Arno, & Allison-Bunnell, 2002; Davis et al., 1959; Pyne, 1984; Chuvieco, Salas, & Vega, 1997; Vadrevu et al, 2008). Climatic factors closely related to the ignition of wildfires include air temperature, humidity, annual rainfall values, and wind speed and direction (Sastry et al., 2002; Jaiswal et al., 2002; Fuller, 1991; Arno, & Allison-Bunnell, 2002; Davis et al., 1959; Pyne, 1984; Chuvieco, Salas, & Vega, 1997; Vadrevu et al, 2008). All of these factors have considerable influence on the condition of regional fuel sources and play dominant roles in creating the necessary conditions for an ignition to occur.

Vegetation type and density are two of the most important floristic factors related to the ignition of wildfires. Dry, unhealthy vegetation is considerably more susceptible to ignition than vegetation which is moist

and vigorous. Vegetation type has a significant effect on wildfire ignition and behavior as certain vegetation types ignite and are consumed more readily than others (Sastry et al., 2002, Jaiswal et al., 2002; Chuvieco et al., 1997; Fuller, 1991; Arno, & Allison-Bunnell, 2002; Pyne, 1984; Davis et al., 1959; Vadrevu et al, 2008). The density of regional vegetation also affects the probability of an ignition and subsequent wildfire behavior. Densely compacted vegetation is significantly more likely to ignite and burn with increased intensity (Sastry et al., 2002, Jaiswal et al., 2002; Chuvieco et al., 1997; Fuller, 1991; Arno, & Allison-Bunnell, 2002; Pyne, 1984; Davis et al., 1959; Vadrevu et al, 2008). The greater degree of available fuel allows for wildfires to burn over larger areas and with increased severity.

Physiographic factors have a pronounced effect on wildfire ignitions and behavior. Factors such as slope, aspect and elevation play vital roles in creating the necessary conditions for ignitions to occur. Wildfires travel rapidly up slope, with steeper slopes resulting in quicker spreading fires (Sastry et al., 2002, Jaiswal et al., 2002; Chuvieco et al.,

1997; Roy, 2004; Fuller, 1991; Arno, & Allison-Bunnell, 2002; Pyne, 1984; Davis et al., 1959; Hussin et al., 2008; Vadrevu et al, 2008). Slope also has a significant effect on wind speed and direction, which can greatly influence wildfire behavior through oxygen transportation (Sastry et al., 2002, Jaiswal et al., 2002; Chuvieco et al., 1997; Roy, 2004; Fuller, 1991; Arno, & Allison-Bunnell, 2002; Pyne, 1984; Davis et al., 1959; Hussin et al., 2008; Vadrevu et al, 2008). Aspect creates conditions which can either promote or discourage wildfires. The direct sun exposure which south facing slopes receive results in increased drying of fuels, making southern slopes more vulnerable to ignitions (Sastry et al., 2002, Jaiswal et al., 2002; Chuvieco et al., 1997; Roy, 2004; Fuller, 1991; Arno, & Allison-Bunnell, 2002; Pyne, 1984; Davis et al., 1959; Hussin et al., 2008; Vadrevu et al, 2008).

Edaphic factors such as soil type and condition have considerable influence on regional vegetation types and health (Sastry et al., 2002; Chuvieco et al., 1997; Fuller, 1991; Arno, & Allison-Bunnell, 2002; Pyne, 1984; Davis et al., 1959; Vadrevu et al, 2008). Rich, healthy soils create

the conditions necessary for vigorous vegetation growth. Soil type and condition greatly influence the type of vegetation which can grow and prosper within a region (Sastry et al., 2002; Chuvieco et al., 1997; Fuller, 1991; Arno, & Allison-Bunnell, 2002; Pyne, 1984; Davis et al., 1959; Vadrevu et al, 2008). Soil's influence on vegetation type and rigor make it an important contributing factor to the occurrence of wildfires.

Factors such as distance to road features, distance to water features, and distance to settlements also have a substantial influence on the probability of wildfire ignitions (Sastry et al., 2002; Jaiswal et al., 2002; Chuvieco et al., 1997; Roy, 2004; Hussin et al., 2008). These sociological and environmental factors influence ignition probabilities by allowing human activities to more readily enter wildfire susceptible environments. Movements of people and vehicles along and near roads and highways provide the opportunity for human induced and accidental ignitions to occur (Sastry et al., 2002; Jaiswal et al., 2002; Chuvieco et al., 1997; Roy, 2004; Hussin et al., 2008). The distance to water features and human settlements combined with regional customs and cultural

practices result in both purposeful and accidental ignitions which can lead to the occurrence of destructive wildfire events and unnatural wildfire regimes (Sastry et al., 2002; Jaiswal et al., 2002; Chuvieco et al., 1997; Roy, 2004; Hussin et al., 2008).

There are a number of methods that have been proposed by policy makers and land managers to reduce wildfire ignitions and minimize the related economic, environmental, and societal losses. Proposed mitigation methods include mechanical thinning, increased timber harvesting, and a greater degree of prescribed burns (Prestemon et al., 2002; Fuller, 1991; Arno, & Allison-Bunnell, 2002; Pyne, 1984; Davis et al., 1959). All of the proposed methods to minimize wildfires require effective research into the locations, timing, and causal factors that result in regional wildfire ignitions (Prestemon et al., 2002; Fuller, 1991; Arno, & Allison-Bunnell, 2002; Pyne, 1984; Davis et al., 1959).

Most studies of wildfire events have been performed under carefully controlled conditions utilizing only fine scale data for limited areas and locations (Prestemon et al., 2002). Effective wildfire ignition

mitigation practices would benefit from broad scale research studies which utilize moderate or course resolution data sources. The data could be used to identify wildfire prone environments and factors which contribute to regional wildfire ignitions over extensive areas (Prestemon et al., 2002).

Broad scale research is also effective at identifying and isolating knowledge gaps (Prestemon et al., 2002). These gaps can then be further analyzed utilizing finer scale data sources to aid in greater understanding of the topic at hand, or identify areas requiring additional research. Studies performed at finer scales of analysis could also be used to validate findings from broad scale research (Prestemon et al., 2002).

Satellite Detection of Wildfires

Wildfire detection and monitoring is traditionally performed by human spotters placed at key locations throughout a forested area. However, this traditional detection method is only marginally effective and heavily dependent on the alertness and abilities of the spotters (Stipanicev et al., 2007; Pyne, 1984; Davis et al., 1959). More effective

methods of wildfire detection utilize networks of satellite based remote sensors deployed for the purpose of wildfire recognition, monitoring, and reporting. These satellite networks are capable of accurately detecting the location, intensity, and spread of wildfires across a landscape at local, regional, and global scales (Pyne, 1984; Frost, & Vosloo, 2006; Vadrevu et al, 2008; Hawbaker et al., 2008; Giglio, Csiszar, & Justice, 2006).

To detect wildfires from space, satellite based sensors along with terrestrial based communications infrastructure and detection algorithms are used to distinguish and track the progression of wildfire events. Satellite platforms with sensors capable of detecting and tracking wildfire events include Polar Operational Environmental Satellites (POES), Geostationary Operational Environmental Satellites (GOES), Along Track Scanning Radiometer (ATSR), Defense Meteorological Satellite Program Operational Linescan System (DMSP-OLS), Multi-functional Transport Satellites (MTSAT), Visible and Infrared Scanner (VIRS), Meteosat, SPOT VEGETATION, and the Terra and Aqua platforms (Frost, & Vosloo, 2006; Li et al., 2001; Li et al., 2003; Hawbaker et al., 2008; Pyne, 1984).

These satellites utilize moderate to coarse resolution sensors to detect wildfire events using specialized platform and sensor specific detection algorithms. The moderate and course resolution sensors make use of the relatively high temporal resolution of the satellites geostationary and polar orbits to make sufficient daily overpasses to effectively monitor wildfire events at regional and global scales.

The satellite based detection of wildfires is accomplished through the use of specialized fire detection algorithms which use satellite sensor data to identify and track wildfire events on the planet's surface. The majority of wildfire event detections are achieved through sub-pixel data analysis. The moderate to coarse resolution of sensors capable of wildfire recognition makes sub-pixel analysis essential to the detection of wildfire events (Li et al., 2001). Many wildfire events that occur across the planet are not large enough to occupy an entire pixel, resulting in the need for sub-pixel analysis in wildfire identification and tracking (Li et al., 2001). Through sub-pixel analysis the detection algorithms identify and separate wildfire events from pixel backgrounds.

There are three types of algorithms that are commonly used in the detection of wildfire events. These include single channel threshold algorithms, multi-channel threshold algorithms, and spatial contextual algorithms (Li et al., 2001; Boles, & Verbyla, 2000). Single channel threshold algorithms use fixed threshold values to detect wildfire events. In a single channel threshold algorithm the data from a satellites mid-infrared band is compared to the threshold value (Li et al., 2001; Li et al., 2003). Values which exceed the threshold are classified as wildfire events. Those which do not exceed the threshold are either not classified, or classified as non-fire thermal anomalies.

When using single channel threshold algorithms, reflected solar radiation can be problematic. This is particularly true of reflections generated by clouds and bright surfaces such as bare soil, water bodies, and paved areas (Li et al., 2001; Li et al., 2003; Giglio, Descloitres, Justice, & Kaufman, 2003; Flasse, & Ceccato, 1996; Boles, & Verbyla, 2000). Due to the limitations of single channel threshold algorithms and their sensitivity to reflected solar radiation, the algorithms are most often

used to identify wildfire events during satellites overpasses which occur at night (Li et al., 2001). Multi-channel threshold algorithms were developed in order to address the limitations of single channel thresholding.

Multi-channel threshold algorithms also utilize fixed threshold values to detect wildfire events. Multi-channel threshold algorithms use satellite based infrared sensor channels to identify pixels which contain potential wildfire events (Li et al., 2001; Li et al., 2003). A series of statistical tests are then applied to the candidate pixels to identify and eliminate potential errors of commission (Li et al., 2001; Li et al., 2003; Giglio et al., 2003). The thermal channel is used to identify and remove cloud pixels. The brightness temperatures from the potential wildfire event pixels are then compared to data from a near-infrared or second mid-infrared channel (Li et al., 2001). The comparison to coincident data is performed to allow for the separation of wildfire events from pixel background values (Li et al., 2001; Giglio et al., 2003; Boles, & Verbyla, 2000). Supplementary tests can also be performed at this time to assist

in the identification and removal of highly reflective surfaces (Li et al., 2001; Li et al., 2003; Giglio et al., 2003; Boles, & Verbyla, 2000).

The addition of quality assurance tests allows multi-channel threshold algorithms to remove clouds, separate wildfire events from background values, and remove highly reflective surfaces which could generate commission errors (Li et al., 2001; Li et al., 2003; Giglio et al., 2003; Boles, & Verbyla, 2000). The ability to identify areas of potential commission errors and remove false fire detections makes multi-channel thresholding considerably more effective than single channel threshold algorithms. Multi-channel threshold algorithms are effective at both day and night overpass detection. This allows multi-channel threshold algorithms to be effectively used in regional and global wildfire events detection and tracking (Li et al., 2001).

Spatial contextual algorithms improve upon the capabilities of multi-channel thresholding techniques. Contextual algorithms detect wildfire events using variable threshold values calculated on a per pixel basis (Li et al., 2001; Li et al., 2003; Giglio et al., 2003). The contextual

algorithms calculate an initial threshold value to identify potential wildfire events. A series of tests are then run to identify potential errors of omission and errors of commission (Li et al., 2001; Li et al., 2003; Giglio et al., 2003; Flasse, & Ceccato, 1996; Boles, & Verbyla, 2000; Morisette et al., 2005). The statistical tests employed in a contextual algorithm are much more liberal than the ones employed in multi-channel thresholding (Li et al., 2001; Boles, & Verbyla, 2000). This is done to minimize the occurrence of omission errors in order to maximize the number of actual wildfire events detected by the algorithm.

Once the initial threshold value has been set and preliminary wildfire detection has occurred, statistics are calculated for surrounding non-fire background pixels (Li et al., 2001; Giglio et al., 2003; Flasse, & Ceccato, 1996). Using a varying window ranging from 3x3 to 21x21 pixels, basic descriptive statistics are calculated for the background pixels (Li et al., 2001; Giglio et al., 2003; Flasse, & Ceccato, 1996). Window size for the statistical calculations is varied to allow for the inclusion of a minimum number of background pixels required to

calculate statistically significant values of the mean, median, standard deviation, and mean absolute deviation of the surrounding pixels (Li et al., 2001; Giglio et al., 2003; Flasse, & Ceccato, 1996; Li et al., 2003; Justice at al., 2002). These statistics are used to refine the detection threshold. The refined detection threshold is then used to re-evaluate the potential wildfires and confirm the detection of an event (Li et al., 2001).

Spatial contextual algorithms are much more efficient at wildfire event detection then multi-channel threshold techniques. The contextual algorithms have considerably improved detection rates and are more adept at the detection of cool and small scale wildfire events (Giglio et al., 2003; Flasse, & Ceccato, 1996). Regional and global wildfire event detection and monitoring can be performed using contextual detection algorithms with a high degree of accuracy. Contextual algorithms can use supplementary data including wildfire event strengths, seasonal surface conditions, fuel types, and fuel concentrations to develop efficient regional detection algorithms (Li et al., 2001; Giglio et al., 2003;

Flasse, & Ceccato, 1996; Boles, & Verbyla, 2000). Contextual algorithms can also be developed for global wildfire detection, though the global detection algorithms are designed to be more conservative than regional algorithms (Li et al., 2001). Successful applications of global contextual algorithms effectively detect and monitor global wildfire event activity while minimizing the number of commission errors (Li et al., 2001; Giglio et al., 2003; Flasse, & Ceccato, 1996).

Satellite based sensors for wildfire event detection operate by using onboard computing resources to process and automatically downlink satellite sensor data to processing centers to identify and analyze wildfire events using specialized platform-specific wildfire detection algorithms. When an ignition has been detected a wildfire event is automatically produced by the sensor system and an alert with relevant data is sent to a ground receiving station. Alert messages, data publishing, and requests to redirect satellites of higher scientific value or resolution can then be generated and distributed (Frost, & Vosloo, 2006).

Alert messages and data can be disseminated to interested parties by way of the internet, email, and SMS text message (Chien et. al., 2005; Frost, & Vosloo, 2006). These alerts can be simple notifications of a wildfire event, or they can include additional detailed information about the event such as location, size, severity, and relevant meteorological information (Chien et. al., 2005; Frost, & Vosloo, 2006).

If the request to redirect an additional satellite can be accommodated, the request will be uplinked from the processing center to the appropriate satellite platform. Once uplinked, the satellite will incorporate the request into its normal operations and the data will be downlinked to the processing center upon acquisition. When the sensor data from the second satellite is acquired and downlinked to the processing center it is automatically processed and published for retrieval (Chien et. al., 2005). Additional alerts can also be generated at this time to inform interested parties of the availability of additional wildfire event data sources.

The MODIS Active Fire Mapping Program is a model example of an operational satellite based sensor network which has been successfully used to detect and monitor wildfire events (Justice et al., 2002). The MODIS Active Fire Mapping Program makes use of onboard computing assets and artificial intelligence to image and report wildfire events on the Earth's surface (Quayle, 2002; Chien et. al., 2005; Giglio et al., 2003). The MODIS Active Fire Mapping Program utilizes the MODIS sensor onboard the National Aeronautics and Space Administration (NASA) Earth Observing Systems (EOS) Terra and Aqua satellites. The sensor data collected from the Terra and Aqua satellites is downlinked to the EOS Data and Operations System center (Quayle, 2002; Chien et. al., 2005; Giglio et al., 2003).

At the EOS Data and Operations System center the raw MODIS data is transferred to the NASA Goddard Space Flight Center where it is processed using an application-specific contextual wildfire detection algorithm designed specifically for the MODIS sensor and the Terra and Aqua platforms (Quayle, 2002; Chien et. al., 2005; Giglio et al., 2003).

The detection algorithm is designed to detect and separate active wildfire events from background pixels using the MODIS thermal bands, while using platform specific contextual tests minimizing the number of commission errors produced by the system (Giglio et al., 2003; Quayle, 2002; Hawbaker et al., 2008). The system is capable of detecting wildfires 100 m^2 and larger with an accuracy level of greater than or equal to 50% (Giglio et al., 2003; Hawbaker et al., 2008; Frost, & Vosloo, 2006).

Although remote sensing offers great potential in the areas of wildfire detection and monitoring, there are limitations to the effective recognition of wildfire events. Limitations of MODIS and satellite based detections can result in biased wildfire counts and distributions. These limitations can lead to errors of commission resulting from reflective surfaces with properties similar to wildfire signatures. Errors of commission can be generated by cloud shadows and edge effects. Urban and built-up areas contain reflective surfaces capable of producing false detections. Commission errors can be generated by sun glint on water

surfaces and coastlines. Barren soil, wet soil, and decaying vegetation, as well as areas with significant differences in radiometric contrast, are also known to generate errors of commission (Hawbaker et al., 2008; Giglio et al., 2006; Giglio et al., 2003).

Errors of omission also occur and can result from differences between wildfire occurrence and the overpass times of satellites capable of wildfire recognition (Hawbaker et al., 2008; Giglio et al., 2006; McNamara et al., 2002). Small scale fires are difficult to detect due to the resolution of sensors with wildfire detection capabilities. The moderate resolutions of currently operating infrared and thermal sensors make the detection of low intensity wildfires and events smaller than 1 km^2 difficult to achieve (Giglio et al., 2003). Omission errors can also be generated when a wildfire pixel contains multiple underlying individual wildfires. The inability of satellite based wildfire detection and monitoring to accurately differentiate between event types, including controlled burns, agricultural fires, and naturally occurring wildfires is another notable

limitation (Hawbaker et al., 2008; Giglio et al., 2006; McNamara et al., 2002).

Moderate Resolution Imaging Spectroradiometer

The Moderate Resolution Imaging Spectroradiometer is a 36 band multispectral sensor which acquires data from the visible, near-infrared, short-wave infrared, and long-wave infrared regions of the electromagnetic spectrum (Barnes, Pagano, & Salomonson, 1998; Guenther, Xiong, Salomonson, Barnes, & Young, 2002; Morisette et al., 2005). The sensor has a spectral response ranging from 0.4 to 0.6 µm in the visible spectrum, 0.6 to 1.0 µm in the near-infrared spectrum, 1.0 to 5.0 µm in the short-wave infrared spectrum, and 5.0 to 15.0 µm in the long-wave infrared spectrum (Table 1) (Barnes et al., 1998; Guenther et al., 2002). Data is collected at spatial resolutions of 250 m for bands 1 and 2, 500 m for bands 3 to 7, and 1 km for bands 8 through 36 to accommodate the needs of the wildfire user community (Barnes et al., 1998; Justice et al., 1998; Guenther et al., 2002; Chand et al. 2007).

Table 1: MODIS Spectral Bands and Primary Usage
(Source: Barnes et al., 1998; Guenther et al., 2002)

Primary Use	Band	Bandwidth (μm)	Spectral Radiance[1]	Required SNR[2]/NEDT[3]
Land/Cloud/Aerosols Boundaries	1	.620 – .670	21.8	128 (SNR)
	2	.841 – .876	24.7	201 (SNR)
Land/Cloud/Aerosols Properties	3	.459 – .479	35.3	243 (SNR)
	4	.545 – .565	29.0	228 (SNR)
	5	1.230 – 1.250	5.4	74 (SNR)
	6	1.628 – 1.652	7.3	275 (SNR)
	7	2.105 – 2.155	1.0	110 (SNR)
Ocean Color/ Phytoplankton/ Biogeochemistry	8	.405 – .420	44.9	880 (SNR)
	9	.438 – .448	41.9	838 (SNR)
	10	.483 – .493	32.1	802 (SNR)
	11	.526 – .536	27.9	754 (SNR)
	12	.546 – .556	21.0	750 (SNR)
	13	.662 – .672	9.5	910 (SNR)
	14	.673 – .683	8.7	1087 (SNR)
	15	.743 – .753	10.2	586 (SNR)
	16	.862 – .877	6.2	516 (SNR)
Atmospheric Water Vapor	17	.890 – .920	10.0	167 (SNR)
	18	.931 – .941	3.6	57 (SNR)
	19	.915 – .965	15.0	250 (SNR)
Surface/Cloud Temperature	20	3.660 – 3.840	0.45 (300K)	0.05 (NEDT)
	21	3.929 – 3.989	2.38 (335K)	2.00 (NEDT)
	22	3.929 – 3.989	0.67 (300K)	0.07 (NEDT)
	23	4.020 – 4.080	0.79 (300K)	0.07 (NEDT)
Atmospheric Temperature	24	4.433 – 4.498	0.17 (250K)	0.25 (NEDT)
	25	4.482 – 4.549	0.59 (275K)	0.25 (NEDT)
Cirrus Clouds Water Vapor	26	1.360 – 1.390	6.00	150 (SNR)
	27	6.535 – 6.895	1.16 (240K)	0.25 (NEDT)
	28	7.175 – 7.475	2.18 (250K)	0.25 (NEDT)
Cloud Properties	29	8.400 – 8.700	9.58 (300K)	0.05 (NEDT)
Ozone	30	9.580 – 9.880	3.69 (250K)	0.25 (NEDT)
Surface/Cloud Temperature	31	10.780 – 11.280	9.55 (300K)	0.05 (NEDT)
	32	11.770 – 12.270	8.94 (300K)	0.05 (NEDT)
Cloud Top Altitude	33	13.185 – 13.485	4.52 (260K)	0.25 (NEDT)
	34	13.485 – 13.785	3.76 (250K)	0.25 (NEDT)
	35	13.785 – 14.085	3.11 (240K)	0.25 (NEDT)
	36	14.085 – 14.385	2.08 (220K)	0.35 (NEDT)

[1]Spectral Radiance values = W/m^2 -μm-sr

[2]SNR = Signal-to-noise ratio

[3]NEDT = Noise-equivalent delta temperature (K)

The MODIS sensor is flown onboard the Terra (AM1) and Aqua (PM1) platforms of the National Aeronautics and Space Administration's (NASA) Earth Observing System (EOS) (Figure 6) (Morisette et al., 2005; Giglio et al., 2006; Barnes et al., 1998). The satellites operate at an altitude of 705 km in near-polar, sun-synchronous orbits. MODIS is a cross track sensor with a swath width of 2,330 km and an along track swath length of 10 km at nadir (Barnes et al., 1998). The Terra platform has a daily descending equatorial crossing that occurs at 10:30 a.m. The Aqua platform has a daily ascending equatorial crossing that take place at 1:30 p.m. (Barnes et al., 1998; Morisette et al., 2005; Giglio et al., 2006). The swath width and length along with the orbital characteristics and temporal resolution of the platform allow the MODIS sensor to image the entire surface of the Earth every 1 to 2 days (Barnes et al., 1998; Guenther et al., 2002).

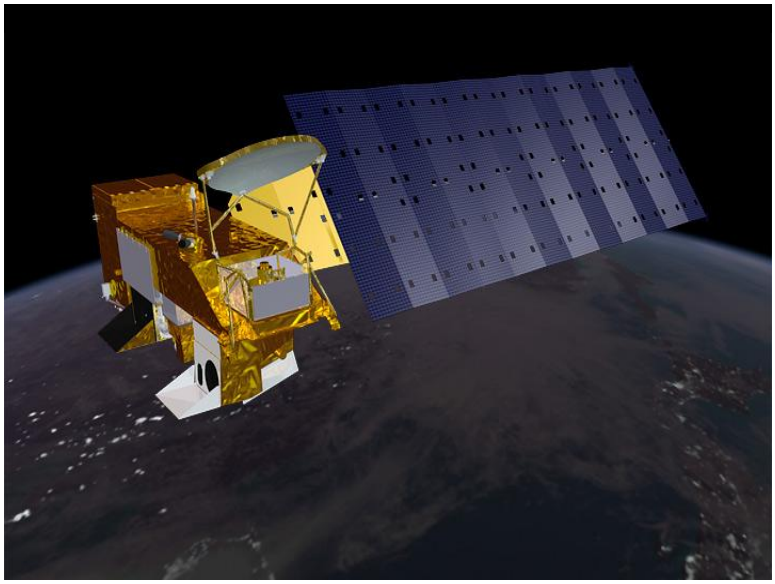

Figure 6: Terra and Aqua Satellite Platform
(Source: NASA Earth Observatory)

Data from the Terra and Aqua MODIS is used to generate a suite of standard data products designed to maximize ease of use while minimizing data processing. The MODIS standard data products are generated using rigorously developed application specific peer-reviewed algorithms. The standard data products include a series of basic land, ocean, cryosphere, and atmospheric variables (Giglio et al., 2003).

The MODIS standard land and surface products comprise spectral reflectance (MOD09/MYD09), land surface temperature (MOD11/MYD11), land cover and land cover change (MOD12/MCD12), vegetation indices

(MOD13/MYD13), thermal anomalies and fires (MOD14/MYD14), leaf area index, and fraction of absorbed photosynthetically active radiation (FPAR) (MOD15/MYD15) (Justice et al., 1998; Guenther et al., 2002; NASA MODIS Web, 2011; NASA LPDAAC, 2011). Evapotranspiration (MOD16), net photosynthesis and gross primary productivity (MOD17/MYD17), albedo and bidirectional reflectance distribution function (BRDF) adjusted reflectance (MCD43), vegetation cover conversion (MOD44B), a land water mask (MOD44W), and burned area (MCD45) products are also generated (Justice et al., 1998; Guenther et al., 2002; NASA MODIS Web, 2011; NASA LPDAAC, 2011).

Standard ocean products generated from the Terra and Aqua MODIS include normalized water-leaving radiance (MOD18/MYD18), chlorophyll-a concentration (MOD19/MYD19), surface photosynthetically active radiation (PAR), and instantaneous photosynthetically active radiation (IPAR) (MOD20/MYD20) (Esaias et al., 1998; Franz et al., 2006; MODIS Web, 2011). Clear water epsilons (MOD21/MYD21), chlorophyll fluorescence (MOD22/MYD22), coccolith concentration (MOD23/MYD23),

ocean primary productivity (MOD24/MYD24), and sea surface temperature (MOD25/MYD25) products are also produced (Esaias et al., 1998; Franz et al., 2006; MODIS Web, 2011).

Cryosphere products generated from the Terra and Aqua MODIS include the snow cover (MOD10/MYD10) and sea ice cover (MOD29/MYD29 standard data products (Hall, Riggs, Salomonson, DiGirolamo, & Bayr, 2002; Hall et al., 2001; Justice et al., 1998; MODIS Web, 2011). Snow cover variables included in the snow cover product (MOD10/MYD10) consist of fractional snow cover and snow albedo (Hall et al., 2002; Hall et al., 2001; Justice et al., 1998; MODIS Web, 2011). The sea ice cover product (MOD29/MYD29) includes sea ice extent and ice-surface temperature (IST) variables for day and night scenes (Hall et al., 2002; Hall et al., 2001; Justice et al., 1998; MODIS Web, 2011).

The atmospheric products from Terra and Aqua MODIS comprise a combination of standard atmospheric, water vapor, and cloud variables (Remer at al., 2005; King, Kaufman, Menzel, & Tanré, 1992). The MODIS atmosphere products are generated for both land and ocean scenes

(Remer at al., 2005; King et al., 1992). Standard atmosphere products generated include an aerosol product (MOD04/MYD04), total precipitable water (MOD05/MYD05), a cloud product (MOD06/MYD06), atmospheric profiles (MOD07/MYD07), a gridded atmospheric product (MOD08/MYD08), and a cloud mask (MOD35/MYD35) (Remer at al., 2005; King et al., 1992; MODIS Web, 2011).

Aerosol variables in the standard aerosols product (MOD04/MYD04) include aerosol optical thickness, aerosol type, particle size distribution, and optical properties (Remer at al., 2005; King et al., 1992; MODIS Web, 2011). Water vapor variables included in the total precipitable water product are atmospheric water vapor concentration and amount of precipitable water (Remer at al., 2005; King et al., 1992; MODIS Web, 2011). The standard cloud product (MODMOD06/MYD06) includes cloud optical thickness, cloud top height, cloud top temperature, cloud top pressure, cloud particle radius, cloud particle phase, cloud integrated water path, cloud shadow effects, effective emissivity, day and night cloud fraction, cirrus reflectance, and thermodynamic phase

variables (Platnick et al., 2003; King et al., 1992; MODIS Web, 2011). Variables in the standard atmospheric profiles product (MOD07/MYD07) include total-ozone burden, atmospheric stability, temperature and moisture profiles, and atmospheric water vapor (King et al., 1992; Remer at al., 2005; Platnick et al., 2003; MODIS Web, 2011).

The MODIS standard data products were designed to meet the needs of global to regional monitoring, assessment, and modeling with an emphasis on global change research (Justice et al., 1998). MODIS standard data products are generated at various levels of processing, each representing an increased degree of validation and calibration (Justice et al., 1998). Level 0 data represents raw MODIS data which has not undergone any level of processing, calibration or validation. MODIS level 0 data is a sequence of digital counts in Consultative Committee for Space Data Systems (CCSDS) packets that are about one gigabit in size and produced for every MODIS scene collected (Xiong et al., 2005; Read et al., 2004; Justice et al., 1998).

Level 1 data products undergo two stages of processing, level 1A and level 1B. The level 1A data processing converts MODIS digital counts into raw radiance and reflectance values (Nishihama et al., 1997; Xiong et al., 2005; Read et al., 2004). To process MODIS digital count data to level 1A spatial values along with Earth location information is generated for the ground location of each spatial element in the scene. During level 1A processing metadata describing the data product being produced is generated and included with each data file (Nishihama et al., 1997; Xiong et al., 2005; Read et al., 2004).

Data processing to level 1B involves additional analysis and calibration steps. The level 1B data applies a radiometric calibration to the raw radiance and reflectance data contained in the level 1A product. Level 1B products are fully calibrated to the spatial and temporal resolutions of the Terra and Aqua MODIS in sensor units (Xiong et al., 2005; Savtchenko et al., 2004; Justice et al., 1998; Read et al., 2004). The nadir pixel for each scene is also calculated allowing the Level 1B products to contain calibrated radiance and reflectance data at a 250 m

to 1 km resolution (Xiong et al., 2005; Savtchenko et al., 2004; Justice et al., 1998; Read et al., 2004).

Processing to level 2 data products involves the use of satellite range and height above the ellipsoid as well as solar and satellite azimuth angles to perform additional calibration (Justice et al., 1998). These parameters are used to perform atmospheric correction of each data scene collected by the MODIS sensor (Justice et al., 1998). In the final stage of processing, level 2 MODIS data scenes are converted to an Earth based grid using one of the MODIS standard projection systems. Projection systems used to create the MODIS grids include the Integerized Sinusoidal, Goode Homolosine, or Lambert's Azimuthal Equal Area projection (Justice et al., 2002; Justice et al., 1998; Wolfe, Roy, & Vermote, 1998; Nishihama et al., 1997). Projection onto an Earth based grid is performed to create the level 2G MODIS products.

MODIS level 3 data undergoes additional processing steps to produce data products that are resampled to higher resolutions and temporally composited. Level 2G data in projected coordinate systems

are resampled to 500 m and 250 m resolutions to produce higher order data products (Read et al., 2004). Once resampled, the data products at all three MODIS standard product resolutions are then temporally composited to application specific time intervals. The data products are temporally composited to produce 8-day, 16-day, monthly, 32-day, 96-day, and yearly data sets (Read et al., 2004; Justice et al., 1998; Justice et al., 2002). The spatially resampled and temporally composited MODIS level 3 data products have then undergone sufficient calibration and processing for use in high level modeling and analysis (Read et al., 2004; Justice et al., 1998; Justice et al., 2002).

Level 4 data products are generated using the highest level of processing applied to MODIS data. The MODIS level 4 data products are the modeling outputs and results from the analysis of lower level data products (Read et al., 2004; Justice et al., 1998; Justice et al., 2002). Modeling outputs and analysis results used to produce level 4 data are derived from multiple measurements of MODIS level 2, 2G, and 3 data (Read et al., 2004). The methods used to generate the level 4 data

products are derived from peer-reviewed algorithms and comparison to airborne and in-situ data sources to insure data quality and scientific applicability. Once the modeling and analyses are completed, the outputs are projected into the most applicable MODIS standard projection system (Read et al., 2004).

Western Hindu Kush-Himalayas

The Western Hindu Kush-Himalayas are located in South Asia and include the mountainous regions of Afghanistan, Pakistan, and northern India (Figure 7). The region encompasses an area of 1,080,570 km^2, running a total length of 10,635 km. The Western Hindu Kush region is part of the Himalayan mountain range, the tallest and one of the geologically youngest folded mountain ranges in the world (Ahmad, 1993; TERI-NA, 2002; Menon, 1954; Schweinfurth, 1992). With a calculated relative relief of 7,989 m, the Western Hindu Kush region contains ecological zones ranging from tropical, subtropical, temperate, subalpine, to alpine (Ohsawa, Shakya, & Numata, 1986). Having elevations ranging from 11 m to greater than 8,000 m, the Western

Hindu Kush-Himalayas contain a variety of prominent topological and environmental features.

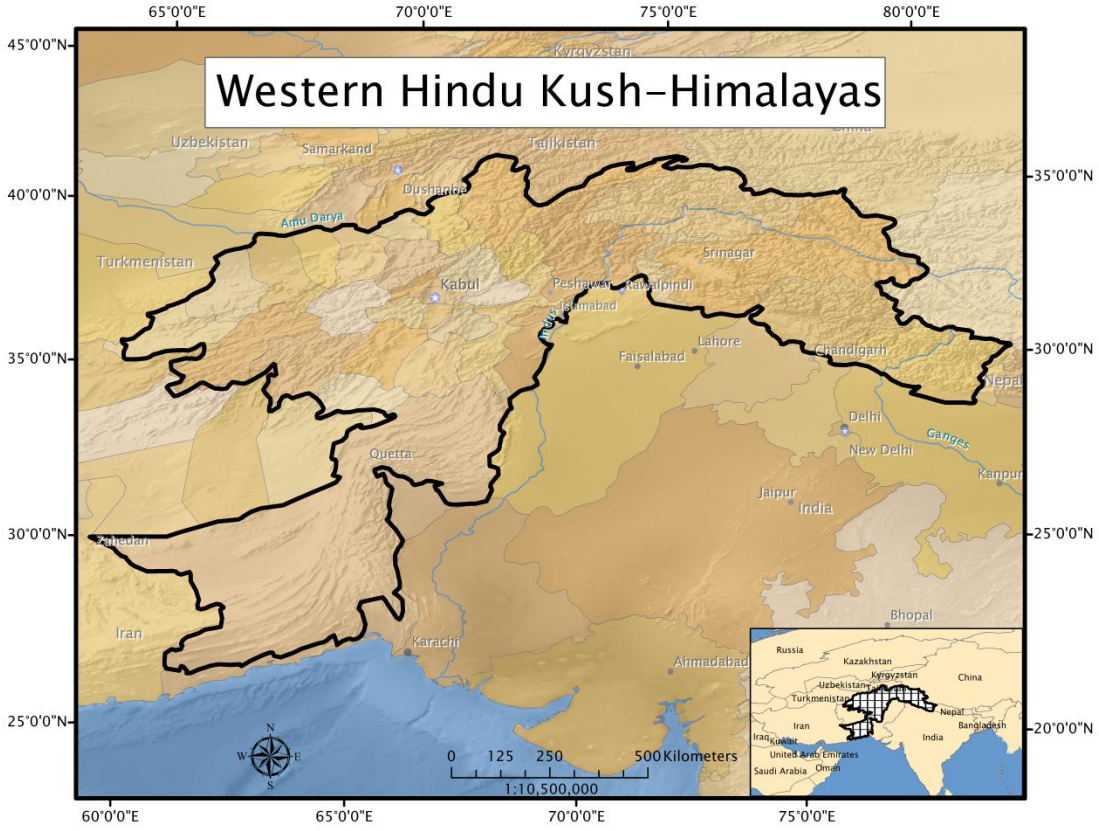

Figure 7: The Western Hindu Kush-Himalayan Region
(Data Source: ESRI Inc., 2004; ICIMOD, 2010)

In the Western Hindu Kush region, large valley glaciers, mighty rivers, and towering mountain peaks dominate the landscape. Some of the planet's most prevalent glaciers have developed and continue to persist in the region. The Majiacangbu, Baltoro, Biafo, Gangotri, Siachen,

and Daoliqu glaciers are all located in the Western Hindu Kush-Himalayas (TERI-NA, 2002; Naithani, Nainwal, Sati, & Prasad, 2001; Hewitt, Wake, Young, & David, 1989; Mayer, Lambrecht, Belò, Smiraglia, & Diolaiuti, 2006). These represent some of the largest glaciers in the world beyond the planet's Polar Regions. The melt and runoff from these glaciers are important sources of regional tributaries and river flow (TERI-NA, 2002; Ahmad, 1993; Naithani et al., 2001; Hewitt et al., 1989; Mayer et al., 2006).

Increased retreat of regional glaciers over the past century has resulted in decreased annual runoff levels. This has caused rivers and tributaries throughout the Western Hindu Kush-Himalayas to flow with decreased length and volume (TERI-NA, 2002; Hewitt et al., 1989; Naithani et al., 2001; Mayer et al., 2006). Estimates have shown that regional glacial retreat is occurring at an annual rate of at least 30 m (TERI-NA, 2002). Research indicates that if current trends in glacial retreat continue, many of the glaciers in the Western Hindu Kush-Himalayas could decrease to levels that would no longer make them

viable water sources (TERI-NA, 2002; Naithani et al., 2001; Hewitt et al., 1989; Mayer et al., 2006). This would have a disastrous effect on the millions of people living in the region that are dependent on the rivers and tributaries fed by the glaciers.

The Indus, Ganges, and Amu Darya, three of the world's largest rivers, flow through the Western Hindu Kush-Himalayas (Hewitt et al., 1989; TERI-NA, 2002; Adil, 2001; Menon, 1954). The Indus and Amu Darya rivers both originate from within the region. These large and vitally important regional water bodies derive from sources high in the Western Hindu Kush-Himalayan Mountains (Hewitt et al., 1989; TERI-NA, 2002; Adil, 2001). The Ganges River flows through the Himalayan Mountain range and the Western Hindu Kush region. These three rivers provide vital water and transportation sources to millions of people throughout South Asia.

Rugged terrain throughout the Western Hindu Kush has resulted in the formation of some of the tallest mountains in the world in the region's upper elevations. Some of the planet's most formidable

mountains have developed in the Western Hindu Kush-Himalayas, including many of the planets tallest peaks. The region's notable peaks exceeding 8,000 m include Nanga Parbat in northern Pakistan's Nanga Parbat range at 8,125 m and Gasherbrum I in the Baltoro Karakoram range of northern Pakistan, which stands at 8,068 m. Also located in the Baltoro Karakoram are Broad Peak which measures 8,047 m and Gasherbrum II at 8,035 m (ICIMOD, 2010; TERI-NA, 2002;).

In the Hindu Kush Himalayas of northern India, towering peaks such as Nanda Devi at 7,816 m in the Kumoan range and Saser Kangri I at 7,672 m in the Saser Karakoram range can be found. The Himalayas of northern India is also home to Kamet which stands at 7,756 m and Mana standing at 7,272 m, both located in the Garhwal range (ICIMOD, 2010; TERI-NA, 2002;). The prominent peak of Noshaq measuring in at 7,485 m in Afghanistan's Hindu Kush range is another notable peak located in the region (ICIMOD, 2010; TERI-NA, 2002).

The Western Hindu Kush-Himalayas is home to an abundance of plant and animal species. Unique geology and topology in the region

combine to create environmental gradients that are conducive to the development of many types of flora and fauna. The Western Hindu Kush-Himalayas contain numerous types of flora, including grasses, scrubs, herbs, and tree species (Singh, & Singh, 1987). Many grass species can be found in the hot, humid lower elevation tropical and subtropical zones of the region. *Bothriochloa spp.*, *Cynodon dactylon*, *Chrysopogon fluvus*, *Themeda anathera*, *Arundinella setosa*, *Heteropogon contortus*, *Sporobolus marginatus*, *Chloris spp.*, *Eulaliopsis binata*, *and Cenchrus ciliaris* are all widespread in these zones (Gupta, 1978; Agrawal, 1990).

The warm middle elevation temperate zones of the Western Hindu Kush are also home to numerous grass species. This zone is the optimum habitat to support such species as *Bothriochloa spp.*, *Cynodon dactylon*, *Chrysopogon gryllus*, *Poa annua*, *Poa alpina*, *Poa stewartiana*, *Poa pratensis*, *Themeda triandra*, *Heteropogon contortus*, *Cymbopogon stracheyii*, *and Koeleria cristata* (Gupta, 1978; Agrawal, 1990).

In the subalpine and alpine zones of the Western Hindu Kush region high altitude grass species dominate the landscape. These

species have adapted to the high Himalayas, allowing them to prosper despite the harsh environment. In these zones, species such as *Agrostis spp.*, *Poa spp.*, *Phleum alpinum*, *Puccinellia kashmiriana*, *Trisetum spp.*, *Danthonia spp.*, *Helictotrichon spp.*, *Deschampsia caespitosa*, *Andropogon spp.*, *and Agropyron spp.* are common (Gupta, 1978; Gupta, 1972; Klimeš, 2003). The region also contains discontiguous patches of *Kobresia pygmaea*, *Carex spp.*, *Stipa spp.*, *Puccinellia himalaica*, *Eleocharis quinqueflora*, *Juncus thomsonii*, *Blysmus compressus*, and *Triglochin palustre* (Gupta, 1978; Gupta, 1972; Klimeš, 2003).

Scrubs and other ground species in the Western Hindu Kush-Himalayas are widespread and can be found throughout the region. The primary scrub types found in the low to middle elevation Western Hindu Kush mountains include such diverse species as *Acantholimon kokandense*, *Acantholimon lycopodioides*, *Astragalus section Aegacantha*, *Juniperus communis*, *Juniperus excelsa polycarpos*, *Artemisia santolinifolia*, *Ephedra gerardiana*, *Salix hastate*, *Sorbus tianschanica*, *Hippophaë rhamnoides*, *and Myricaria germanica*

alopecuroides (Miehe, Miehe, & Schlütz, 2009; Ohsawa, Shakya, & Numata, 1986; Singh, & Singh, 1987).

The low and middle elevations are also home to many herbaceous and flowering plant species. *Polygonum plebejum*, *Potentilla bifurca*, *Malva pusilla*, *Lamiaceae spp.*, *Plantago spp.*, *Tribulus terrestris*, *Eremurus stenophyllus*, *Festuca olgae*, and the poisonous *Arisaema flavum and Stellera chamaejasme* are all widespread and commonly found throughout the Western Hindu Kush (Miehe et al., 2009; Ohsawa et al., 1986; Singh, & Singh, 1987). Patches of *Boraginaceae spp.*, *Cyananthus spp.*, *Cousinia spp.*, *Hepaticae spp.*, as well as *Botrychium lunaria* and *Ophioglossum vulgatum*, can also be found in the region (Miehe et al., 2009; Ohsawa et al., 1986; Singh, & Singh, 1987).

Throughout the upper elevations, alpine scrub and steppe vegetation dominate the landscape. High altitude adapted scrub species including *Artemisia spp.*, *Celtis caucasica*, *Galium spp.*, *Lonicera webbiana*, *Potentilla spp.*, *Berberis petiolaris garhwalensis*, *Juniperus communis nana*, *Myricaria germanica*, *Lycopodium clavatum*, *Pyrola*

rotundifolia, *Sorbus spp.*, *Pedicularis spp.*, and *Myricaria spp.* are all widely distributed throughout the alpine zones of the Western Hindu Kush (Gupta, 1972; Miehe et al., 2009; Breckle, 1971; Singh, & Singh, 1987, Klimeš, 2003). Also commonly identified in the region are areas containing individual and small patches of *Lonicera spinosa* and *Dasiphora parvifolia* (Klimeš, 2003).

Many herbaceous species can also be indentified throughout the region's alpine zones. These species consist of *Arabis pterosperma*, *Hedera nepalensis*, *Salvia nubicola*, *Euphorbia indica*, *Agrimonia pilosa nepalensis*, *Sanicula europaea elata*, *Thymus spp.*, *Veronica spp.*, *Delphinium elatum*, *Valeriana spp.*, *Saxifraga spp.*, *Nepeta spp.*, *Astragalus spp.*, and *Erysium hieracifolium* (Gupta, 1972; Miehe et al., 2009; Breckle, 1971; Singh, & Singh, 1987, Klimeš, 2003). Additional species commonly encountered in the highest elevations of the Western Hindu Kush include *Alyssum spp.*, *Oxytropis microphilla*, *Tanacetum fruticulosum*, *Thylacospermum cespitosum*, *Potentilla pamirica*, *Pegaeophyton scapiflorum*, *Ranunculus trichophyllus*, *Actinocarya acaulis*,

Hedinia tibetica, *Waldheimia tridactylites*, *Christolea pumila*, and *Saussurea gnaphalodes* (Gupta, 1972; Miehe et al., 2009; Breckle, 1971; Singh, & Singh, 1987, Klimeš, 2003).

The alpine zones also contain patches of many flowering species intermixed with the scrub and herbaceous plant life of the upper Hindu Kush Mountains. Species such as *Circaea imaicola*, *Gnaphalium affine*, *Gentiana spp.*, *Filago spathulata*, *Prunus cornuta*, *Carduus onopordioides*, *Drapa alpine*, *Lychnis apetala*, *Saxifraga spp.*, *Gagea lutea*, *Leontopodium campestre*, *Ranunculus shaftoana*, *Delphinium brunonianum*, and *Eremurus stenophyllus* are also quite common in the region (Gupta, 1972; Breckle, 1971; Miehe et al., 2009; Singh, & Singh, 1987, Klimeš, 2003).

In the Western Hindu Kush-Himalayas, diverse forest types can be found throughout the region. The principal species commonly identified in the Western Hindu Kush region include *Quercus semecarpofolia*, *Quercus lanuginosa*, *Pinus wallichiana*, and *Pinus roxburghii* (Ohsawa, Shakya, & Numata, 1986; Miehe et al., 2009; Singh, & Singh, 1987;

Gupta, 1978; Shrestha, 2003). The tropical zones are populated by heat tolerant, low elevation adapted tree species including stands of *Shorea robusta*, *Adina cordifolia*, Engelhardtia spicata, and the dominant *Pinus roxburghii* (Ohsawa et al., 1986; Miehe et al., 2009; Singh, & Singh, 1987; Gupta, 1978; Shrestha, 2003).

In the mid-elevation temperate zones of the Western Hindu Kush, a diverse array of tree species can be identified throughout the landscape. The temperate zones are dominated by stands of *Quercus lanuginosa*, *Quercus semecarpifolia* and *Pinus wallichiana* (Ohsawa et al., 1986; Miehe et al., 2009; Singh, & Singh, 1987; Gupta, 1978; Shrestha, 2003). Intermixed with the temperate zones predominant species are stands and individual *Alnus nepalensis and Lyonia ovalifolia*. In the cool upper temperate regions *Rhododendron arboretum* can also be found (Ohsawa et al., 1986; Miehe et al., 2009; Singh, & Singh, 1987; Gupta, 1978; Shrestha, 2003).

Tree species adapted to high elevation and cold climate dominate in the alpine zones of the Western Hindu Kush-Himalayan region. The

upper elevations of the Western Hindu Kush are known to contain only two predominant tree species, *Abies spectabilis* and *Betula utilis* (Ohsawa et al., 1986; Miehe at al., 2009; Singh, & Singh, 1987; Gupta, 1978; Gupta, 1972; Shrestha, 2003). These two species dominate the landscape of the region's cold, high elevation subalpine zones.

In the alpine zones, the number of tree species capable of establishing is low due to limitations created by harsh climatic conditions. The upper elevation zones are dominated by dwarf species which have adapted to the extreme conditions that prevail in the region's alpine environments. Stands and individual *Betula jacquemonti*, *Picea smithiana* and *Juniperus semiglobosa* are commonly identified in the region's alpine zones (Breckle, 1971; Gupta, 1972; Ohsawa et al., 1986; Shrestha, 2003; Singh, & Singh, 1987; Miehe et al., 2009). The alpine zones also contain discontinuous stands of *Juglans regia kumaonica* and *Corylus jacquemonti* (Gupta, 1972; Singh, & Singh, 1987; Miehe et al., 2009). These tree species prevail throughout the region's upper elevations.

A diverse array of animal life inhabits the Western Hindu Kush-Himalayas. Throughout the region, species adapted to the mountains steep slopes and rugged terrain flourishes. The region is home to a diverse array of mammals, reptiles, and avian species; as well as amphibians and aquatic fauna. Carnivorous species such as *Canis lupus chanco*, *Cuon alpinus*, *Python molurus*, *Vulpes vulpes*, *Vulpes ferrilata*, and *Lynx lynx isabellinus* can be found throughout the region (Bagchi, Mishra, & Bhatnagar, 2004; Ahmad, 1993; TERI-NA, 2002; Adil, 2001; Verma, 2002). Additionally, herbivores including *Ovis vignei*, *Ovis ammon poli*, *Procapra picticaudata*, *Cervus elaphus hanglu*, *Equus kiang*, *Pseudois nayaur*, *Bos grunniens*, and *Pantholops hodgsoni* are commonly encountered in the mountains of the Western Hindu Kush (Bagchi et al., 2004; Ahmad, 1993; TERI-NA, 2002; Adil, 2001; Verma, 2002).

The region is home to numerous small mammals as well. The predominant species include squirrels, rabbits, and rodents. *Pataurista petusista albiventer*, *Eoglaucomys fimbriatus*, *Presbytis entellus*, *Alticola roylei*, *Alticola argentatus*, *Nyctalus leisleri*, and *Murina grisea* are all

commonly found in the forests and meadows of the Western Hindu Kush Mountains (Wilson, & Reeder, 2005; TERI-NA, 2002; Singh, & Singh, 1987; Verma, 2002). The mountains are also home to groups of *Ailurus fulgens*, *Marmota caudate*, *Microtus transcaspicus*, *Prionodon pardicolor*, *Apodemus pallipes*, *Conothoa macrotis*, and *Mus musculus* (Wilson, & Reeder, 2005; TERI-NA, 2002; Singh, & Singh, 1987; Verma, 2002). Small mammals flourish throughout the Western Hindu Kush feeding on the rich foliage of the meadows and forests.

Avian and aquatic species also thrive throughout the mountains of the Western Hindu Kush, though in smaller numbers than their mammalian counterparts. Avian species can be found flying throughout the skies and inhabiting the lakes and rivers of the Western Hindu Kush region. A diverse array of avifauna including Gypaetus *barbatus*, *Gyps himalayensis*, *Falco cherrug*, *Falco tinnunculus*, *Phoenicopterus roseus*, *Picoides himalaensis*, *Collacalia brevirostris*, *Scolopax rusticola*, *Sitta cashmirensis*, and *Ficedula subrubra* inhabit the region (Price, Zee, Jamdar, & Jamdar, 2003; Adil, 2001; TERI-NA, 2002;). Along with

Tragopan spp., *Buteo* spp., Lophophorus *impejanus*, *Turdus spp.*, *Ficedula spp.*, *Certhia himalayana*, *Parus spp.*, *Phylloscopus spp.*, and *Carpodacus spp.*, *Leucosticte nemoricola*, and *Mycerobas spp*. which are all commonly found throughout the mountains of the region (Price et al., 2003; Adil, 2001; TERI-NA, 2002;).

In the rivers, lakes, and streams of the Western Hindu Kush-Himalayas fish species can be found in abundance. The region's plentiful water bodies contain *Tor tor*, *Garra gotyla*, *Garra prashadi*, *Oreinus plagiostomus*, *Psilorhynchus balitora*, *Botia almorhae*, and *Botia lohachata* (Menon, 1954). The lakes and large flowing rivers of the region also contain large populations of *Nemachilus spp.*, *Amblyceps mangois*, *Bagarius bagarius*, *Glyptothorax spp.*, and *Sisor rhabdophorus* (Menon, 1954). Although many animal species can be found throughout the region, their numbers have been declining at a steady rate. Habitat destruction along with illegal poaching and competition from domestic livestock has seriously impacted most of the region's fauna (Bagchi et al., 2004; Ahmad, 1993; TERI-NA, 2002; Menon, 1954).

The Western Hindu Kush-Himalayas is also home to a number of endangered species. Limited natural resources along with increased exploitation by humanity threaten the livelihood of many of the region's fauna. The mammal species *Ursus arctos*, *Panthera unica*, *Selenactos himalayanus*, *Elephas maximus*, *Capra sibirica*, *Moschus mischiferus*, and *Hemitragus jamlahicus* are all endangered (Verma, 2002; TERI-NA, 2002; Ahmad, 1993; Bagchi et al., 2004; Adil, 2001; Singh, & Singh, 1987). In the Western Hindu Kush region, the endemic *Nycticebus bengalensis*, *Bunopithecus hoolock*, *Neofelis nebulosa* and *Caprolagus hispidus* are also in decline and classified regionally as endangered (Verma, 2002; TERI-NA, 2002; Ahmad, 1993; Bagchi et al., 2004; Adil, 2001; Singh, & Singh, 1987).

Regional avian species have been adversely impacted by increased resource exploitation and deforestation. *Oreortyx pictus*, *Grus leucogeranus*, *Tetraogallus tibetanus*, and *Aviceda leuphotes* are now classified as endangered in the Western Hindu Kush-Himalayas. The *Crossoptilon harmani*, *Tragopan spp.*, and *Grus nigricollis* are also

threatened throughout the region (TERI-NA, 2002; Ahmad, 1993; Wilson, & Reeder, 2005; Adil, 2001; Verma, 2002). Disruption of migratory routes and breeding grounds has had serious consequences for the region's avifauna resulting in decreased population numbers (TERI-NA, 2002; Ahmad, 1993; Wilson, & Reeder, 2005; Adil, 2001; Verma, 2002).

Fish species are also under threat in the lakes and streams of the region. Decreased numbers of *Tor putitora* and *Salmo trutta fario* have been seen throughout the upper elevations of the Western Hindu Kush Mountains (Ahmad, 1993; TERI-NA, 2002). This has affected catch numbers and species regeneration down river in the heavily populated lower elevations (Ahmad, 1993; TERI-NA, 2002). Environmental degradation along with decreases in habitat has negatively impacted many of these regional species and they are now at risk of extinction.

In the Western Hindu Kush-Himalayan region, agrarian and pastoral populations deriving their livelihoods from a combination of subsistence farming and animal husbandry practices prosper (Ahmad, 1993; Tiwari, 2000; Singh, & Singh, 1987; Gupta, 1978; TERI-NA, 2002; Tucker, 1982;

Adil, 2001). Human impact has had a considerable influence on the ecology of the Western Hindu Kush-Himalayan region. Historically, the ecosystem has been utilized by local peoples for the grazing of cattle, fodder and firewood collection, charcoal manufacturing, slash and burn agriculture, and as building material (Ahmad, 1993; Tiwari, 2000; Singh, & Singh, 1987; Gupta, 1978; TERI-NA, 2002; Tucker, 1982; Adil, 2001). In recent centuries, the region has seen increased exploitation for surface mining, road construction, reservoir and dam building, recreation, and tourism (Ahmad, 1993; Tiwari, 2000; Singh, & Singh, 1987; Gupta, 1978; TERI-NA, 2002; Tucker, 1982; Adil, 2001). These activities have resulted in alterations in regional species types and composition as well as a high degree of environmental degradation.

Environmental pressures created by anthropogenic land use along with the fragility of the Western Hindu Kush-Himalaya's ecology have resulted in degradation of the landscape throughout the region. Many of the region's natural resources have been adversely affected by increases in the human population and the resulting increase in resource use.

Exploitation of the Western Hindu Kush to support large human and livestock populations has resulted in the carrying capacity of the land being surpassed (Ahmad, 1993; Tiwari, 2000; Singh, & Singh, 1987; Gupta, 1978; TERI-NA, 2002). This has led to the development of a multitude of environmental issues throughout the Western Hindu Kush region.

Unplanned land use, overgrazing by cattle, deforestation, the removal of broad leaved flora, and excess exploitation of community and village forests have had disastrous effects on the region's environment (Ahmad, 1993; Gupta, 1978; TERI-NA, 2002; Singh, & Singh, 1987; Adil, 2001; Verma, 2002). The practice of crop cultivation on steep slopes, surface mining, large scale engineering projects, and increased urbanization have all contributed to environmental degradation throughout the Western Hindu Kush-Himalayas (Ahmad, 1993; Gupta, 1978; TERI-NA, 2002; Singh, & Singh, 1987; Adil, 2001; Verma, 2002).

These activities have led to increased incidence of wild fires, landslides, and avalanches; soil nutrient and moisture loss; decreasing

water resources; and increased water pollution along the entire Himalayan range and throughout the Western Hindu Kush region (Ahmad, 1993; Gupta, 1978; TERI-NA, 2002; Singh, & Singh, 1987; Adil, 2001; Verma, 2002). The region is also suffering from the effects of receding glaciers, wide-scale landscape transformation, arrested succession in the region's forests and meadows, and atmospheric changes including broad scale pollution and alterations at the microclimatic level (Ahmad, 1993; Gupta, 1978; TERI-NA, 2002; Singh, & Singh, 1987; Adil, 2001; Verma, 2002).

Method

This study is representative of regional wildfire counts and distributions as detected by the Terra and Aqua MODIS sensors. Limited daily satellite overpasses along with sensor and detection algorithm constraints limit the number of wildfire detections that the Terra and Aqua MODIS can achieve. These limitations prevent the satellites from characterizing the occurrence of all wildfires that ignited throughout the region, resulting in biased wildfire counts and distributions. This limits the study to wildfire events that occurred during the Terra and Aqua regional overpass times and that were of sufficient size and intensity to be detected by the MODIS sensor.

The study determined the most relevant environmental, topological, and sociological factors that contribute to the ignition of wildfire events in the Western Hindu Kush-Himalayas region of South Asia. Environmental variables investigated included land cover type, vegetation health, and distance to water. Topological variables examined included slope, aspect, and elevation. Regional sociological variables

evaluated for the model included distance to roads and distance to settlements.

To accurately determine relevant environmental, topological, and sociological factors a statistical evaluation of MODIS and GIS data sources was performed. A multi-criteria evaluation was then executed to model regional wildfire potential. The statistical analysis and multi-criteria evaluation were performed using 1 km resolution MODIS Terra and Aqua data obtained during the regional 2009 peak wildfire season. Peak wildfire season in the Western Hindu Kush region lasts for 3 months, beginning in February and lasting until the end of April (Ichoku, Giglio, Wooster, & Remer, 2008).

To allow for accurate identification of regional wildfire variables, data were analyzed based on the 3 month February through April regional peak wildfire season. MODIS MCD14ML global monthly fire location data for the peak wildfire season was used to characterize regional wildfire events. The location of each regional wildfire event was determined from the wildfire event data set derived from the MODIS

MCD14ML global monthly fire location data.

A total of 1,959 wildfire events were detected by the Terra and Aqua MODIS during the 2009 peak wildfire season in the Western Hindu Kush-Himalayas. The wildfire events were compared to regional MODIS land cover data to allow for the removal of blatant commission errors. Comparison to land cover data revealed 16 false wildfire event detections during the 2009 peak wildfire season. Of the 16 total commission errors eight occurred in the region's permanent wetlands, six in urban and built-up areas, and two in barren or sparsely vegetated land. This represented a false detection rate of only .82% in the Western Hindu Kush-Himalayas during the 2009 peak wildfire season. The 1,943 wildfire events remaining after the removal of commission errors comprised the regional wildfire events data set for the 2009 peak wildfire season. These wildfire event points were used to represent the geographic locations of known wildfire events and as sampling points to extract variable data.

A series of 1,074 sampling points were used to extract variable data for analysis. The sample size was determined based on a 95% confidence level with a confidence interval of 2%. Cochran's sampling statistic in Figure 8 was used to calculate the minimum number of sampling points required to maintain an error (ϵ) of no more than 2% (Cochran, 1977; Bartlett, Kotrlik, & Higgens, 2001).

$$n_0 = \frac{(z_{\alpha/2})^2(\rho)(1-\rho)}{\epsilon^2} \quad (1)$$

Where

n_0 = Sample Size

$z_{\alpha/2}$ = Value of Selected Alpha Level

ρ = Estimate of Variance

ϵ = Accepted Margin of Error

Figure 8: Sample Size Formula
(Source: Cochran, 1977; Bartlett et al., 2001)

The minimum number of sampling points determined by the equation exceeded 5% of the total population of regional wildfire events.

Therefore, Cochran's correction formula in Figure 9 was used to determine the optimum number of sampling points (Cochran, 1977; Bartlett et al., 2001).

$$n_1 = \frac{n_0}{1+(n_0 - 1/N)} \quad (2)$$

Where

n_1 = Corrected Sample Size

n_0 = Sample Size Determined by Cochran's Formula

N = Population Size

Figure 9: Sample Size Correction Formula
(Source: Cochran, 1977; Bartlett et al., 2001)

The 1,074 sampling points were selected from the 1,943 total wildfire events that occurred during the 2009 peak wildfire season using a random selection function. To perform the random selection the R software environment for statistical computing (R Development Core Team, 2008) was used. The remaining 869 wildfire event data points were set aside as a holdout data set for use in model validation.

MODIS raster data were acquired from the NASA Warehouse Inventory Search Tool (WIST) and the University of Maryland. MODIS data obtained from WIST included regional land cover (MCD12Q1) and vegetation indices (MOD13A3). Global monthly fire location (MCD14ML) data were obtained from the University of Maryland. The project's large study area encompassed six MODIS tiles including h23v05, h23v06, h24v05, h24v06, h25v05, and h25v06. All preprocessing of data including the mosaicing of tiles was performed using IDRISI Taiga (Eastman, 2009).

Topographic factors were extracted from a 1 km resolution NASA Shuttle Radar Topography Mission (SRTM) digital elevation model (DEM). A regional SRTM DEM was obtained from the Consultative Group for International Agriculture Research (CGIAR). The regional DEM was used to extract topological variables including slope, aspect, and elevation for the entire Western Hindu Kush-Himalayas.

Geographic information systems data were obtained from two resources, the International Centre for Integrated Mountain Development

(ICIMOD) and the Environmental Systems Research Institute (ESRI). A boundary for the Hindu Kush-Himalayas was acquired from ICIMOD through the Mountain Environment and Natural Resources Information System (MENRIS). Once retrieved, the boundary for the Western Hindu Kush-Himalayas was delineated from the Hindu Kush-Himalayas vector data source. The Western Hindu Kush-Himalayas for the purpose of this study incorporated the Hindu Kush-Himalayan regions of Afghanistan, Pakistan, and northern India.

High level road networks, water features, and settlement locations vector data for the entire Western Hindu Kush-Himalayas region was acquired from the ESRI. The ESRI road networks and water features data sources were obtained online through the GeoCommunity. Settlement locations for the Western Hindu Kush-Himalayas were obtained from the ESRI Data and Maps: World, Europe, Canada, and Mexico compact disc (ESRI Inc., 2004).

Once all of the vector and raster data sources were obtained, required preprocessing was performed. Preprocessing of the data

included the merging, scaling, and clipping of data sets to conform to the boundaries of the Western Hindu Kush-Himalayas. The data sets were then projected into the Asia South Albers equal area coordinate system. An Albers equal area coordinate system was selected to accommodate the region's size and the east-west orientation of the project's study area. The Albers equal area coordinate system was also selected to maintain accurate area calculations for regional land cover and the wildfire zones generated by the wildfire potential model, while minimizing shape distortion.

Once the data was processed a through point pattern and statistical analysis was performed. The point pattern analysis included the calculation of kernel density estimation to test the wildfire event points for clustering (O'Sullivan, & Unwin, 2003; Burt, Barber, & Rigby, 2009). The Ripley's K(t) function to determine spatial association of the wildfire points was then computed (O'Sullivan, & Unwin, 2003; Burt et al., 2009). The point patterns of the wildfire events were visualized and further

analyzed using the Anselin Local Moran's I statistic (O'Sullivan, & Unwin, 2003; Burt et al., 2009).

The study's independent variables included land cover type, enhanced vegetation index (EVI), slope, aspect, elevation, distance to road features, distance to water features, and distance to settlements. Dependent variables included wildfire location as latitude and longitude, wildfire temperature (T31), and fire radiative power (FRP). Preliminary data exploration and pilot statistics revealed that the study's independent and dependent variables did not conform to a Gaussian distribution.

A series of nonparametric tests were selected to statistically analyze the data. Statistical analysis of the wildfire events and factors data included a Chi-square test of independence to evaluate the statistical significance of the independent variables to the dependent variables (Burt et al., 2009; O'Sullivan, & Unwin, 2003). The strength of the relationship between the independent and dependent variables was determined using a Spearman's rho correlation (Burt et al., 2009; O'Sullivan, & Unwin, 2003). Kruskal-Wallis H tests were performed to

determine the difference between levels of the independent variables and dependent variables (Burt et al., 2009). Kruskal-Wallis H tests were also used to evaluate how the independent variables influence the dependent variables and to what degree.

Robust regression analyses were completed to determine the relationship between the independent and dependent variables (Berk, 1990; Anderson, 2008; Rousseeuw, & Leroy, 1987). The robust regression equations allow for prediction of values of the dependent variables from values of the independent variables using nonparametric data sources (Berk, 1990; Anderson, 2008; Rousseeuw, & Leroy, 1987). A land cover sub-model was also created to determine the most significant land cover types that contribute to regional wildfire ignitions.

After the point pattern and statistical analyses were completed, a pair-wise comparison was performed to determine appropriate weights to apply to each model factor. A summary of the pair-wise comparison is shown in Table 2.

Table 2: Pair-wise Comparison

	Land Cover	Vegetation Health	Slope	Aspect	Elevation	Road Distance	Water Distance	Settlement Distance
Land Cover	1	2	8	6	4	9	3	9
Vegetation Health	1/2	1	5	4	3	8	2	8
Slope	1/8	1/5	1	1/4	1/7	3	1/6	3
Aspect	1/6	1/4	4	1	1/4	4	1/7	4
Elevation	1/4	1/3	7	4	1	6	1/3	5
Road Distance	1/9	1/8	1/3	1/4	1/6	1	1/6	2
Water Distance	1/3	1/2	6	7	3	6	1	8
Settlement Distance	1/9	1/8	1/3	1/4	1/5	1/2	1/8	1

With the pair-wise comparison completed, model weights were calculated for each factor along with the overall consistency ratio. Results of the weights calculation produced an acceptable consistency ratio of .08. The weights calculated for the model are summarized in Table 3.

Table 3: Model Weights

Factor	Weight
Land Cover	0.3265
Vegetation Health	0.2163
Slope	0.0356
Aspect	0.0616
Elevation	0.1220
Road Distance	0.0234
Water Distance	0.1953
Settlement Distance	0.0194
Consistency Ratio = 0.08	

The factors' data was then standardized using fuzzy set membership functions to facilitate the execution of the multi-criteria

evaluation. The range of values of each factor conducive to wildfire ignition was standardized using an appropriate fuzzy set membership function to values from 0 to 255 (Figure 10).

A user defined method of fuzzy set membership standardization was applied to the land cover data. The membership values selected for the standardization of the land cover data are shown in Table 4. Vegetation health was standardized using a symmetrical sigmoidal membership function with membership values that began at 0 EVI, plateaued between .2 to .4 EVI, and then decreased to .5 EVI. To standardize slope a symmetrical sigmoidal membership function was utilized. The membership values used to standardize slope began at 0°, plateaued between .1° to 15°, and then decreased to 30°. A symmetrical sigmoidal membership function was also used to standardize aspect. Membership values used to standardize aspect began at -.000001°, plateaued at 202.5°, and then decreased to 360°.

Elevation was standardized using a monotonically decreasing sigmoidal membership function with membership values that began at 0

m and decreased to 4,000 m. Each of the distance factors were also standardized using monotonically decreasing sigmoidal membership functions. To standardize distance to road features the membership values began at 0 m and decreased to 31 km. The membership values used to standardize distance to water features began at 0 m and decreased to 38 km. Distance to settlements was standardized using membership values that began at 0 m and decreased to 53 km. The membership values used in the fuzzy set membership standardization of each factor are summarized in Table 5.

Table 4: Land Cover Fuzzy Set Membership Values

Land Cover Class	Fuzzy Set Membership Value
Water	0
Evergreen Needleleaf Forests	0.3
Evergreen Broadleaf Forests	0.2
Deciduous Needleleaf Forests	0.1
Deciduous Broadleaf Forests	0.2
Mixed Forests	1
Closed Shrublands	0.4
Open Shrublands	0.4
Woody Savannas	0.9
Savannas	0.1
Grasslands	0.3
Permanent Wetlands	0
Croplands	0.7
Urban and Built-up	0
Cropland/Natural Vegetation Mosaic	0.6
Snow and Ice	0
Barren or Sparsely Vegetated	0

Table 5: Factor Fuzzy Set Membership Values

Factor	Fuzzy Set Membership Shape	Fuzzy Set Membership Type	Membership Values
Land Cover	User Defined	User Defined	0 – 1
Vegetation Health	Symmetric	Sigmoidal	0 – 0.2 – 0.4 – 0.5 (EVI)
Slope	Symmetric	Sigmoidal	0 – 0.1 – 15 – 30 (deg)
Aspect	Symmetric	Sigmoidal	-0.000001 – 202.5 – 202.5 – 360 (deg)
Elevation	Monotonically Decreasing	Sigmoidal	0 – 4,000 (m)
Road Distance	Monotonically Decreasing	Sigmoidal	0 – 31 (km)
Water Distance	Monotonically Decreasing	Sigmoidal	0 – 38 (km)
Settlement Distance	Monotonically Decreasing	Sigmoidal	0 – 53 (km)

Fuzzy set membership was selected for standardization to compensate for the ambiguous nature of the data and the project's research question (Woodcock, & Gopal, 2000; Cornelis, Deschrijver, & Kerre, 2004; Singpurwalla, & Booker, 2004). The use of fuzzy set membership also allowed for uncertainty in the data to be accounted for in the model (Woodcock, & Gopal, 2000; Cornelis et al., 2004; Singpurwalla, & Booker, 2004).

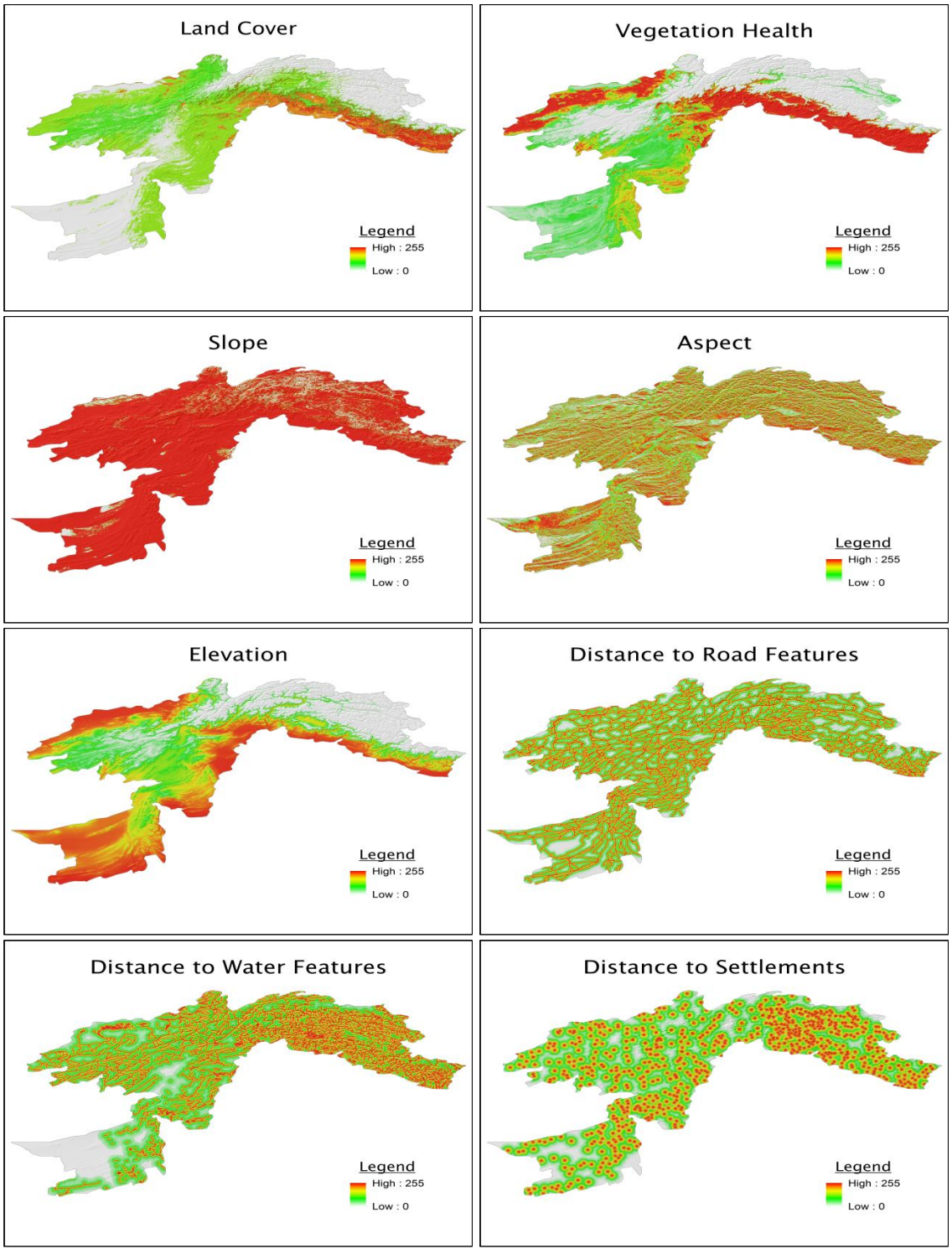

Figure 10: Maps of Standardized Factors

With the data processed, statistically analyzed, and standardized, the multi-criteria evaluation based on a weighted linear combination was performed to model wildfire potential in the Western Hindu Kush-Himalayas. The wildfire potential model was constructed using a modification of the methods of Jaiswal et al. (2002) and Sastry, Jadhav, and Thakker (2002).

Once the model was completed the output of the multi-criteria evaluation was classified into six categories of wildfire potential based on the natural breaks methodology of Jenks and Caspall (1971). Categories utilized for the classification included very high, high, moderate, low, very low, and no wildfire potential.

Model validation was then performed to assess the accuracy of the wildfire potential zones. The model was evaluated for accuracy through validation with the holdout data derived from the 2009 regional peak wildfire season MODIS MCD14ML wildfire event location data set (Kohavi, 1995; Molinaro, Simon, & Pfeiffer, 2005; Refaeilzadeh, Tang, & Liu, 2009; Burt et al., 2009). Accuracy of the model was determined through a Chi-

square goodness of fit test and correlation of the wildfire potential zones with the locations of wildfire events from the holdout data set (Jaiswal et al., 2002). A significant Chi-square and correlation of the wildfire potential zones with the locations of wildfire events from the holdout data set was indicative of the reliability of the modeling technique and the accuracy of the wildfire potential zones (Jaiswal et al., 2002).

Results

During the 2009 peak wildfire season, MODIS data indicated that the Western Hindu Kush-Himalayas experienced a total of 1,943 wildfire events. Of the total number of wildfire events that were detected in the region, 1,620 events were detected in the Western Hindu Kush-Himalayas of India. This represented 83.4% of the region's total detected wildfire events. Uttarakhand State experienced the greatest number of wildfire events detected in the Western Hindu Kush-Himalayas, with a total of 1,340. Uttarakhand State alone accounted for 68.9% of all wildfire event activity detected in the region. In Himachal Pradesh State, a total of 224 wildfire events were detected, and Jammu and Kashmir State experienced a modest total of 56 wildfire events.

In the Western Hindu Kush-Himalayas of Pakistan, a total of 306 wildfire events were detected during the 2009 peak wildfire season, accounting for 15.7% of the region's wildfire event activity. The majority of wildfire events detected in Pakistan occurred in the North-West Frontier Province, where a total of 262 wildfire events were detected.

Baluchistan Province experienced a total of 24 wildfire events, and 13 events were detected in the Federally Administered Tribal Areas Territory. A small number of wildfire events were also detected in Azad Kashmir Province, where a total of seven events occurred.

Afghanistan experienced the least amount of wildfire activity during the 2009 peak wildfire season. In the Western Hindu Kush-Himalayas of Afghanistan, a total of only 17 wildfire events were detected, which accounted for just 0.9% of the region's total wildfire activity during the 2009 peak wildfire season. The greatest number of wildfire events that occurred in Afghanistan were identified in Balkh Province, where a total of seven events were detected. In Kunduz Province a total of four wildfire events were detected, and Takhar Province experienced three wildfire events. The provinces of Badakhshan, Nangarhar, and Samangan each experienced only one wildfire event during the 2009 peak wildfire season. Total wildfire events by Western Hindu Kush-Himalayan nation are indicated in Figure 11.

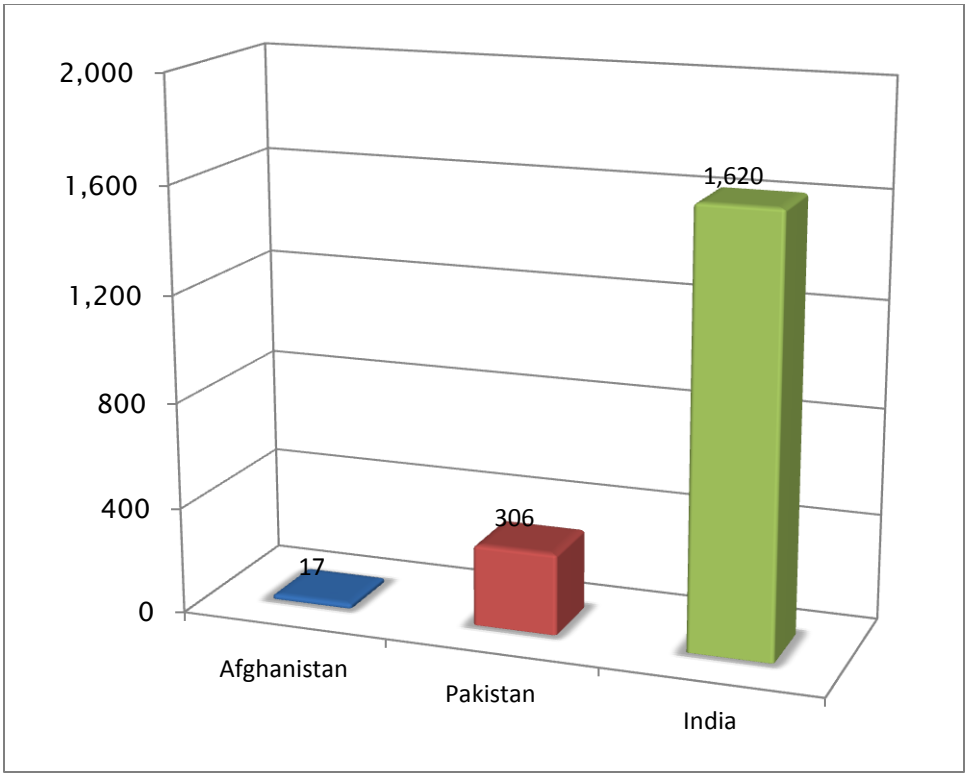

Figure 11: Regional Wildfire Events by Country

During the 2009 peak wildfire season, wildfires in the Western Hindu Kush-Himalayas burned with low intensity and produced generally very low levels of fire radiative power. Mean wildfire event temperature was 301.9 °K, with a median of 301.8 °K, and a mode of 296.2 °K. Fire radiative power generated by wildfire events in the Western Hindu Kush-Himalayas had a mean value of 25.5 Mw, a median of 18.1 Mw, and a mode of 11.7 Mw. In Table 6 a summary of the dependent variable

classes are shown.

Table 6: Dependent Variable Classes

Dependent Variable		1	2	3	4	5
Latitude	Class	Low	Mid	Upper		
	Values	25.478 – 29.815°	29.815 – 34.152°	34.152 – 38.489°		
Longitude	Class	West	Central	East		
	Values	60.854 – 67.579°	67.579 – 74.303°	74.303 – 81.028°		
Temperature	Class	Very Low	Low	Moderate	High	Very High
	Values	250 – 280 K	280 – 310 K	310 – 340 K	340 – 370 K	370 – 400 K
Fire Radiative Power	Class	Very Low	Low	Moderate	High	Very High
	Values	0 – 100 MW	100 – 200 MW	200 – 300 MW	300 – 400 MW	400 – 500 MW

Low to very low vegetation health in the Western Hindu Kush-Himalayas was found to be highly conducive to regional wildfire activity. Wildfire events in the Western Hindu Kush-Himalayas had a mean EVI of .241, a median of .240, and a mode of .12. This was consistent with the behavior that is expected from wildfires, where low-health vegetation is more likely to burn than healthy vegetation. A summary of the independent variable classes are shown in Table 7.

Table 7: Independent Variable Classes

Independent Variable		1	2	3	4	5
Vegetation Health	Class	Very Low Health	Low Health	Moderate Health	Healthy	Very Healthy
	Values	0 – .2 EVI	.2 – .4 EVI	.4 – .6 EVI	.6 – .8 EVI	.8 – 1 EVI
Slope	Class	Very Gentle	Gentle	Moderate	Steep	Very Steep
	Values	0 –5°	5 – 15°	15 – 30°	30 – 50°	50 – 75°
Elevation	Class	Very Low	Low	Moderate	High	Very High
	Values	0 – 800 m	800 – 1,600 m	1,600 – 2,400 m	2,400 – 3,200 m	3,200 – 4,000 m
Road Distance	Class	Very Close	Close	Moderate	Far	Very Far
	Values	0 – 2,500 m	2,500 – 5,000 m	5,000 – 10,000 m	10,000 – 20,000 m	20,000 – 40,000 m
Water Distance	Class	Very Close	Close	Moderate	Far	Very Far
	Values	0 – 2,500 m	2,500 – 5,000 m	5,000 – 10,000 m	10,000 – 20,000 m	20,000 – 40,000 m
Settlement Distance	Class	Very Close	Close	Moderate	Far	Very Far
	Values	0 – 3,500 m	3,500 – 7,000 m	7,000 – 14,000 m	14,000 – 28,000 m	28,000 – 56,000 m

Topographic factors had a significant influence on the location of wildfire event activity in the Western Hindu Kush-Himalayas. In the region, wildfire events occurred on gentle slopes with a mean of 7.2°, a median of 6.87°, and a mode of 5.43°. Wildfire events occurred predominantly on east to southeast facing slopes with a mean aspect of 173.425°, a median of 175.779°, and a mode of 137.931°. The aspect classes are summarized in Table 8. In the low to very low elevations of the Western Hindu Kush-Himalayas wildfire event activity was greatest. Mean elevation for wildfire occurrence in the region was 1,186 m, with a median of 1,225 m, and a mode of 180 m.

Table 8: Aspect Classes

Aspect	Class	Values
1	Flat	-0.000001 - 0°
2	North	0 - 67.5°
3	northeast	67.5 - 112.5°
4	East	112.5 - 157.5°
5	southeast	157.5 - 202.5°
6	South	202.5 - 247.5°
7	southwest	247.5 - 292.5°
8	West	292.5 - 337.5°
9	northwest	337.5 - 360°

The majority of wildfire events in the Western Hindu Kush-Himalayas occurred at distances close or very close to regional road features. Mean distance to road features was 4,966.01 m, with a median of 3,757.23 m, and a mode of less than 1 m. Wildfire events in the region also occurred close or very close to regional water features. Distance to water features had a mean of 3,469 m, a median of 2,515.33 m, and a mode of less than 1 m. Regional wildfire events occurred predominantly at distances far from the settlements of the Western Hindu Kush-Himalayas. Mean distance to settlements was 15,190.95 m, with a median of 14,138.7 m, and a mode of 4,017.74 m.

Of the 1,943 total wildfire events detected in the Western Hindu Kush-Himalayas during the 2009 peak wildfire season, 11 were very low temperature events, 1,636 were low temperature events, and 296 were of moderate temperature (Figure 12). An overwhelming majority of wildfire events in the region generated very low levels of fire radiative power (Figure 13). A total of 1,906 very low fire radiative power wildfire events were detected along with 32 low power events, two moderate power

events, two high power events, and one very high power event.

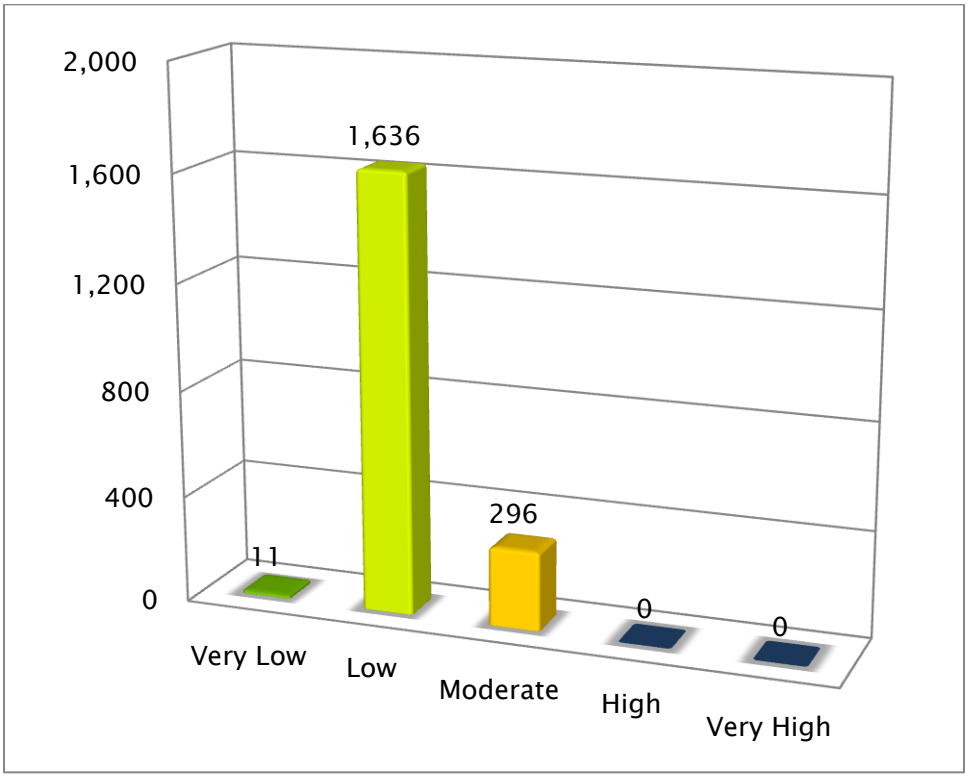

Figure 12: Wildfire Events by Temperature

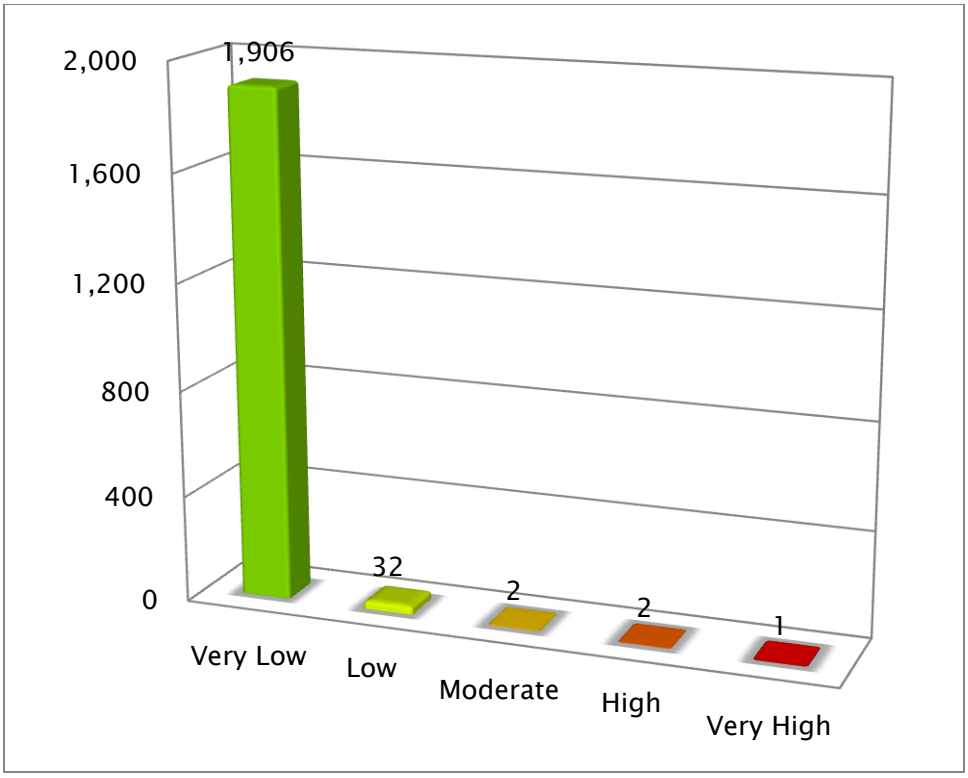

Figure 13: Wildfire Events by Fire Radiative Power

Wildfire events in the Western Hindu Kush-Himalayas occurred predominately in the region's mixed forests, where 677 events were detected (Figure 14). There were 529 wildfire events detected in the woody savannas of the Western Hindu Kush-Himalayas, and 338 in the region's croplands. Cropland and natural vegetation mosaics accounted for 239 of the Western Hindu Kush-Himalayas wildfire events, 59 were detected in open shrublands, and 47 in closed shrublands. Evergreen

needleleaf forests were home to 27 wildfire events, 20 occurred in grasslands, five in deciduous broadleaf forests, and two in evergreen broadleaf forests.

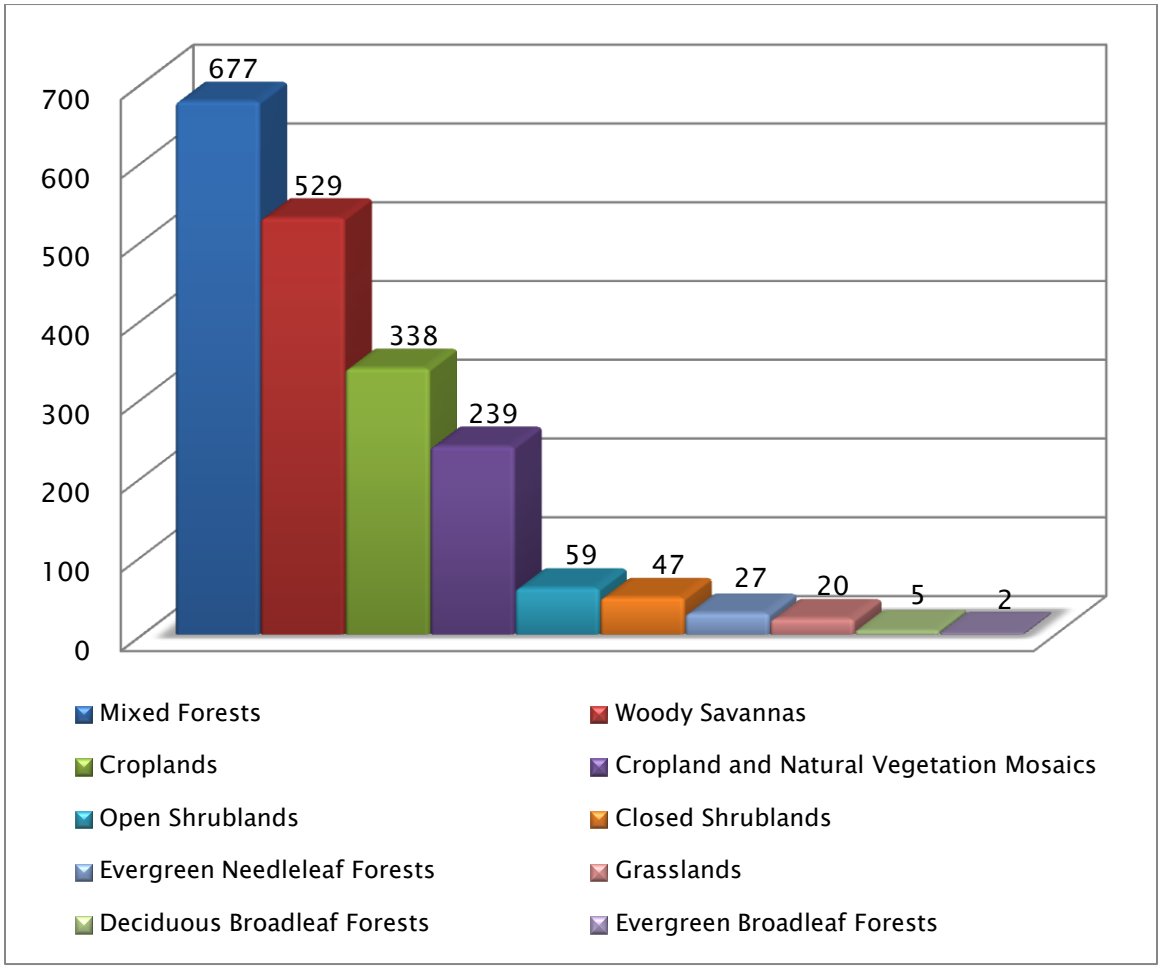

Figure 14: Wildfire Events by Land Cover Type

Very low health vegetation in the Western Hindu Kush-Himalayas experienced a total of 257 wildfire events during the 2009 peak wildfire

season. The majority of wildfire events were located in the region's low health vegetation, where 1,685 wildfire events were detected (Figure 15). In the Western Hindu Kush-Himalayas moderate health vegetation, only one wildfire event was detected.

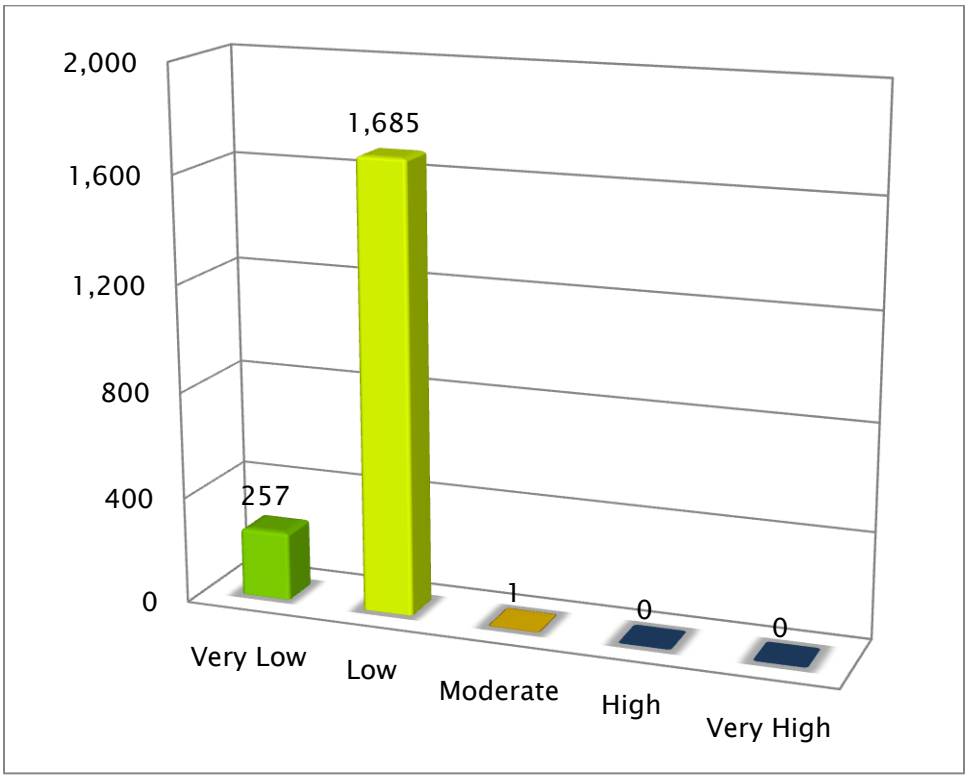

Figure 15: Wildfire Events by Vegetation Health

In the Western Hindu Kush-Himalayas, topographic factors had a considerable impact on the location and intensity of wildfires. A total of 745 wildfire events occurred on very gentle slopes, 1,018 wildfire events

occurred on gentle slopes, and 180 events were detected on moderate slopes (Figure 16). Figure 17 shows the distribution of wildfire events by aspect. Most wildfire events in the Western Hindu Kush-Himalayas occurred on South facing slopes. There were 559 wildfire events detected on South facing slopes, 320 were detected on southwest slopes, 157 were detected on West facing slopes, and 127 occurred on northwest slopes. On North facing slopes only 46 wildfire events were detected, 140 events were detected on northeast slopes, 236 occurred on East facing slopes, and 358 were detected on southeast slopes.

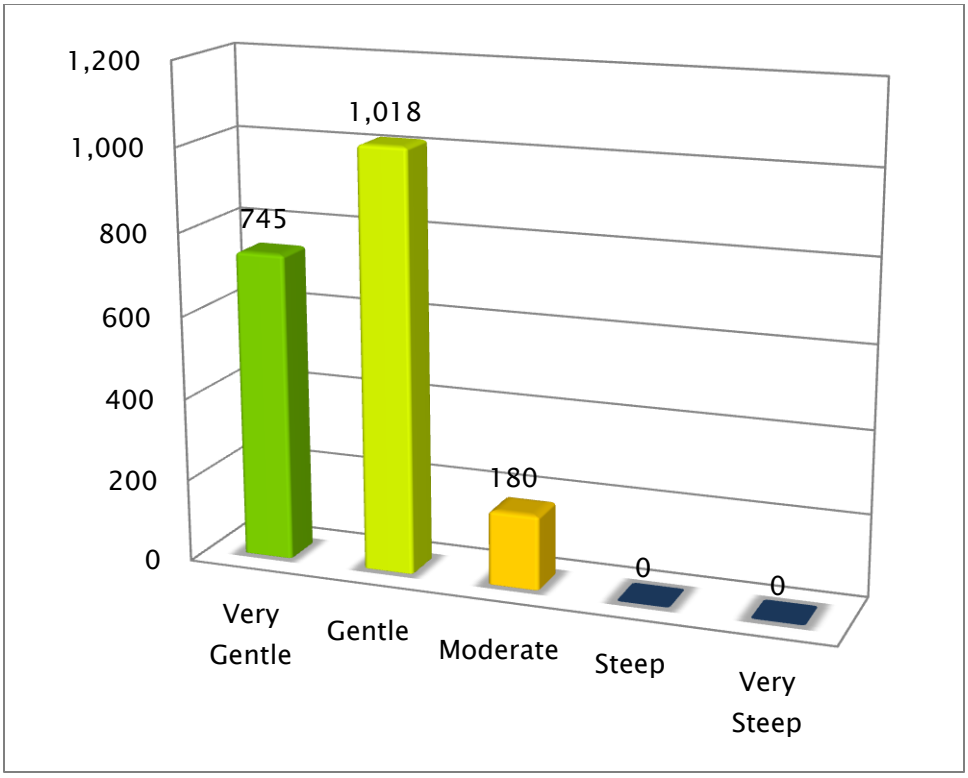

Figure 16: Wildfire Events by Slope

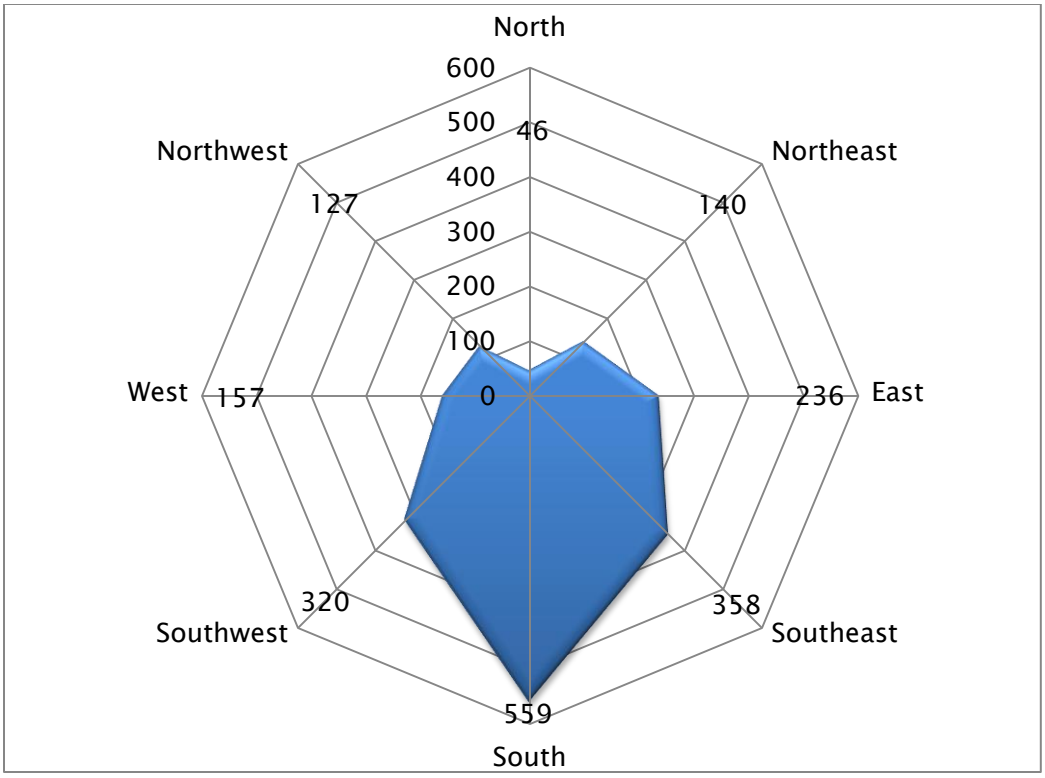

Figure 17: Wildfire Events by Aspect

Wildfire events in the Western Hindu Kush-Himalayas occurred predominantly in the region's lower elevations. In the very low elevations 687 wildfire events were detected, at low elevations 604 wildfire events were detected, and 566 were detected at moderate elevations. Wildfire events in the Western Hindu Kush-Himalaya's upper elevations were considerably less numerous. A total of 80 wildfire events were detected in the region's high elevations, and six wildfire events were detected at

very high elevation. The distribution of wildfire events by elevation is shown in Figure 18.

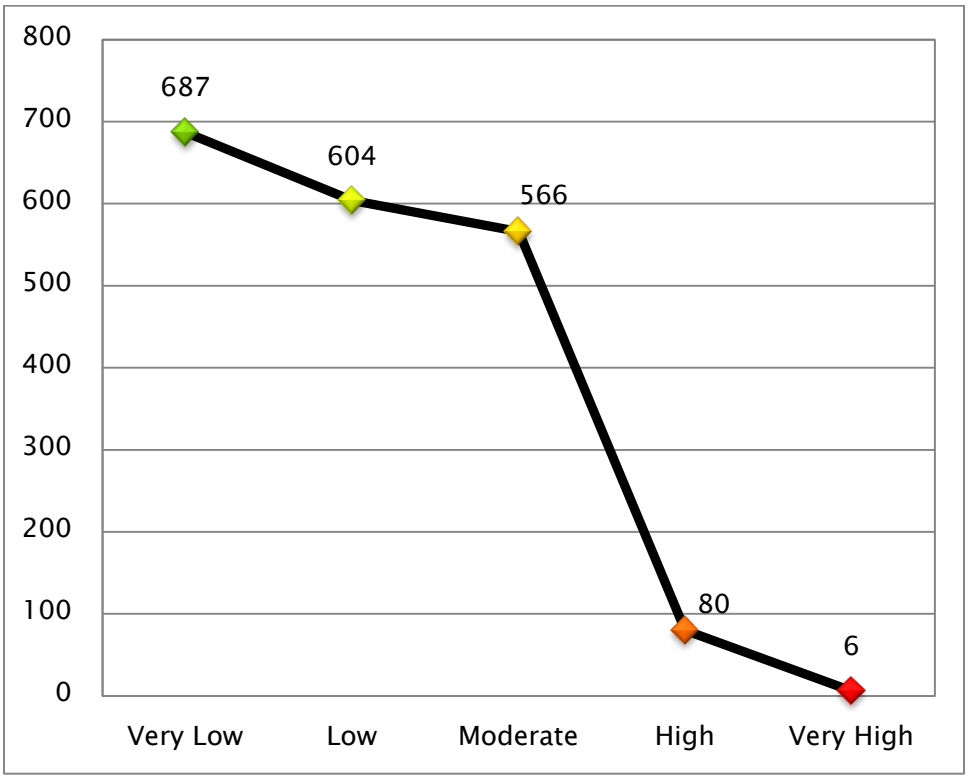

Figure 18: Wildfire Events by Elevation

The Western Hindu Kush-Himalayas experienced a significant number of wildfire events very close to regional road features during the 2009 peak wildfire season. Very close to road features a total of 658 wildfire events were detected, 548 were detected close to road features, and 487 occurred at moderate distances to road features. At distances

far from road features 233 wildfire events were detected in the region and 17 events were detected at distances very far from road features. Figure 19 shows the distribution of wildfire events by distance to road features.

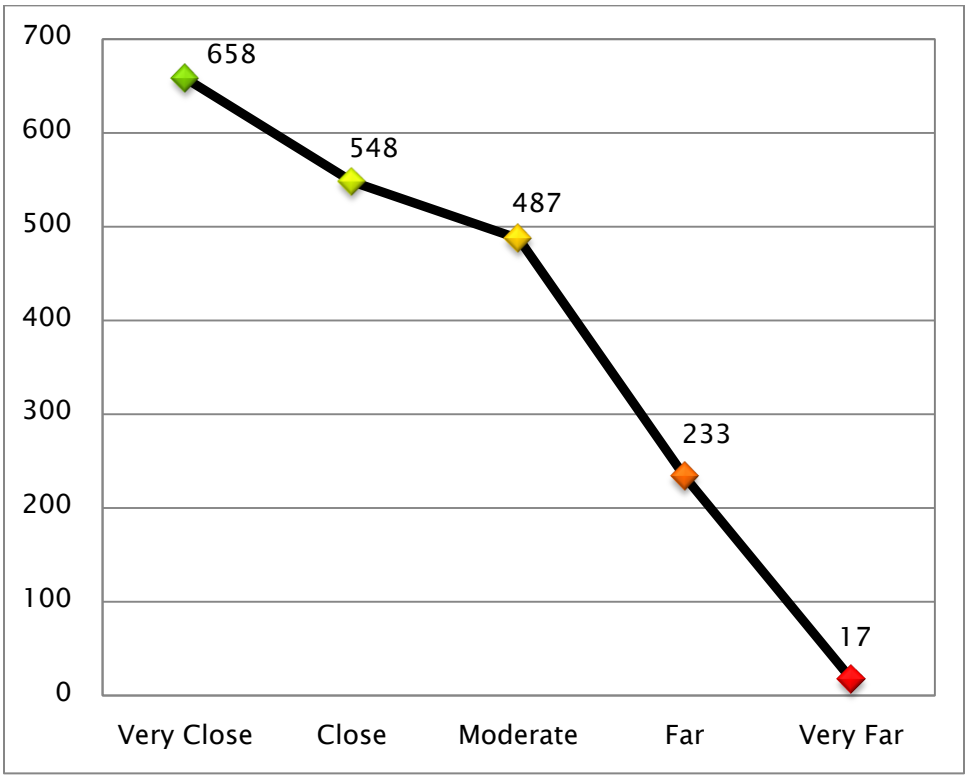

Figure 19: Wildfire Events by Distance to Road Features

The majority of wildfire events in the Western Hindu Kush-Himalayas were detected very close to water features, where 968 wildfire events were detected. At distances close to water features 566 wildfire

events were detected, and 298 events were detected at moderate distances to water features. Far from water features 95 wildfire events were detected, and at distances very far from water features 16 events were detected. In Figure 20, the distribution of wildfire events by distance to water features in shown.

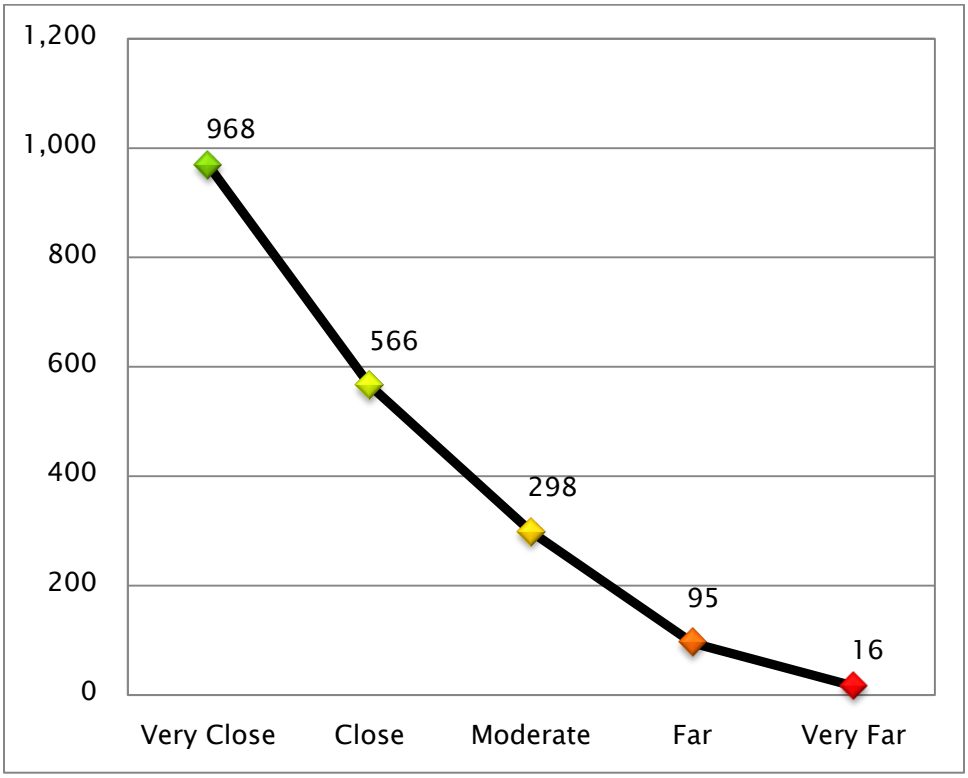

Figure 20: Wildfire Events by Distance to Water Features

Most wildfire events detected in the Western Hindu Kush-Himalayas occurred at distances far from settlements. Only 43 wildfire events were

detected very close to settlements, 210 were detected close to settlements, and 707 were detected at moderate distances from settlements. Far from settlements a total of 854 wildfire events were detected, and 129 wildfire events were detected at distances very far from settlements. Figure 21 shows the distribution of wildfire events by distance to settlements.

Figure 21: Wildfire Events by Distance to Settlements

Chi-square tests of independence were performed to examine the degree of dependence between the study's independent and dependent variables. It was hypothesized that the study's dependent variables would be dependent on the independent variables. Results of the Chi-square tests of independence are summarized in Table 9.

Table 9: Chi-square Tests of Independence Results

		Latitude	Longitude	Temperature	Fire Radiative Power
Land Cover	X^2	127.452	561.048	26.372	15.783
	df	18	18	18	36
	Sig.	.000	.000	.092	.999
Vegetation Health	X^2	86.756	67.803	33.925	9.587
	df	4	4	4	8
	Sig.	.000	.000	.000	.295
Slope	X^2	45.328	224.224	30.092	5.434
	df	4	4	4	8
	Sig.	.000	.000	.000	.710
Aspect	X^2	53.823	150.958	35.583	14.830
	df	16	16	16	32
	Sig.	.000	.000	.003	.996
Elevation	X^2	97.847	177.94	94.982	20.803
	df	8	8	8	16
	Sig.	.000	.000	.000	.186
Road Distance	X^2	85.370	18.813	13.813	6.945
	df	8	8	8	16
	Sig.	.000	.016	.087	.974
Water Distance	X^2	223.723	605.054	25.868	11.189
	df	8	8	8	16
	Sig.	.000	.000	.001	.798
Settlement Distance	X^2	56.101	27.204	21.028	64.566
	df	8	8	8	16
	Sig.	.000	.001	.007	.000

Land cover type was compared to latitude and longitude, T31 temperature, and fire radiative power. The null hypothesis was that latitude and longitude, temperature, and fire radiative power of wildfire events in the Western Hindu Kush-Himalayas are independent of land cover type. The alternate hypothesis was that latitude and longitude, temperature, and fire radiative power of wildfire events in the Western Hindu Kush-Himalayas and land cover type are dependent. A significant interaction was found between latitude and longitude, and land cover type ($X^2(18) = 127.452$, $p < .05$, $X^2(18) = 561.048$, $p < .05$). The locations of wildfire events in the Western Hindu Kush-Himalayas are dependent on land cover type.

Vegetation health was then compared to latitude and longitude, T31 temperature, and fire radiative power of Western Hindu Kush-Himalayan wildfire events. The null hypothesis was that latitude and longitude, temperature, and fire radiative power of wildfire events in the Western Hindu Kush-Himalayas are independent of vegetation health. The alternate hypothesis was that latitude and longitude, temperature,

and fire radiative power of wildfire events in the Western Hindu Kush-Himalayas and vegetation health are dependent.

A significant interaction was found between latitude and longitude, and vegetation health ($X^2(4) = 86.756$, $p < .05$, $X^2(4) = 67.803$, $p < .05$). The locations of wildfire events in the Western Hindu Kush-Himalayas are dependent on vegetation health. A significant interaction between the temperatures of wildfire events and vegetation health was also found ($X^2(4) = 33.925$, $p < .05$). The temperatures of wildfire events in the Western Hindu Kush-Himalayas are dependent on vegetation health.

The topographic variables were compared to latitude and longitude, T31 temperature, and fire radiative power of Western Hindu Kush-Himalayan wildfire events. The null hypotheses were that latitude and longitude, temperature, and fire radiative power of wildfire events in the Western Hindu Kush-Himalayas are independent of slope, aspect, and elevation. The alternate hypotheses were that latitude and longitude, temperature, and fire radiative power of wildfire events in the Western Hindu Kush-Himalayas are dependent on slope, aspect, and elevation.

Significant interactions were found between latitude and longitude and slope ($X^2(4) = 45.328$, $p < .05$, $X^2(4) = 224.224$, $p < .05$), aspect ($X^2(16) = 53.823$, $p < .05$, $X^2(16) = 150.958$, $p < .05$), and elevation ($X^2(8) = 97.847$, $p < .05$, $X^2(8) = 177.940$, $p < .05$). The locations of wildfire events in the Western Hindu Kush-Himalayas are dependent on slope, aspect, and elevation.

A significant interaction was also found between wildfire event temperatures and slope ($X^2(4) = 30.092$, $p < .05$), aspect ($X^2(16) = 35.583$, $p < .05$,), and elevation ($X^2(8) = 94.982$, $p < .05$). The temperatures of wildfire events in the Western Hindu Kush-Himalayas are dependent on slope, aspect, and elevation.

The distance factors were then compared to the latitude and longitude, T31 temperature, and fire radiative power of wildfire events in the Western Hindu Kush-Himalayas. The null hypotheses were that latitude and longitude, temperature, and fire radiative power of wildfire events in the Western Hindu Kush-Himalayas are independent of distance to road features, distance to water features, and distance to settlements.

The alternate hypotheses were that latitude and longitude, temperature, and fire radiative power of wildfire events in the Western Hindu Kush-Himalayas are dependent on distance to road features, distance to water features, and distance to settlements.

Significant interactions were found between latitude and longitude and distance to road features ($X^2(8) = 85.370$, $p < .05$, $X^2(4) = 18.813$, $p < .05$), distance to water features ($X^2(8) = 223.723$, $p < .05$, $X^2(8) = 605.054$, $p < .05$), and distance to settlements ($X^2(8) = 56.101$, $p < .05$, $X^2(8) = 27.204$, $p < .05$). The locations of wildfire events in the Western Hindu Kush-Himalayas are dependent on distances to road features, water features, and settlements.

A significant interaction was found between wildfire event temperatures and distance to water features ($X^2(8) = 25.968$, $p < .05$) as well as distance to settlements ($X^2(8) = 21.028$, $p < .05$). Temperatures of wildfire events in the Western Hindu Kush-Himalayas are dependent on distance to water features and distance to settlements. The interaction between wildfire event fire radiative power and distance to settlements

was also significant ($X^2(16) = 64.566$, $p < .05$). The fire radiative power of wildfire events in the Western Hindu Kush-Himalayas are dependent on distance to settlements.

Spearman's rho correlations were performed to determine the strength of the relationship between the study's independent and dependent variables. Correlations were calculated to compare land cover type and latitude and longitude, T31 temperature, and fire radiative power. The null hypotheses were that no association exists between land cover type and the latitude and longitude, temperature, and fire radiative power of wildfire events in the Western Hindu Kush-Himalayas. The alternate hypotheses were that associations exist between land cover type and the latitude and longitude, temperature, and fire radiative power of wildfire events in the Western Hindu Kush-Himalayas. The Spearman's rho correlation results are summarized in Table 10.

Table 10: Spearman's Rho Correlation Results

		Latitude	Longitude	Temperature	Fire Radiative Power
Land Cover	rho	.296	-.314	.031	-.010
	df	1072	1072	1072	1072
	Sig.	.000	.000	.303	.744
Vegetation Health	rho	-.389	.297	.080	-.132
	df	1072	1072	1072	1072
	Sig.	.000	.000	.009	.000
Slope	rho	-.096	.360	-.065	.072
	df	1072	1072	1072	1072
	Sig.	.002	.000	.033	.018
Aspect	rho	-.173	.177	.172	.014
	df	1072	1072	1072	1072
	Sig.	.000	.000	.000	.658
Elevation	rho	-.015	.303	-.166	.098
	df	1072	1072	1072	1072
	Sig.	.634	.000	.000	.001
Road Distance	rho	.130	-.074	-.032	.028
	df	1072	1072	1072	1072
	Sig.	.000	.015	.268	.352
Water Distance	rho	.146	-.303	-.095	-.062
	df	1072	1072	1072	1072
	Sig.	.000	.000	.002	.041
Settlement Distance	rho	-.036	.052	.004	.061
	df	1072	1072	1072	1072
	Sig.	.218	.091	.889	.047

A weak positive correlation was found between land cover type and latitude ($rho(1072) = .296$, $p < .05$), and a moderate negative correlation was found between land cover type and longitude ($rho(1072) = -.314$, $p < .05$). Wildfire event locations alter along with change in land cover type in the Western Hindu Kush-Himalayas.

The relationship between vegetation health and latitude and longitude, T31 temperature, and fire radiative power was then evaluated. The null hypotheses were that no association exists between vegetation health and the latitude and longitude, temperature, and fire radiative power of wildfire events in the Western Hindu Kush-Himalayas. The alternate hypotheses were that associations exist between vegetation health and the latitude and longitude, temperature, and fire radiative power of wildfire events in the Western Hindu Kush-Himalayas.

A moderate negative correlation was found between vegetation health and latitude ($rho(1072) = -.389$, $p < .05$), and a weak positive correlation was found between vegetation health and longitude ($rho(1072) = .297$, $p < .05$). The locations of wildfire events in the Western Hindu Kush-Himalayas vary along with change in vegetation health.

A weak positive correlation was found between vegetation health and wildfire event temperatures ($rho(1072) = .080$, $p < .05$). The greater vegetation health, the higher wildfire event temperatures in the Western

Hindu Kush-Himalayas tends to be. The correlation between vegetation health and wildfire event fire radiative power produced a weak negative correlation ($rho(1072) = -.132$, $p < .05$). As vegetation health decreases, the fire radiative power of wildfire events in the Western Hindu Kush-Himalayas tends to decline.

Correlations were calculated for the topographic variables and latitude and longitude, T31 temperature, and fire radiative power of wildfire events in the Western Hindu Kush-Himalayas. The null hypotheses were that no association exists between slope, aspect, and elevation and the latitude and longitude, temperature, and fire radiative power of wildfire events in the Western Hindu Kush-Himalayas. The alternate hypotheses were that associations exist between slope, aspect, and elevation and the latitude and longitude, temperature, and fire radiative power of wildfire events in the Western Hindu Kush-Himalayas.

A weak negative correlation was found between slope and latitude ($rho(1072) = -.096$, $p < .05$), and a moderate positive correlation was found between slope and longitude ($rho(1072) = .360$, $p < .05$). The

locations of wildfire events in the Western Hindu Kush-Himalayas vary along with change in slope. Additionally, a weak negative correlation was found between aspect and latitude ($rho(1072) = -.173$, $p < .05$), and a weak positive correlation was found between aspect and longitude ($rho(1072) = .177$, $p < .05$). The locations of wildfire events in the Western Hindu Kush-Himalayas vary along with change in aspect. A moderate positive correlation was also found between elevation and longitude ($rho(1072) = .303$, $p < .05$). The longitude of wildfire events in the Western Hindu Kush-Himalayas varies along with change in elevation.

A weak negative correlation was found between slope and wildfire event temperatures ($rho(1072) = -.065$, $p < .05$). Wildfire event temperatures tend to decrease along with slope. A weak positive correlation was found between aspect and wildfire event temperatures ($rho(1072) = .172$, $p < .05$). As aspect increases, wildfire event temperatures in the Western Hindu Kush-Himalayas tend to increase. The correlation between elevation and wildfire event temperatures produced a weak negative correlation ($rho(1072) = -.166$, $p < .05$). The

temperatures of wildfire events in the Western Hindu Kush-Himalayas tend to decline along with decreases in elevation.

A weak positive correlation was found between slope and wildfire event fire radiative power ($rho(1072) = -.065$, $p < .05$). As slope increases, the fire radiative power of wildfire events in the Western Hindu Kush-Himalayas tends to increase. A weak positive correlation was found between elevation and wildfire event fire radiative power ($rho(1072) = .098$, $p < .05$). The fire radiative power of wildfire events in the Western Hindu Kush-Himalayas tends to increase along with elevation.

Correlations were then calculated for the distance variables and latitude and longitude, T31 temperature, and fire radiative power of wildfire events in the Western Hindu Kush-Himalayas. The null hypotheses were that no association exists between distance to road features, distance to water features, and distance to settlements and the latitude and longitude, temperature, and fire radiative power of wildfire events in the Western Hindu Kush-Himalayas. The alternate hypotheses were that associations exist between distance to road features, distance

to water features, and distance to settlements and the latitude and longitude, temperature, and fire radiative power of wildfire events in the Western Hindu Kush-Himalayas.

A weak positive correlation was found between distance to road features and latitude ($rho(1072) = .130$, $p < .05$), and a weak negative correlation was found between distance to road features and longitude ($rho(1072) = -.074$, $p < .05$). The locations of wildfire events in the Western Hindu Kush-Himalayas vary along with change in distance to road features. A weak positive correlation was found between distance to water features and latitude ($rho(1072) = .146$, $p < .05$), and a moderate negative correlation was found between distance to water features and longitude ($rho(1072) = -.303$, $p < .05$). The locations of wildfire events in the Western Hindu Kush-Himalayas vary along with distance to water features.

A weak negative correlation was found between distance to water features and wildfire event temperatures ($rho(1072) = -.095$, $p < .05$). Wildfire event temperatures in the Western Hindu Kush-Himalayas tend to

decline as distance to water features decreases.

A weak negative correlation was found between distance to water features and wildfire event fire radiative power ($rho(1072) = -.062$, $p < .05$). As distance to water features decreases, the fire radiative power of wildfire events in the Western Hindu Kush-Himalayas tends to decrease. A weak positive correlation was found between distance to settlements and wildfire event fire radiative power ($rho(1072) = .061$, $p < .05$). The fire radiative power of wildfire events in the Western Hindu Kush-Himalayas tends to increase as distance to settlements increases.

A series of Kruskal-Wallis H tests were performed to determine whether the study's independent variables significantly differ based on the dependent variables. Kruskal-Wallis H tests were calculated to compare land cover type and latitude and longitude, T31 temperature, and fire radiative power. The null hypotheses were that latitude and longitude, temperature, and fire radiative power of wildfire events in the Western Hindu Kush-Himalayas do not differ with land cover type. The alternate hypotheses were that latitude and longitude, temperature, and

fire radiative power of wildfire events in the Western Hindu Kush-Himalayas significantly differ with land cover type. A summary of the Kruskal-Wallis H tests are shown in Table 11.

Table 11: Kruskal-Wallis Results

		Latitude	Longitude	Temperature	Fire Radiative Power
Land Cover	H	62.226	544.390	22.698	5.754
	df	9	9	9	9
	Sig.	.000	.000	.007	.764
Vegetation Health	H	25.517	43.979	5.701	3.146
	df	2	2	2	2
	Sig.	.000	.000	.058	.207
Slope	H	26.277	224.007	22.570	.829
	df	2	2	2	2
	Sig.	.000	.000	.000	.661
Aspect	H	40.403	134.958	27.615	6.313
	df	8	8	8	8
	Sig.	.000	.000	.001	.612
Elevation	H	73.664	177.675	68.874	11.587
	df	4	4	4	4
	Sig.	.000	.000	.000	.021
Road Distance	H	79.009	9.937	9.108	2.945
	df	4	4	4	4
	Sig.	.000	.041	.058	.567
Water Distance	H	34.153	259.231	7.221	6.136
	df	4	4	4	4
	Sig.	.000	.000	.125	.189
Settlement Distance	H	26.999	6.880	19.456	11.469
	df	4	4	4	4
	Sig.	.000	.142	.001	.022

The comparison of land cover type to the latitude and longitude of wildfire events in the Western Hindu Kush-Himalayas produced a

significant result ($H(9) = 62.226$, $p < .05$, $H(9) = 544.390$, $p < .05$). The locations of wildfire events in the Western Hindu Kush-Himalayas significantly differ with land cover type. Comparison of land cover type and wildfire event temperatures also produced a significant result ($H(9) = 22.698$, $p < .05$). The temperatures of wildfire events in the Western Hindu Kush-Himalayas significantly differ with land cover type.

Kruskal-Wallis H tests comparing vegetation health and the latitude and longitude, T31 temperature, and fire radiative power of wildfire events in the Western Hindu Kush-Himalayas were conducted. The null hypotheses were that latitude and longitude, temperature, and fire radiative power of wildfire events in the Western Hindu Kush-Himalayas do not differ with vegetation health. The alternate hypotheses were that latitude and longitude, temperature, and fire radiative power of wildfire events in the Western Hindu Kush-Himalayas significantly differ with vegetation health.

The comparison of vegetation health to the latitude and longitude of wildfire events in the Western Hindu Kush-Himalayas produced a

significant result ($H(2) = 25.517$, $p < .05$, $H(2) = 43.979$, $p < .05$). The locations of wildfire events in the Western Hindu Kush-Himalayas are significantly correlated with vegetation health.

Kruskal-Wallis H tests were calculated for the topographic variables and the latitude and longitude, T31 temperature, and fire radiative power of wildfire events in the Western Hindu Kush-Himalayas. The null hypotheses were that latitude and longitude, temperature, and fire radiative power of wildfire events in the Western Hindu Kush-Himalayas do not differ with slope, aspect, and elevation. The alternate hypotheses were that latitude and longitude, temperature, and fire radiative power of wildfire events in the Western Hindu Kush-Himalayas significantly differ with slope, aspect, and elevation.

Significant differences were found through comparison of wildfire event latitude and longitude, and slope ($H(2) = 26.277$, $p < .05$, $H(2) = 224.007$, $p < .05$), aspect ($H(8) = 40.403$, $p < .05$, $H(8) = 134.958$, $p < .05$), and elevation ($H(4) = 73.664$, $p < .05$, $H(4) = 177.675$, $p < .05$). The locations of wildfire events in the Western Hindu Kush-Himalayas

significantly differ with slope, aspect, and elevation.

Significant differences were found between wildfire event temperatures and slope ($H(2) = 22.570$, $p < .05$), aspect ($H(8) = 27.615$, $p < .05$), and elevation ($H(4) = 68.874$, $p < .05$). The temperatures of wildfire events in the Western Hindu Kush-Himalayas significantly differ with slope, aspect, and elevation. The comparison of elevation with the fire radiative power of wildfire events in the Western Hindu Kush-Himalayas also produced a significant result ($H(4) = 11.587$, $p < .05$). The fire radiative power of wildfire events in the Western Hindu Kush-Himalayas significantly differ with elevation.

Kruskal-Wallis H tests were then calculated for the distance variables and latitude and longitude, T31 temperature, and fire radiative power of wildfire events in the Western Hindu Kush-Himalayas. The null hypotheses were that latitude and longitude, temperature, and fire radiative power of wildfire events in the Western Hindu Kush-Himalayas do not differ with distance to road features, distance to water features, and distance to settlements. The alternate hypotheses were that latitude

and longitude, temperature, and fire radiative power of wildfire events in the Western Hindu Kush-Himalayas significantly differ with distance to road features, distance to water features, and distance to settlements.

Significant differences were found between wildfire event latitude and longitude and distance to road features ($H(4) = 79.009$, $p < .05$, $H(4) = 9.937$, $p < .05$), and distance to water features ($H(4) = 34.153$, $p < .05$, $H(4) = 259.231$, $p < .05$). The locations of wildfire events in the Western Hindu Kush-Himalayas significantly differ with distance to road features and distance to water features. Comparison of wildfire event latitude and distance to settlements also produced a significant difference ($H(4) = 26.999$, $p < .05$). The latitude of wildfire events in the Western Hindu Kush-Himalayas significantly differ with distance to road settlements.

The comparison of distance to settlements with wildfire event temperatures in the Western Hindu Kush-Himalayas produced a significant result ($H(4) = 19.456$, $p < .05$). The temperatures of wildfire events in the Western Hindu Kush-Himalayas significantly differ with

distance to settlements. Comparison of distance to settlements with wildfire event fire radiative power in the Western Hindu Kush-Himalayas also produced a significant result ($H(4) = 11.469$, $p < .05$). The fire radiative power of wildfire events in the Western Hindu Kush-Himalayas significantly correlate with distance to settlements.

Robust regressions were calculated to predict the latitude and longitude, T31 temperature, and fire radiative power of wildfire events in the Western Hindu Kush-Himalayas. Robust regression equations predicting latitude and longitude, T31 temperature, and fire radiative power based on land cover type, vegetation health, slope, aspect, elevation, distance to road features, distance to water features, and distance to settlements were evaluated. The null hypotheses were that land cover type, vegetation health, slope, aspect, elevation, distance to road features, distance to water features, and distance to settlements do not explain any of the variation in the latitude and longitude, temperature, and fire radiative power of wildfire events in the Western Hindu Kush-Himalayas. The alternate hypotheses were that land cover

type, vegetation health, slope, aspect, elevation, distance to road features, distance to water features, and distance to settlements explain variation in the latitude and longitude, temperature, and fire radiative power of wildfire events in the Western Hindu Kush-Himalayas.

A significant robust regression equation was found comparing land cover type, vegetation health, slope, aspect, elevation, distance to road features, distance to water features, and distance to settlements with wildfire event latitude ($F(1,8) = 84.049$, $p < .05$), with a coefficient of determination of 43.2% ($R^2 = .432$). A significant robust regression equation was also found comparing land cover type, vegetation health, slope, aspect, elevation, distance to road features, distance to water features, and distance to settlements with wildfire event longitude ($F(1,8) = 16.345$, $p < .05$), with a coefficient of determination of 18.3% ($R^2 = .183$).

The mean latitude of wildfire events in the Western Hindu Kush Himalayas is equal to 31.65 + .03 (land cover) – 8.34 (vegetation health) + .00007 (slope) – .001 (aspect) + .00021 (elevation) + .00002 (road

distance) + .00009 (water distance) – .000007 (settlement distance) degrees when land cover type is measured by class, vegetation health in EVI, slope and aspect in degrees, and elevation, road distance, water distance, and settlement distance in meters.

Mean latitude of wildfire events in the Western Hindu Kush-Himalayas increases .03° for each land cover class, decreases 8.34° for each EVI of vegetation health, increases .00007° for each degree of slope, decreases .001° for each degree of aspect, increases .00021° for each meter of elevation, increases .00002° for each meter of road distance, increases .00009° for each meter of water distance, and decreases .000007° for each meter of settlement distance. Land cover type, vegetation health, aspect, elevation, distance to road features, distance to water features, and distance to settlements were significant predictors of wildfire event latitude. Slope was not a significant predictor of wildfire event latitude.

The mean longitude of wildfire events in the Western Hindu Kush Himalayas is equal to 76.67 – .02 (land cover) + 8.88 (vegetation health)

+ .02 (slope) + .00097 (aspect) + .00001 (elevation) – .00003 (road distance) – .00008 (water distance) + .000007 (settlement distance) degrees when land cover type is measured by class, vegetation health in EVI, slope and aspect in degrees, and elevation, road distance, water distance, and settlement distance in meters.

Mean longitude of wildfire events in the Western Hindu Kush-Himalayas decreases .02° for each land cover class, increases 8.88° for each EVI of vegetation health, increases .02° for each degree of slope, increases .00097° for each degree of aspect, increases .00001° for each meter of elevation, decreases .00003° for each meter of road distance, decreases .00008° for each meter of water distance, and increases .000007° for each meter of settlement distance. Land cover type, vegetation health, slope, aspect, distance to road features, distance to water features, and distance to settlements were significant predictors of wildfire event longitude. Elevation was not a significant predictor of wildfire event longitude.

A regression relative contribution analysis was calculated examining the effect of land cover type, vegetation health, slope, aspect, elevation, distance to road features, distance to water features, and distance to settlements on the latitude and longitude of wildfire events. The contribution to variation in latitude in descending order was land cover (lmg = .393), vegetation health (lmg = .387), distance to water features (lmg = .126), slope (lmg = .036), aspect (lmg = .025), distance to road features (lmg = .016), elevation (lmg = .015), and distance to settlements (lmg = .003). Contribution to variation in longitude in descending order was land cover (lmg = .423), distance to water features (lmg = .174), slope (lmg = .124), vegetation health (lmg = .117), elevation (lmg = .112), aspect (lmg = .038), distance to road features (lmg = .007), and distance to settlements (lmg = .004).

A significant robust regression equation was also found when comparing land cover type, vegetation health, slope, aspect, elevation, distance to road features, distance to water features, and distance to settlements with wildfire event temperature ($F(1,8) = 16.319$, $p < .05$),

with a coefficient of determination of 11.5% (R^2 = .115). The mean temperature of wildfire events in the Western Hindu Kush Himalayas is equal to 297.37 + .03 (land cover) + 17.71 (vegetation health) + .12 (slope) + .01 (aspect) – .003 (elevation) + .00002 (road distance) – .0003 (water distance) + .00006 (settlement distance) °C when land cover type is measured by class, vegetation health in EVI, slope and aspect in degrees, and elevation, road distance, water distance, and settlement distance in meters.

Mean temperature of wildfire events in the Western Hindu Kush-Himalayas increases .03 °C for each land cover class, increases 17.71 °C for each EVI of vegetation health, increases .12 °C for each degree of slope, increases .01 °C for each degree of aspect, decreases .003 °C for each meter of elevation, increases .00002 °C for each meter of road distance, decreases .0003 °C for each meter of water distance, and increases .00006 °C for each meter of settlement distance. Vegetation health, aspect, elevation, and distance to water features were significant predictors of wildfire event temperature. Land cover type, slope, distance

to road features, and distance to settlements were not significant predictors of wildfire event temperature.

A regression relative contribution analysis was calculated examining the effect of land cover type, vegetation health, slope, aspect, elevation, distance to road features, distance to water features, and distance to settlements on the temperature of wildfire events. The contribution to variation in temperature in descending order was elevation (lmg = .319), land cover type (lmg = .263), vegetation health (lmg = .114), distance to water features (lmg = .099), aspect (lmg = .096), slope (lmg = .077), distance to settlements (lmg = .016), and distance to road features (lmg = .015).

A significant robust regression equation was not found when comparing land cover type, vegetation health, slope, aspect, elevation, distance to road features, distance to water features, and distance to settlements with wildfire event fire radiative power ($F(1,8) = 2.191$, $p > .05$), with a coefficient of determination of .7% ($R^2 = .007$). Land cover type, vegetation health, slope, aspect, elevation, distance to road

features, distance to water features, and distance to settlements cannot be used to predict the fire radiative power of wildfire events in the Western Hindu Kush-Himalayas.

Generalized linear modeling with a robust estimator was performed to model latitude and longitude, T31 temperature, and fire radiative power of wildfire events in the Western Hindu Kush-Himalayas based on individual land cover types. Generalized linear models of wildfire event latitude and longitude, temperature, and fire radiative power based on the presence of evergreen needleleaf forests, evergreen broadleaf forests, deciduous broadleaf forests, mixed forests, closed shrublands, open shrublands, woody savannas, grasslands, croplands, and cropland and natural vegetation mosaics were calculated.

The null hypotheses were that the presence of evergreen needleleaf forests, evergreen broadleaf forests, deciduous broadleaf forests, mixed forests, closed shrublands, open shrublands, woody savannas, grasslands, croplands, and cropland and natural vegetation mosaics do not explain any of the variation in the latitude and longitude,

temperature, and fire radiative power of wildfire events in the Western Hindu Kush-Himalayas. The alternate hypotheses were that the presence of evergreen needleleaf forests, evergreen broadleaf forests, deciduous broadleaf forests, mixed forests, closed shrublands, open shrublands, woody savannas, grasslands, croplands, and cropland and natural vegetation mosaics explain variation in the latitude and longitude, temperature, and fire radiative power of wildfire events in the Western Hindu Kush-Himalayas.

Significant robust generalized linear models were found when comparing evergreen needleleaf forests, evergreen broadleaf forests, deciduous broadleaf forests, mixed forests, closed shrublands, open shrublands, woody savannas, grasslands, croplands, and cropland and natural vegetation mosaics with wildfire event latitude ($F(1,9) = 35.521$, $p < .05$), with a coefficient of determination of 22.5% ($R^2 = .225$), and longitude ($F(1,9) = 119.469$, $p < .05$), with a coefficient of determination of 49.8% ($R^2 = .498$).

The mean latitude of wildfire events in the Western Hindu Kush Himalayas is equal to 30.67 – .25 (evergreen needleleaf forests) – 1.71 (evergreen broadleaf forests) – 1.55 (deciduous broadleaf forests) – .61 (mixed forests) + 1.08 (closed shrublands) + .67 (open shrublands) – .34 (woody savannas) + 2.93 (grasslands) + .64 (croplands) + .64 (cropland and natural vegetation mosaics) degrees when evergreen needleleaf forests, evergreen broadleaf forests, deciduous broadleaf forests, mixed forests, closed shrublands, open shrublands, woody savannas, grasslands, croplands, and cropland and natural vegetation mosaics are measured on a per pixel basis.

The mean longitude of wildfire events in the Western Hindu Kush Himalayas is equal to 77.66 + 1.30 (evergreen needleleaf forests) + 2.35 (evergreen broadleaf forests) + 1.87 (deciduous broadleaf forests) + 1.23 (mixed forests) – 2.67 (closed shrublands) – 6.55 (open shrublands) + .93 (woody savannas) – 4.31 (grasslands) – 4.04 (croplands) – 4.04 (cropland and natural vegetation mosaics) degrees when evergreen needleleaf forests, evergreen broadleaf forests, deciduous broadleaf

forests, mixed forests, closed shrublands, open shrublands, woody savannas, grasslands, croplands, and cropland and natural vegetation mosaics are measured on a per pixel basis.

Mean latitude of wildfire events in the Western Hindu Kush-Himalayas decreases .25° for evergreen needleleaf forests, decreases 1.71° for evergreen broadleaf forests, decreases 1.55° for deciduous broadleaf forests, decreases .61° for mixed forests, increases 1.08° for closed shrublands, increases .67° for open shrublands, decreases .34° for woody savannas, increases 2.93° for grasslands, increases .64° for croplands, and increases .64° for cropland and natural vegetation mosaics. Evergreen needleleaf forests, deciduous broadleaf forests, mixed forests, closed shrublands, open shrublands, woody savannas, grasslands, croplands, and cropland and natural vegetation mosaics were significant predictors of wildfire event temperature. Evergreen broadleaf forests were not significant predictors of wildfire event temperature.

Mean longitude of wildfire events in the Western Hindu Kush-Himalayas increases 1.30° for evergreen needleleaf forests, increases

2.35° for evergreen broadleaf forests, increases 1.87° for deciduous broadleaf forests, increases 1.23° for mixed forests, decreases 2.67° for closed shrublands, decreases 6.53° for open shrublands, increases .93° for woody savannas, decreases 4.31° for grasslands, decreases 4.03° for croplands, and decreases 4.04° for cropland and natural vegetation mosaics. Evergreen needleleaf forests, deciduous broadleaf forests, mixed forests, closed shrublands, open shrublands, woody savannas, grasslands, croplands, and cropland and natural vegetation mosaics were significant predictors of wildfire event temperature. Evergreen broadleaf forests were not significant predictors of wildfire event temperature.

Partial eta-squared (η^2) was calculated to determine the effect of evergreen needleleaf forests, evergreen broadleaf forests, deciduous broadleaf forests, mixed forests, closed shrublands, open shrublands, woody savannas, grasslands, croplands, and cropland and natural vegetation mosaics on the latitude and longitude of wildfire events. The contribution to variation in latitude was grasslands ($\eta^2 = .057$), mixed forests ($\eta^2 = .028$), croplands ($\eta^2 = .025$), cropland and natural

vegetation mosaics ($\eta^2 = .025$), closed shrublands ($\eta^2 = .022$), woody savannas ($\eta^2 = .009$), open shrublands ($\eta^2 = .008$), evergreen broadleaf forests ($\eta^2 = .005$), deciduous broadleaf forests ($\eta^2 = .002$), and evergreen needleleaf forests ($\eta^2 = .0007$).

Contribution to variation in longitude was croplands ($\eta^2 = .189$), cropland and natural vegetation mosaics ($\eta^2 = .189$), open shrublands ($\eta^2 = .146$), closed shrublands ($\eta^2 = .030$), grasslands ($\eta^2 = .029$), mixed forests ($\eta^2 = .027$), woody savannas ($\eta^2 = .015$), evergreen needleleaf forests ($\eta^2 = .004$), evergreen broadleaf forests ($\eta^2 = .002$), and deciduous broadleaf forests ($\eta^2 = .0006$).

A significant robust generalized linear model was found when comparing evergreen needleleaf forests, evergreen broadleaf forests, deciduous broadleaf forests, mixed forests, closed shrublands, open shrublands, woody savannas, grasslands, croplands, and cropland and natural vegetation mosaics with wildfire event temperature ($F(1,9) = 5.062$, $p < .05$), with a coefficient of determination of 3.3% ($R^2 = .033$).

The mean temperature of wildfire events in the Western Hindu Kush Himalayas is equal to 304.91 – 7.33 (evergreen needleleaf forests) – .56 (evergreen broadleaf forests) – 2.81 (deciduous broadleaf forests) – 2.88 (mixed forests) – 5.78 (closed shrublands) – 5.79 (open shrublands) – 2.69 (woody savannas) – 9.91 (grasslands) – 4.11 (croplands) – 4.11 (cropland and natural vegetation mosaics) °C when evergreen needleleaf forests, evergreen broadleaf forests, deciduous broadleaf forests, mixed forests, closed shrublands, open shrublands, woody savannas, grasslands, croplands, and cropland and natural vegetation mosaics are measured on a per pixel basis.

Mean temperature of wildfire events in the Western Hindu Kush-Himalayas decreases 7.33 °C in evergreen needleleaf forests, decreases .56 °C in evergreen broadleaf forests, decreases 2.81 °C in deciduous broadleaf forests, decreases 2.88 °C in mixed forests, decreases 5.78 °C in closed shrublands, decreases 5.79 °C in open shrublands, decreases 2.69 °C in woody savannas, decreases 9.91 °C in grasslands, decreases 4.11 °C in croplands, and decreases 4.11 °C in cropland and natural

vegetation mosaics. Evergreen needleleaf forests, deciduous broadleaf forests, mixed forests, closed shrublands, open shrublands, woody savannas, grasslands, croplands, and cropland and natural vegetation mosaics were significant predictors of wildfire event temperature. Evergreen broadleaf forests were not significant predictors of wildfire event temperature.

Partial eta-squared (η^2) was calculated to determine the effect of evergreen needleleaf forests, evergreen broadleaf forests, deciduous broadleaf forests, mixed forests, closed shrublands, open shrublands, woody savannas, grasslands, croplands, and cropland and natural vegetation mosaics on the temperature of wildfire events. The contribution to variation in temperature was croplands ($\eta^2 = .021$), cropland and natural vegetation mosaics ($\eta^2 = .021$), grasslands ($\eta^2 = .014$), mixed forests ($\eta^2 = .013$), closed shrublands ($\eta^2 = .013$), evergreen needleleaf forests ($\eta^2 = .012$), open shrublands ($\eta^2 = .012$), woody savannas ($\eta^2 = .011$), deciduous broadleaf forests ($\eta^2 = .0001$), and evergreen broadleaf forests ($\eta^2 = .00001$).

A significant robust generalized linear model was not found when comparing evergreen needleleaf forests, evergreen broadleaf forests, deciduous broadleaf forests, mixed forests, closed shrublands, open shrublands, woody savannas, grasslands, croplands, and cropland and natural vegetation mosaics with wildfire event fire radiative power ($F(1,9) = .868$, $p > .05$), with a coefficient of determination of -.1% ($R^2 = -.001$). The presence of any of those vegetation categories cannot be used to predict the fire radiative power of wildfire events in the Western Hindu Kush-Himalayas.

Kernel density estimation was performed as a first order analysis of the point pattern of wildfire events in the Western Hindu Kush-Himalayas (Figure 22). The kernel density estimation revealed areas of high wildfire event density in Uttarakhand and Himachal Pradesh States of northern India, and the North-West Frontier province of Pakistan. The area of maximum event density was located in India's Uttarakhand State, where an overwhelming number of the Western Hindu Kush-Himalayas wildfire events were detected. Areas of event density were located in the Indian

state of Jammu and Kashmir, and in Pakistan's Baluchistan province. Areas of light density in the Federally Administered Tribal Areas territory of Pakistan, and along the Western Hindu Kush-Himalayas western boundary in the Afghanistan provinces of Balkh, Kunduz, and Takhar were also identified. Results of the kernel density estimation revealed that wildfire events in the Western Hindu Kush-Himalayas exhibit a density pattern indicative of clustering.

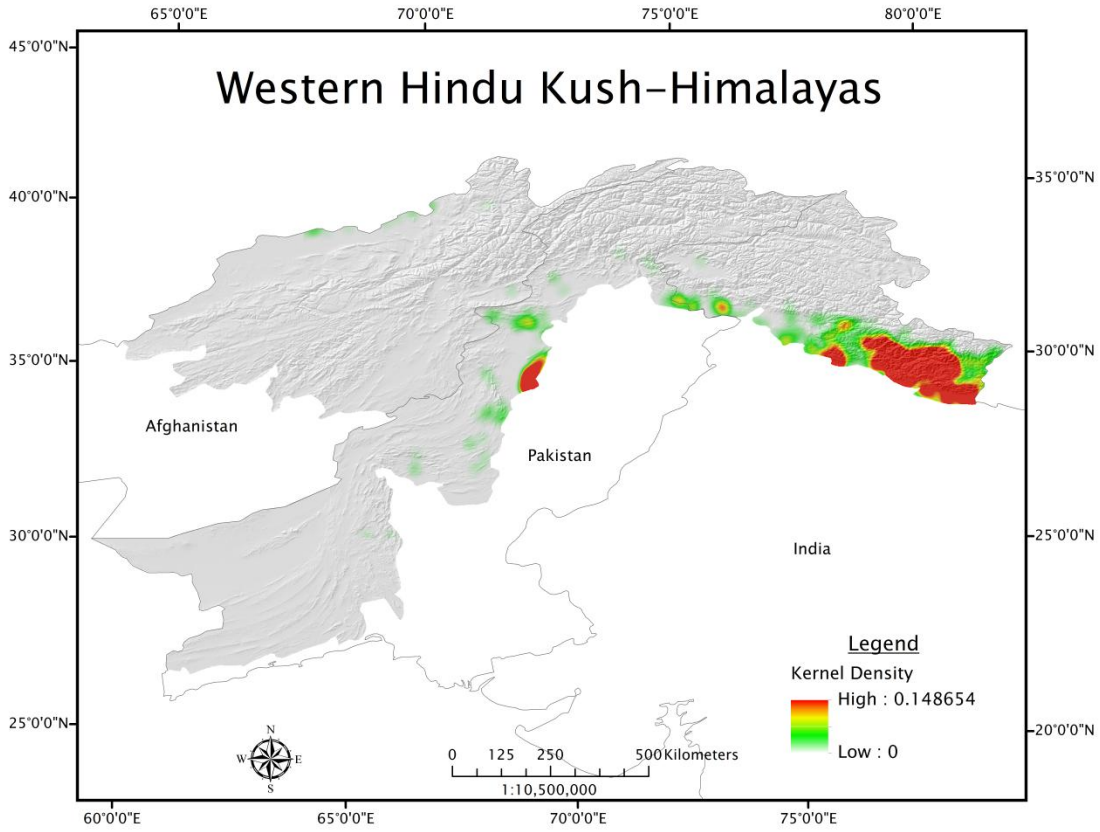

Figure 22: Kernel Density Estimation Results

To confirm the presence of clustering, Ripley's K(t) function was calculated for the wildfire event points. Ripley's K(t) function was used to test the null hypothesis that the pattern of the wildfire events is not significantly more clustered than would occur by chance. The observed results of the K(t) function fell outside of the calculated confidence envelope warranting rejection of the null hypothesis (Figure 23). Wildfire

events in the Western Hindu Kush-Himalayas significantly cluster.

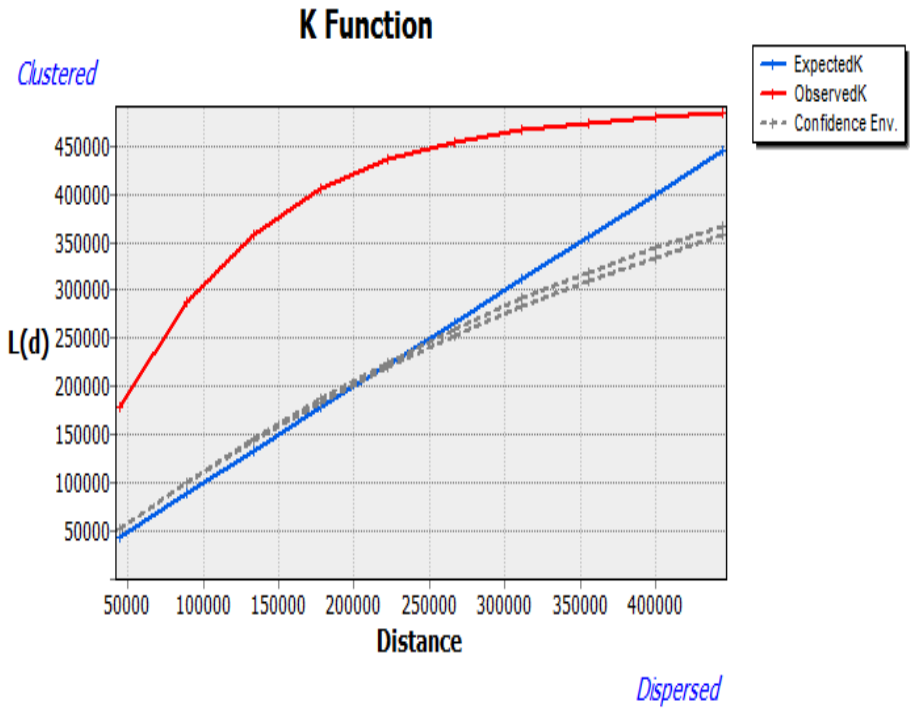

Figure 23: Ripley's K(t) Function Result

The result of Ripley's K(t) function revealed that the wildfire events exhibit a high degree of statistically significant clustering at all distances. These findings support the results of the kernel density estimation; the wildfire event points exhibit a point pattern indicative of clustering.

With the clustering of wildfire events established, Anselin Local Moran's I was calculated to visualize the clusters and reveal the nature of the event clustering. The Anselin Local Moran's I allowed for the wildfire

event clusters to be characterized based on the degree of high or low value clustering. Execution of Anselin Local Moran's I also allowed for visualization of the locations of wildfire event clusters.

Anselin Local Moran's I was calculated for each of the study's independent and dependent variables. Moderate temperature wildfire event clusters were located in the Western Hindu Kush-Himalayas eastern extent (Figure 24). Moderate temperature wildfire events clustered along an area extending from Uttarakhand State to Jammu and Kashmir State in India. The clustering of low temperature wildfire events was located throughout the Western Hindu Kush-Himalayas. Low temperature event clustering occurred in the states of Uttarakhand, Himachal Pradesh, and Jammu and Kashmir in India. Significant low temperature clusters were located in Pakistan's North-West Frontier Province, and along the Western Hindu Kush-Himalayas northwestern boundary in Afghanistan's Balkh and Takhar Provinces.

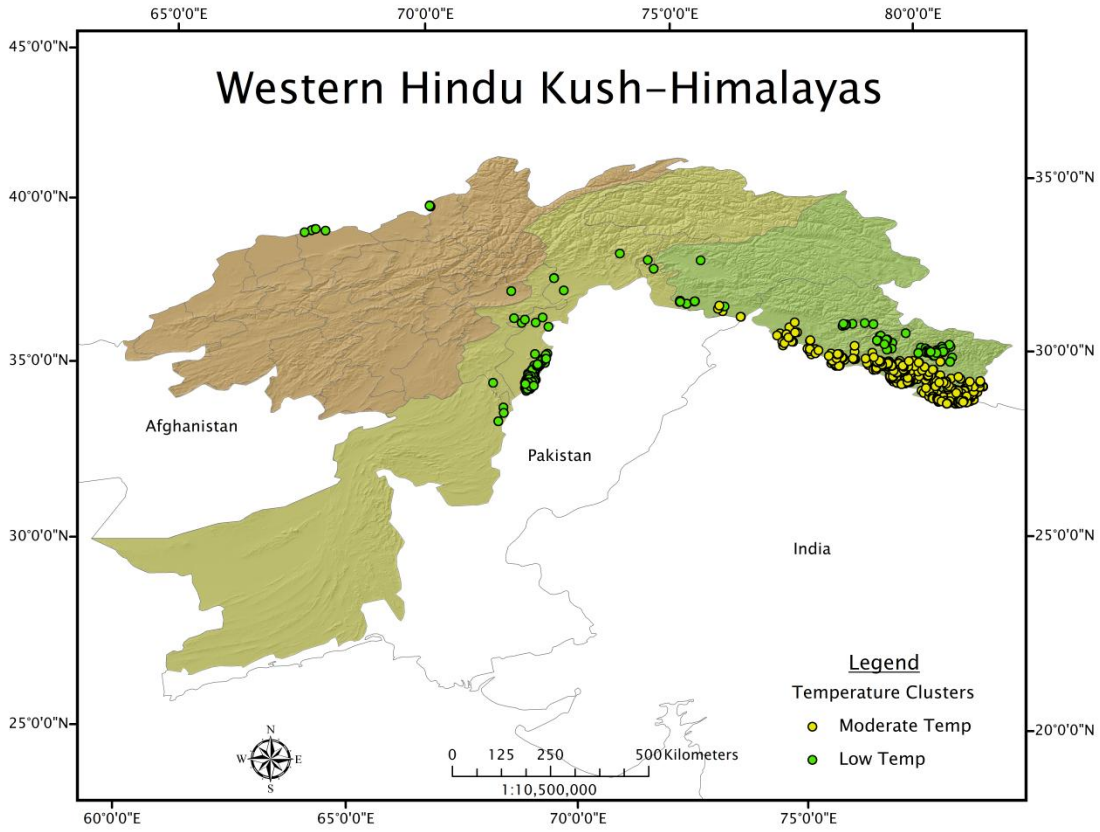

Figure 24: Wildfire Event Temperature Clusters

Wildfire events in the Western Hindu Kush-Himalayas emitted mostly very low to low fire radiative power. The clustering of fire radiative power events occurred with the greatest concentration in Uttarakhand State in India (Figure 25). The south of Uttarakhand contained the only concentration of very low fire radiative power wildfire event clusters located in the region. The north of Uttarakhand contained

a large number of low fire radiative power event clusters. Clusters of low fire radiative power wildfire events were located in Himachal Pradesh State, and along the southern edge of Jammu and Kashmir State in India. The clustering of low fire radiative power events occurred in Pakistan's North-West Frontier Province and Azad Kashmir Province. Significant clusters were also located along the region's western boundary in Balkh and Kunduz Provinces in Afghanistan.

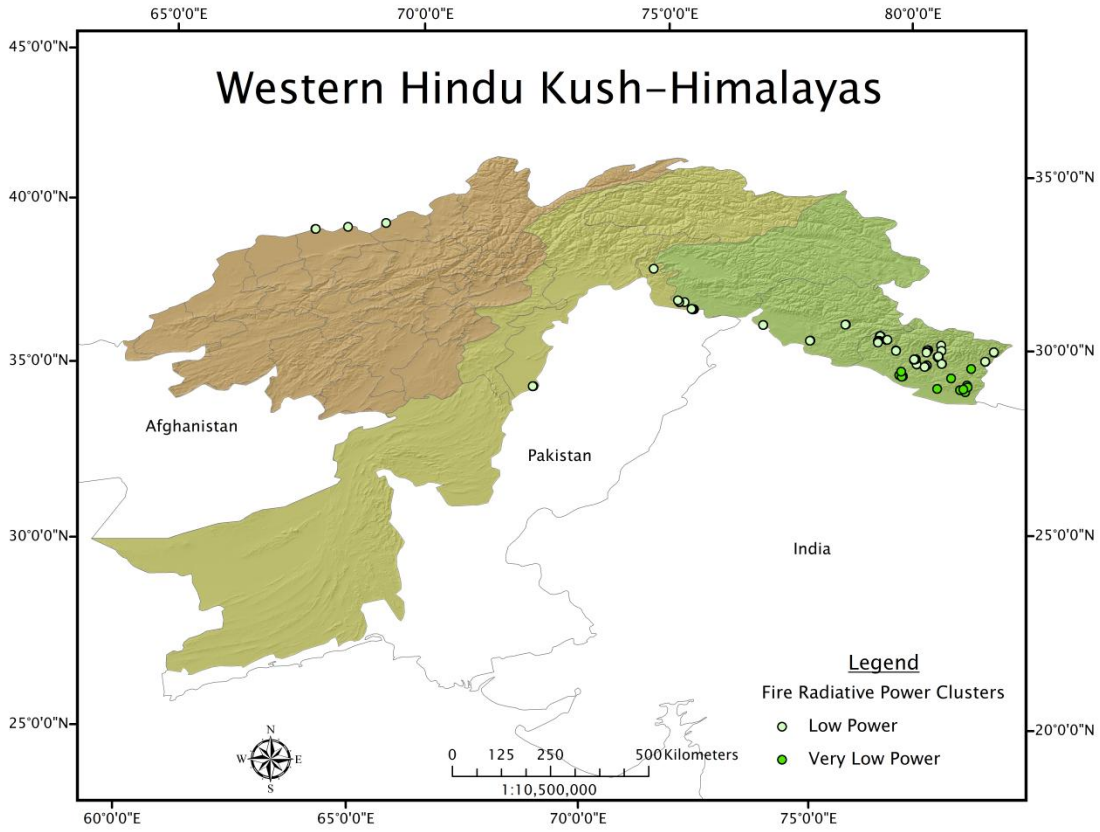

Figure 25: Wildfire Event Fire Radiative Power Clusters

In the Western Hindu Kush-Himalayas, wildfire events occurred predominantly in vegetation that was of low to very low health. The clustering of wildfire events in very low health vegetation occurred all throughout the Western Hindu Kush Himalayas. The largest concentration of very low health wildfire event clusters were located in northern India along the Himachal Pradesh, Uttarakhand border, with the

greatest concentration of very low health event clusters occurring in Himachal Pradesh State. Very low health wildfire event clusters were located throughout the Hindu Kush-Himalayas of Pakistan. Very low health wildfire events occurred in Pakistan's North-West Frontier Province, the Federally Administered Tribal Areas Territory, and in Baluchistan Province. Clusters of very low health wildfire events also occurred in the Western Hindu Kush-Himalayas of Afghanistan in Badakhshan Province, and along the region's western boundary in Balkh Province, Kunduz Province, and Takhar Province.

Low vegetation health wildfire event clusters were located in only two areas of the Western Hindu Kush-Himalayas. The majority of low health event clusters occurred in India's Uttarakhand State (Figure 26). These represented not only the greatest concentration of low health wildfire event clusters but also the largest number of event clusters based on vegetation health that were located in the Western Hindu Kush region. Significant clustering of low health wildfire events was also located in the southern region of Pakistan's North-West Frontier Province.

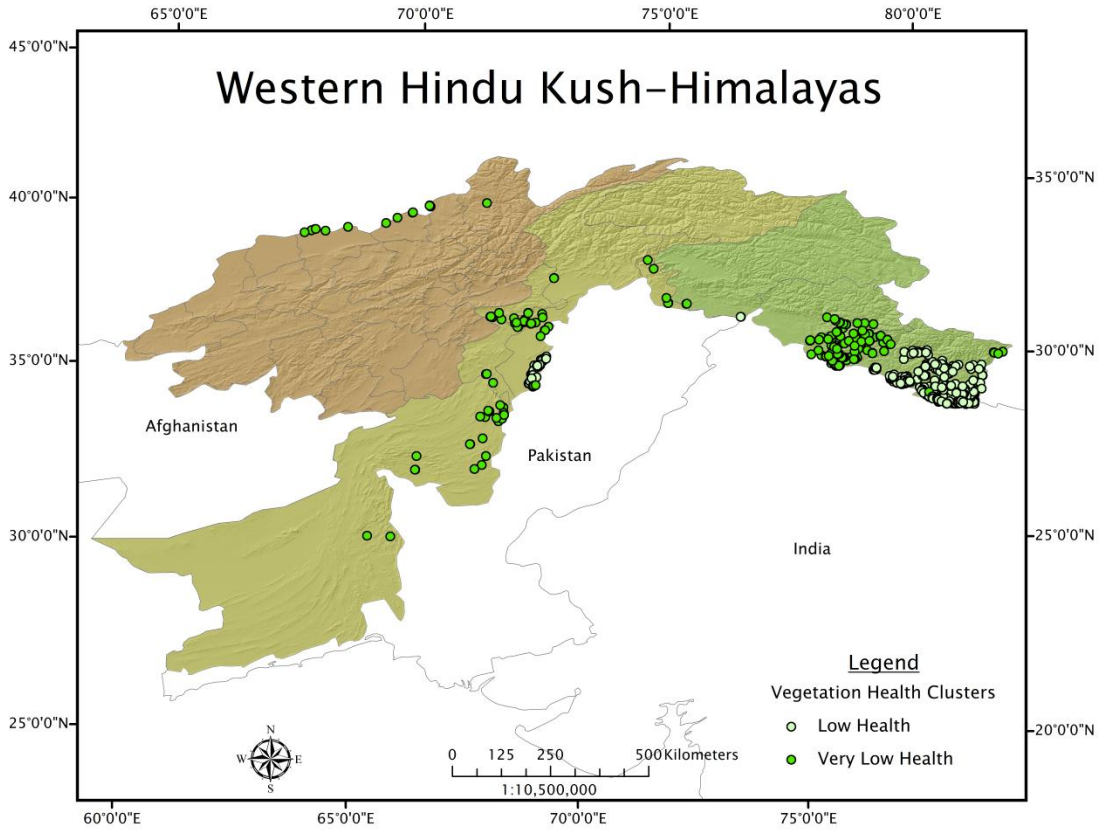

Figure 26: Wildfire Event Vegetation Health Clusters

The majority of wildfire events in the Western Hindu Kush-Himalayas occurred on areas of low slope (Figure 27). Wildfire events were also found in lesser numbers on moderate slopes. Clusters of wildfire events on low slope areas were located throughout the Western Hindu Kush-Himalayas. Low slope wildfire events occurred along the Western Hindu Kush-Himalayas southeastern boundary from Uttarakhand

to Jammu and Kashmir States in northern India. Clusters of wildfire events on low slopes were located in Pakistan concentrated in the North-West Frontier Province, with a small amount of clusters in northeast Baluchistan Province. A number of low slope wildfire events were also located in Afghanistan along the Western Hindu Kush-Himalayas western boundary in Balkh Province, Kunduz Province, and Takhar Province.

Wildfire event clustering on moderate slopes were located in the Western Hindu Kush-Himalayas of northern India. Moderate slope event clusters extended throughout the states of Uttarakhand and eastern Himachal Pradesh. The greatest concentration of moderate slope wildfire event clusters occurred in Uttarakhand State.

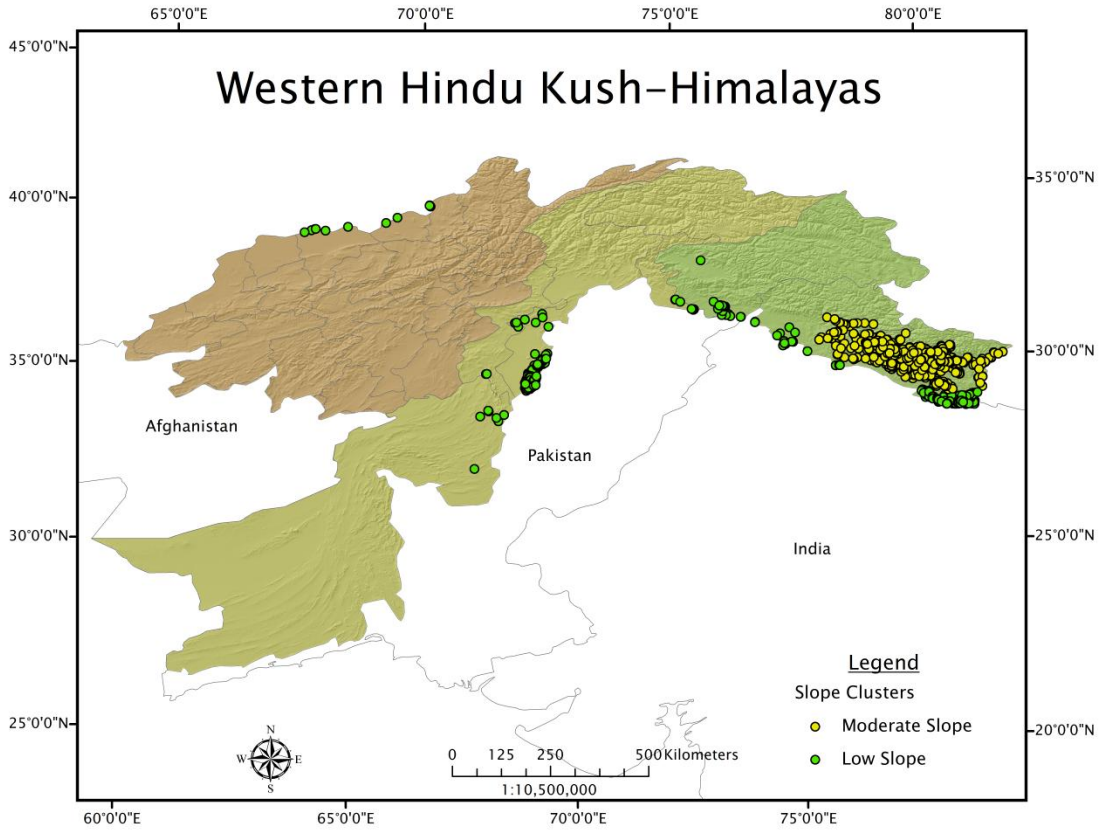

Figure 27: Wildfire Event Slope Clusters

Clusters of wildfire events on similar aspects occurred in the Western Hindu Kush-Himalayas of northern India (Figure 28). The clustering of high aspect wildfire events was located with greatest concentration in Uttarakhand State. High aspect wildfire event clusters also were located In Himachal Pradesh State, Jammu and Kashmir State, as well as in Pakistan's Baluchistan Province. Wildfire events clustered to

a lesser degree on areas of low aspects. Clusters of low aspect events concentrated in the southern region of Pakistan's North-West Frontier Province. Significant low aspect wildfire event clusters were also found in northeastern Baluchistan Province, and in Uttarakhand State in India.

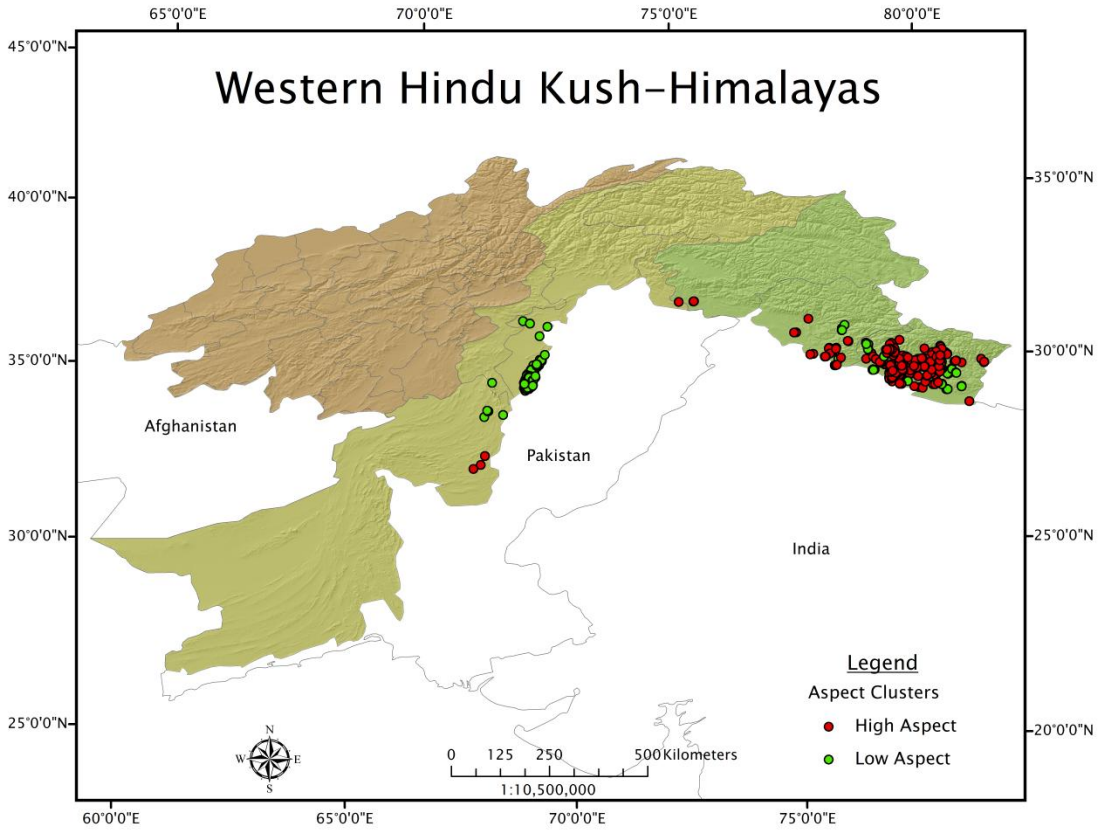

Figure 28: Wildfire Event Aspect Clusters

In the Western Hindu Kush-Himalayas, the majority of wildfire events clustered in the region's upper elevations (Figure 29). The

clustering of wildfire events in the region's upper elevations could be found in Uttarakhand State and Himachal Pradesh State in northern India. A high concentration of wildfire events at upper elevations occurred in Uttarakhand State where the greatest number of event clusters was located.

Lower elevation wildfire event clusters were also located in the Western Hindu Kush-Himalayas. Clusters of lower elevation wildfire events were found along the southeastern boundary of the Western Hindu Kush-Himalayas in Uttarakhand, Himachal Pradesh, and Jammu and Kashmir States. A significant cluster of lower elevation wildfire events were also located in the southern extent of Pakistan's North-West Frontier Province. The clustering of lower elevation wildfire events was also evident along the Western Hindu Kush-Himalayas western boundary in the Afghanistan provinces of Balkh and Kunduz.

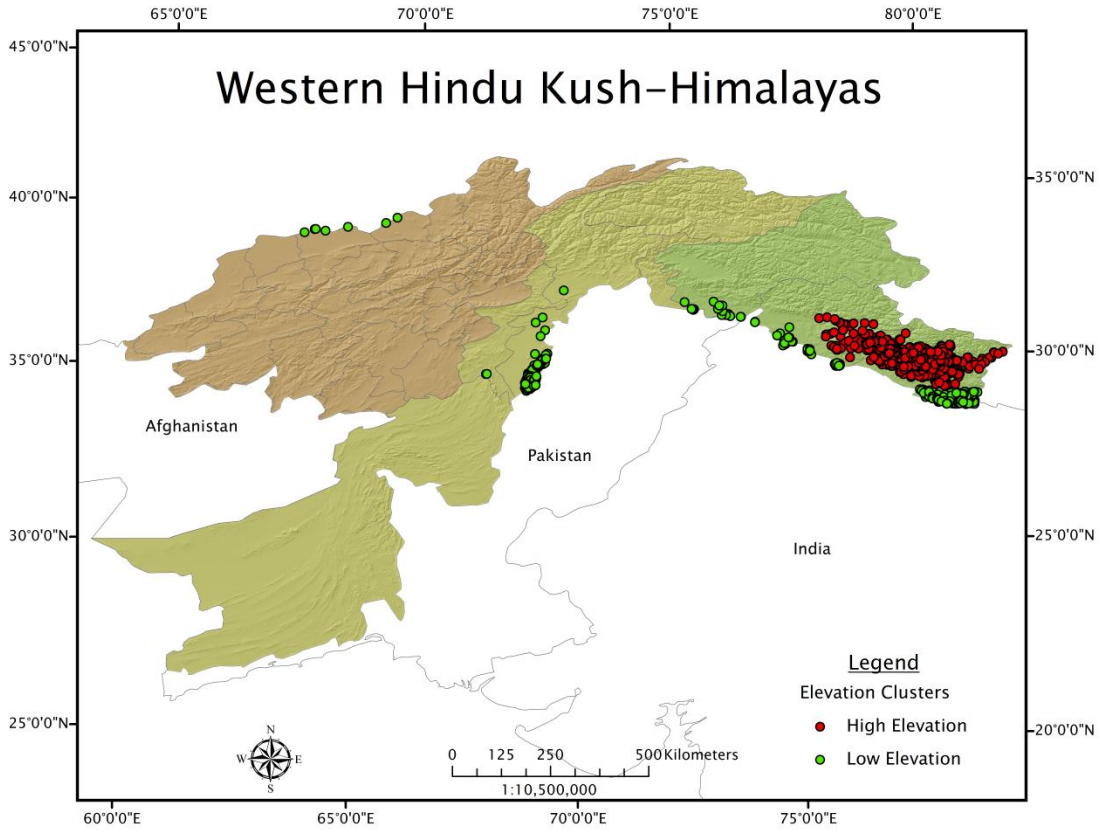

Figure 29: Wildfire Event Elevation Clusters

The clustering of wildfire events predominantly occurred close to road features in the Western Hindu Kush-Himalayas (Figure 30). Significant clusters of wildfire events close to road features were located with greatest concentration in southeast Uttarakhand State in India. Wildfire event clusters close to road features occurred in the south of Jammu and Kashmir State in India as well as in the south of Pakistan's

North-West Frontier Province.

Clusters of wildfire events in the Western Hindu Kush-Himalayas were also located at distances far from road features. The majority of wildfire event clusters that occurred far from road features were found in the western extent of India's Uttarakhand State, and in the eastern extent of Himachal Pradesh State in India. Significant clusters of wildfire events far from road features were also located in northeastern Baluchistan Province in Pakistan, and in Afghanistan's Takhar Province.

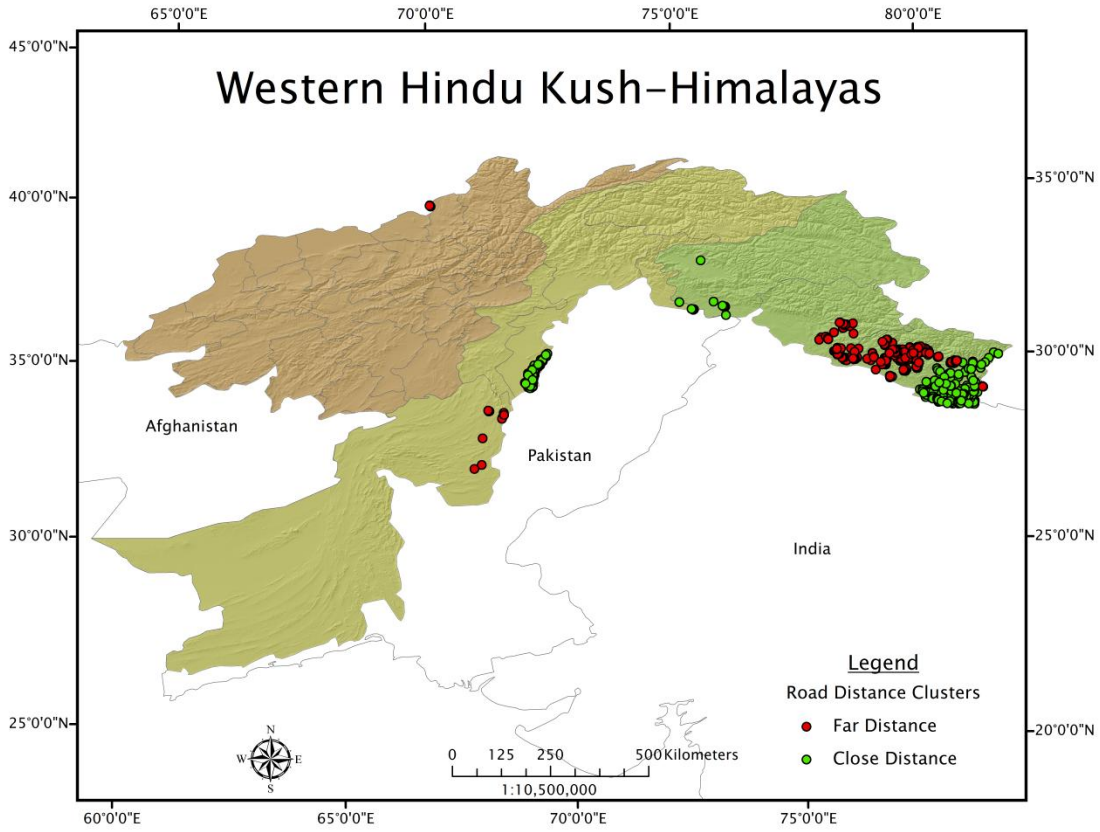

Figure 30: Wildfire Event Road Distance Clusters

Wildfire events in the Western Hindu Kush-Himalayas primarily clustered close to water features (Figure 31). The clustering of wildfire events close to water features occurred in the states of Uttarakhand and Himachal Pradesh in India. Uttarakhand State and Himachal Pradesh State were the only locations in the Western Hindu Kush where clusters of wildfire events close to water features were located.

Significant clusters of wildfire events far from water features were also located in the region. Events far from water features occurred predominantly in the Western Hindu Kush-Himalayas of Pakistan. Clustering of wildfire events far from water features were located in the North-West Frontier Province and in northeastern Baluchistan Province. Clusters of wildfire events far from water features were also located in Afghanistan's Balkh Province.

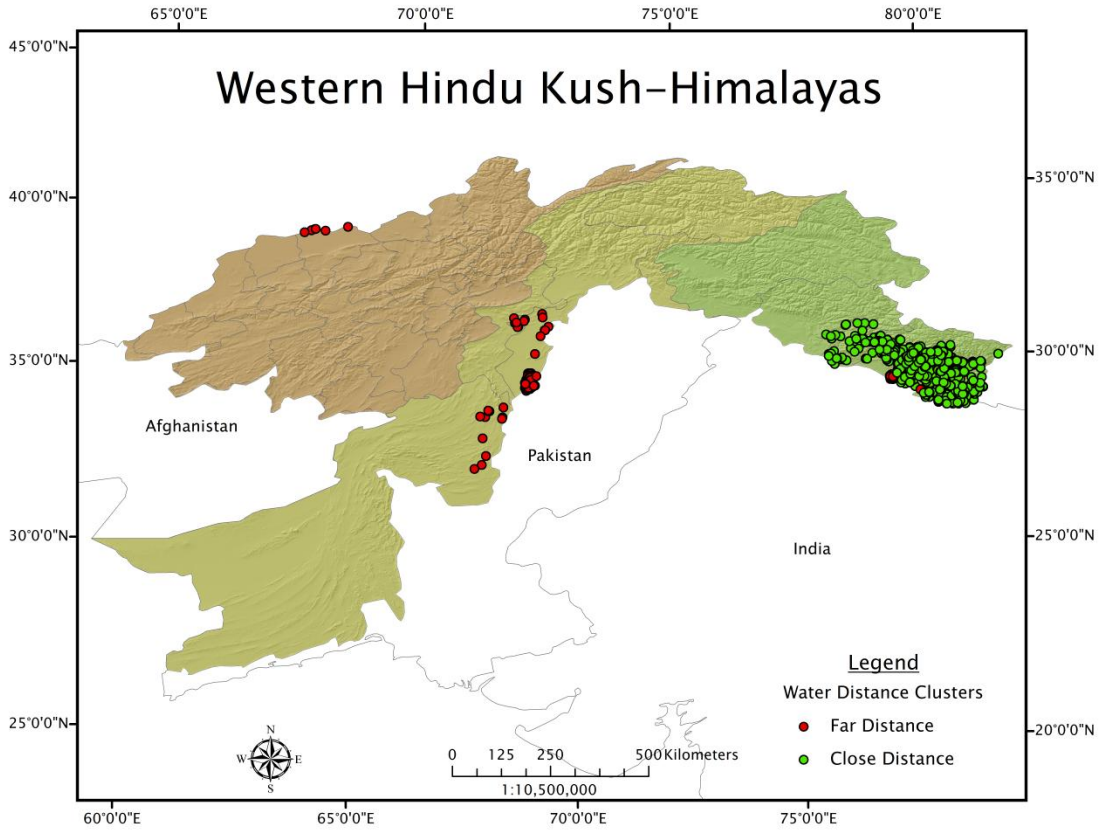

Figure 31: Wildfire Event Water Distance Clusters

Analysis of wildfire event proximity to settlements revealed that the majority of events in the Western Hindu Kush-Himalayas clustered at distances far from settlement locations (Figure 32). The greatest concentration of wildfire event clusters far from settlements occurred throughout Uttarakhand State in northern India. Clusters of wildfire events far from settlements were also identified in the southern extent of

India's Himachal Pradesh State, and in the North-West Frontier Province in Pakistan. Significant clustering of events far from settlements was also found in Nangarhar Province in eastern Afghanistan, and along the Western Hindu Kush-Himalayas western boundary in Afghanistan's Balkh Province.

Significant wildfire event clusters near to settlements were also identified in the Western Hindu Kush-Himalayas. Clusters of wildfire events near to settlements were located in the states of Uttarakhand, Himachal Pradesh, and Jammu and Kashmir in India. The concentration of wildfire event clusters near to settlements was greatest in Uttarakhand State. Wildfire events also significantly clustered near to settlements in the North-West Frontier Province in Pakistan.

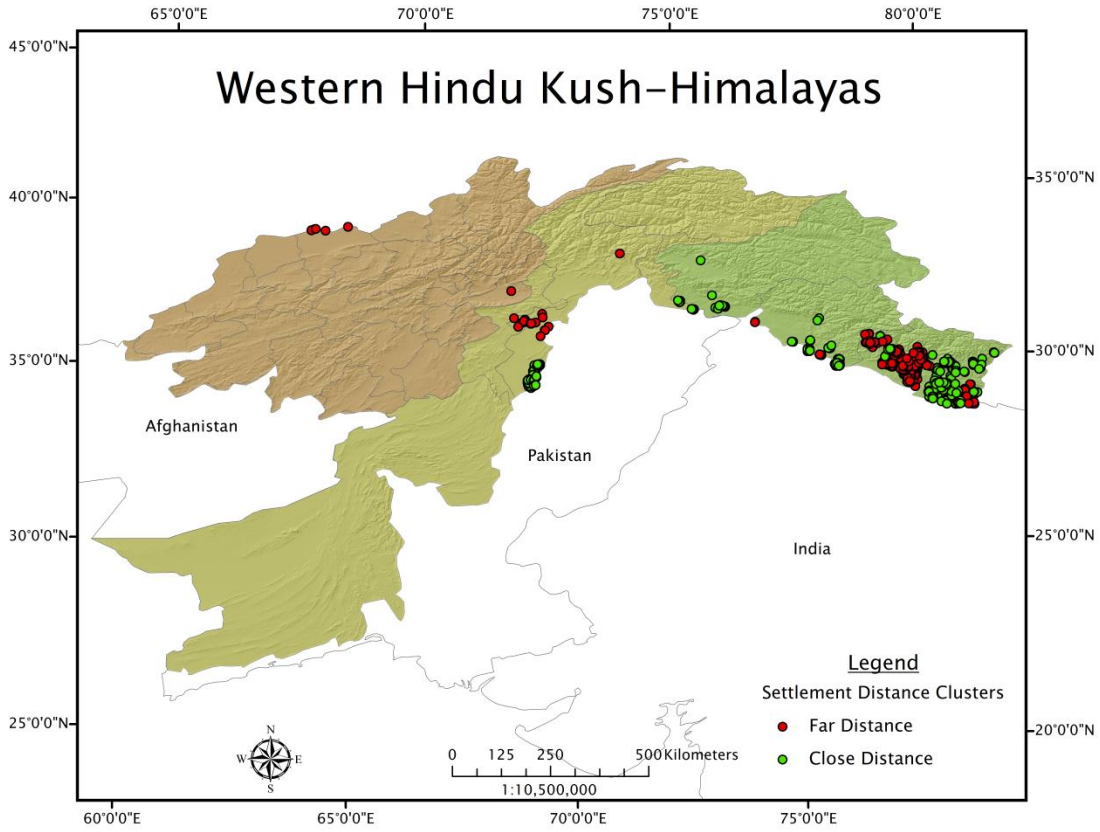

Figure 32: Wildfire Event Settlement Distance Clusters

Analysis of the clustering of regional wildfire events by land cover type was then performed. This allowed for the wildfire event clusters to be characterized based on land cover type, and aided in the identification of wildfire prone environments in the Western Hindu Kush-Himalayas. The clustering of wildfire events in evergreen needleleaf forest occurred only in the Western Hindu Kush-Himalayas of India (Figure 33). The

majority of wildfire event clusters in evergreen needleleaf forest were located in Uttarakhand State. Significant wildfire event clusters were also located in the evergreen needleleaf forests of Himachal Pradesh State.

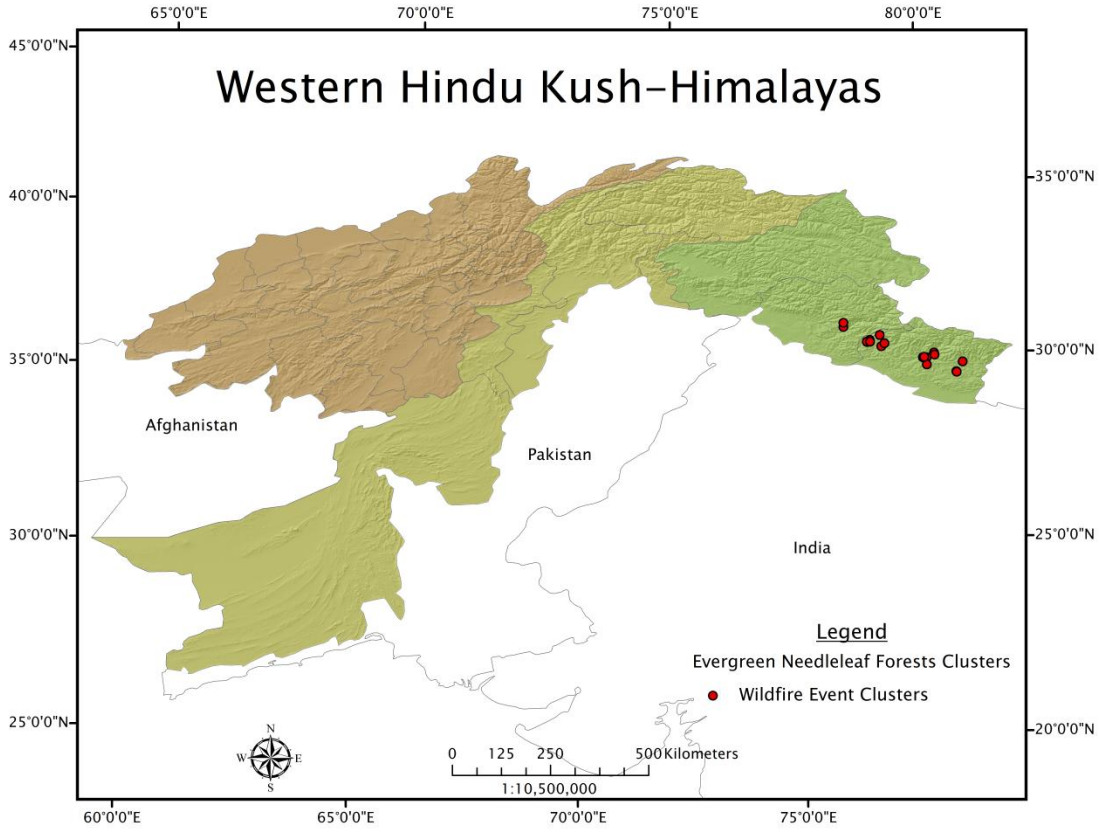

Figure 33: Wildfire Event Clusters in Evergreen Needleleaf Forests

Wildfire events in broadleaf forests were found to cluster in only one area of the Western Hindu Kush-Himalayas (Figure 34). A small cluster of wildfire events in evergreen broadleaf forest were located in

Uttarakhand State along the Western Hindu Kush-Himalayas eastern boundary in India. The clustering of wildfire events in deciduous broadleaf forest were also only located in a single area of the Western Hindu Kush-Himalayas. A cluster of wildfire events in deciduous broadleaf forest were identified in India's Uttarakhand State.

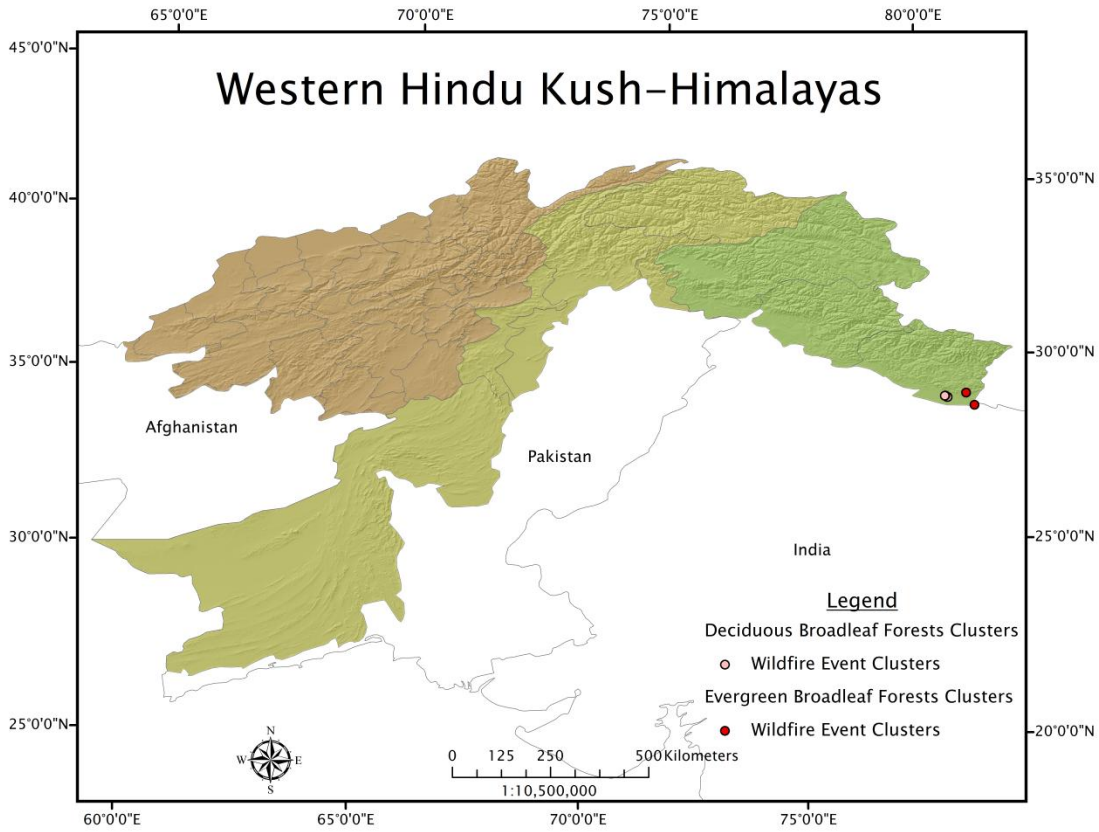

Figure 34: Wildfire Event Clusters in Broadleaf Forests

The clustering of wildfire events in the Western Hindu Kush-Himalayas occurred with greatest concentration in the region's mixed forests. Clusters of wildfire events in mixed forests were located with the greatest concentration in the Western Hindu Kush-Himalayas of India (Figure 35). The largest concentration of wildfire events in mixed forests occurred in Uttarakhand State, while significant clusters of wildfire events were also located in Himachal Pradesh State.

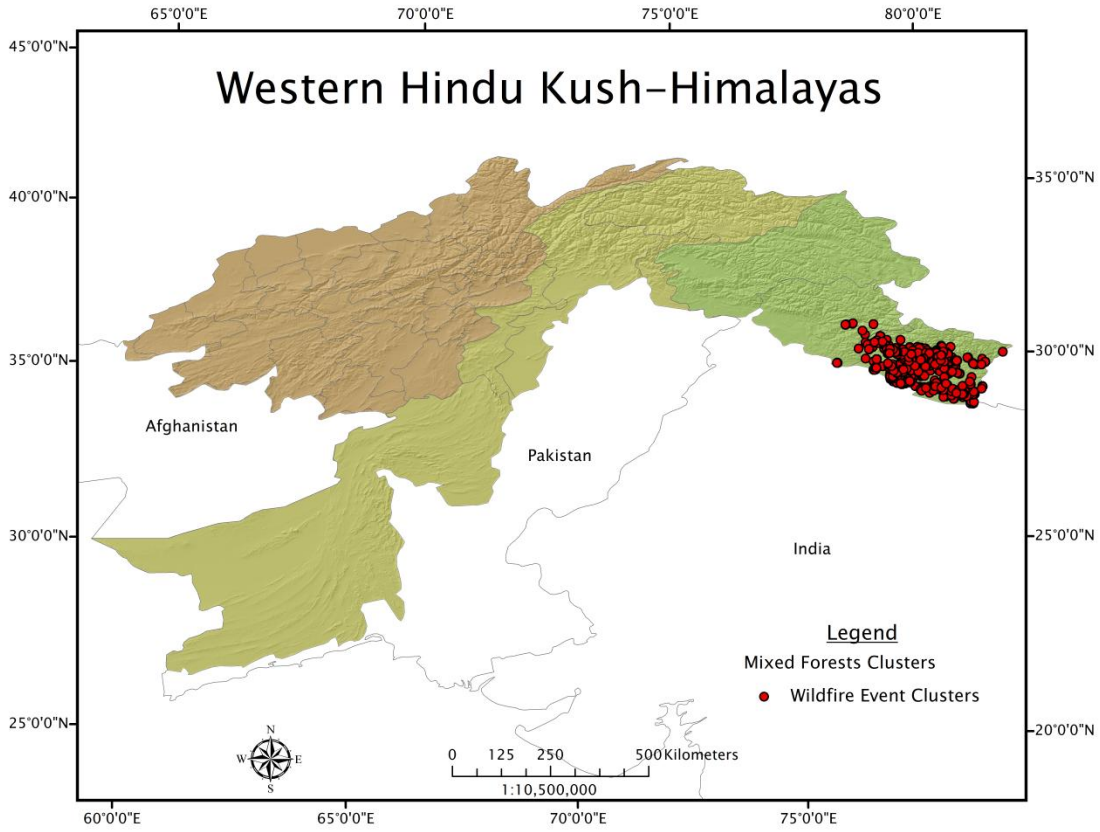

Figure 35: Wildfire Event Clusters in Mixed Forests

Clusters of wildfire events in closed shrublands were identified across the Western Hindu Kush-Himalayas (Figure 36). Wildfire event clusters in closed shrublands occurred predominantly in the Western Hindu Kush-Himalayas of Pakistan. Significant clusters were located in the North-West Frontier Province and in the Federally Administered Tribal Areas Territory. The clustering of wildfire events in closed shrublands

was also identified in Uttarakhand State in India and in Kunduz Province in Afghanistan.

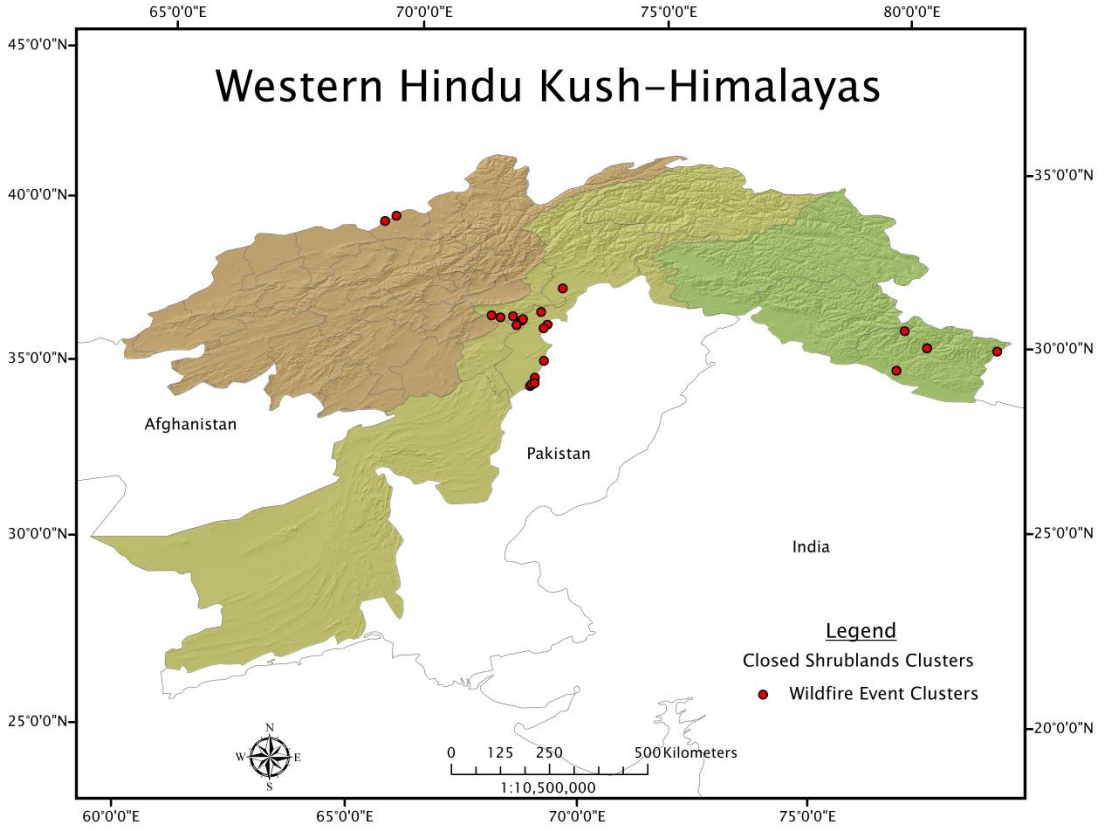

Figure 36: Wildfire Event Clusters in Closed Shrublands

Open shrublands also experienced significant wildfire event clustering. The Western Hindu Kush-Himalayas of Pakistan was the only location in the region where clusters of wildfire events in open shrublands were located (Figure 37). Clusters of wildfire events in open

shrublands occurred in the North-West Frontier Province and in Baluchistan Province. Clustering of wildfire events in open shrublands was also located in the Federally Administered Tribal Areas Territory.

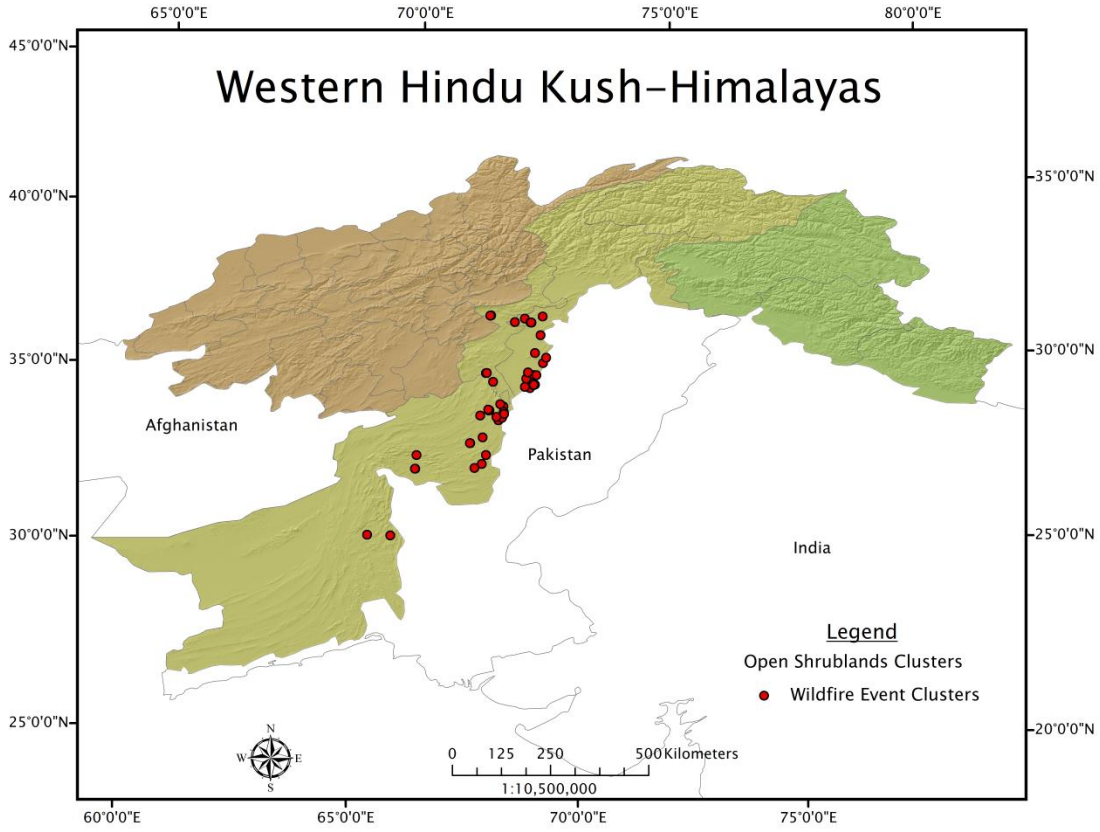

Figure 37: Wildfire Event Clusters in Open Shrublands

The Western Hindu Kush-Himalayas woody savannas experienced a considerable amount of wildfire event clustering. Wildfire event clusters in woody savannas occurred only in the Western Hindu Kush-Himalayas

of India (Figure 38). The greatest concentration of wildfire event clustering occurred in Uttarakhand State. Clusters of wildfire events in woody savannas were also located in Himachal Pradesh State, and a small cluster of events were located in Jammu and Kashmir State.

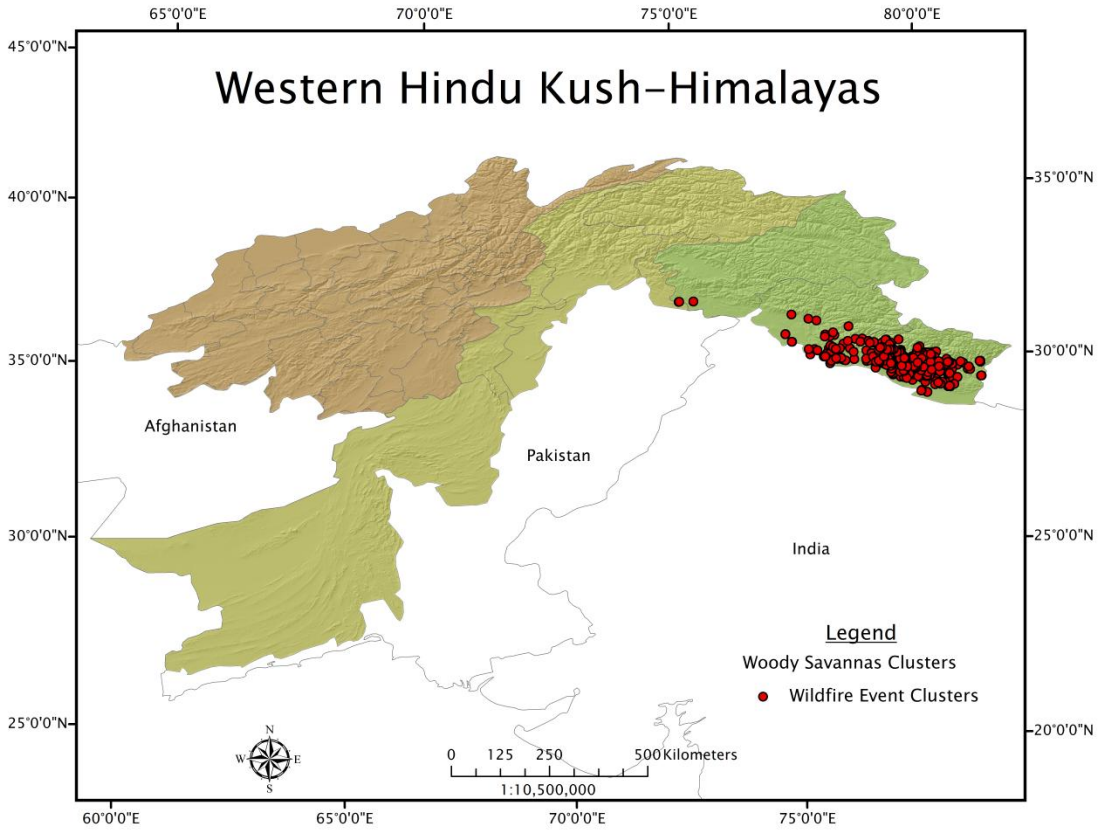

Figure 38: Wildfire Event Clusters in Woody Savannas

Grasslands in the Western Hindu Kush-Himalayas experienced a minimal level of wildfire event clustering (Figure 39). The majority of

wildfire event clusters occurred in the upper elevation grasslands of Uttarakhand State in India. Clusters of wildfire events in the region's grasslands also occurred in Pakistan's North-West Frontier Province, and a significant cluster of wildfire events were also identified in Afghanistan's Takhar Province.

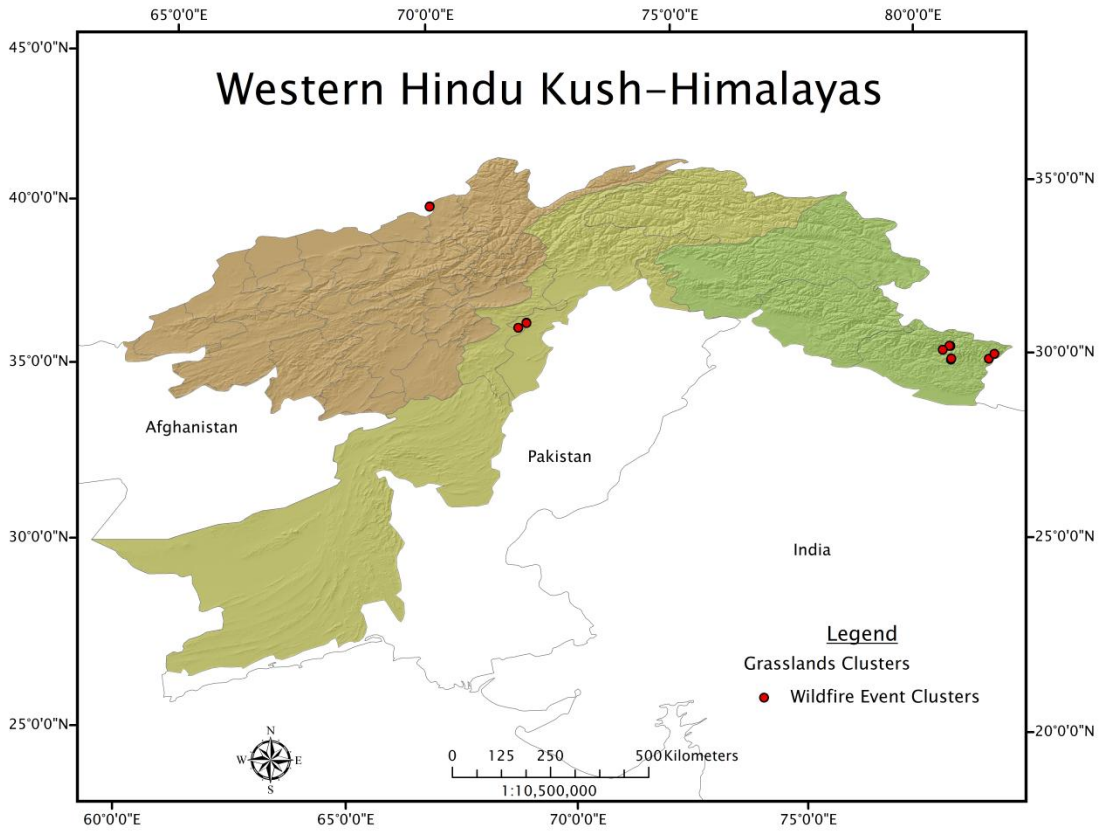

Figure 39: Wildfire Event Clusters in Grasslands

Wildfire event clusters in the croplands of the Western Hindu Kush-Himalayas were located predominantly in Pakistan (Figure 40). The greatest number of wildfire event clusters in croplands was identified in the North-West Frontier Province. The clustering of events in croplands was also located in the Federally Administered Tribal Areas Territory and in Azad Kashmir Province. Significant clustering of wildfire events in croplands were also identified in the Western Hindu Kush-Himalayas of India. Clusters of wildfire events were located in the states of Uttarakhand, Himachal Pradesh, and Jammu and Kashmir.

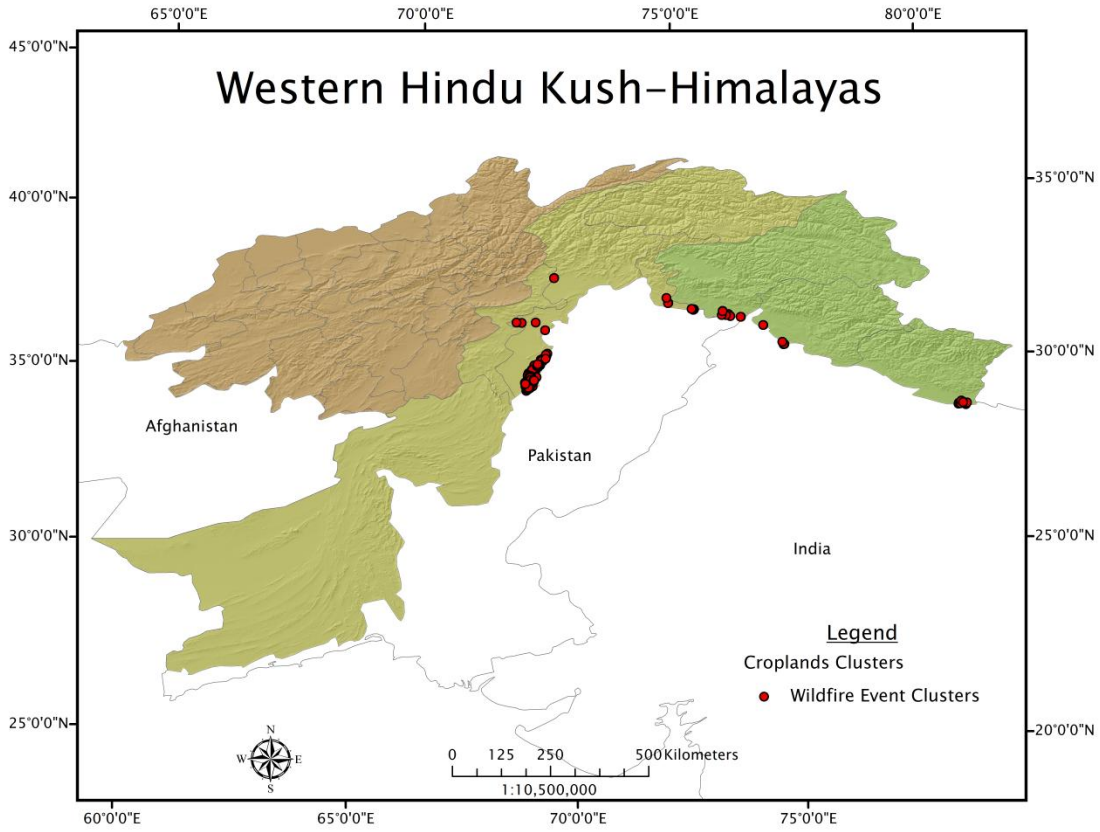

Figure 40: Wildfire Event Clusters in Croplands

Significant clustering of wildfire events in the Western Hindu Kush-Himalayas cropland and natural vegetation mosaics were also identified. The majority of wildfire events clustered in the cropland and natural vegetation mosaics of India (Figure 41). Clustering of wildfire events was identified in Uttarakhand State, Himachal Pradesh State, and in Jammu and Kashmir State. Wildfire events clustered in the cropland and natural

vegetation mosaics of the North-West Frontier Province and the Federally Administered Tribal Area Territory in Pakistan. A small cluster of wildfire events in cropland and natural vegetation mosaics were also located in Balkh Province in Afghanistan.

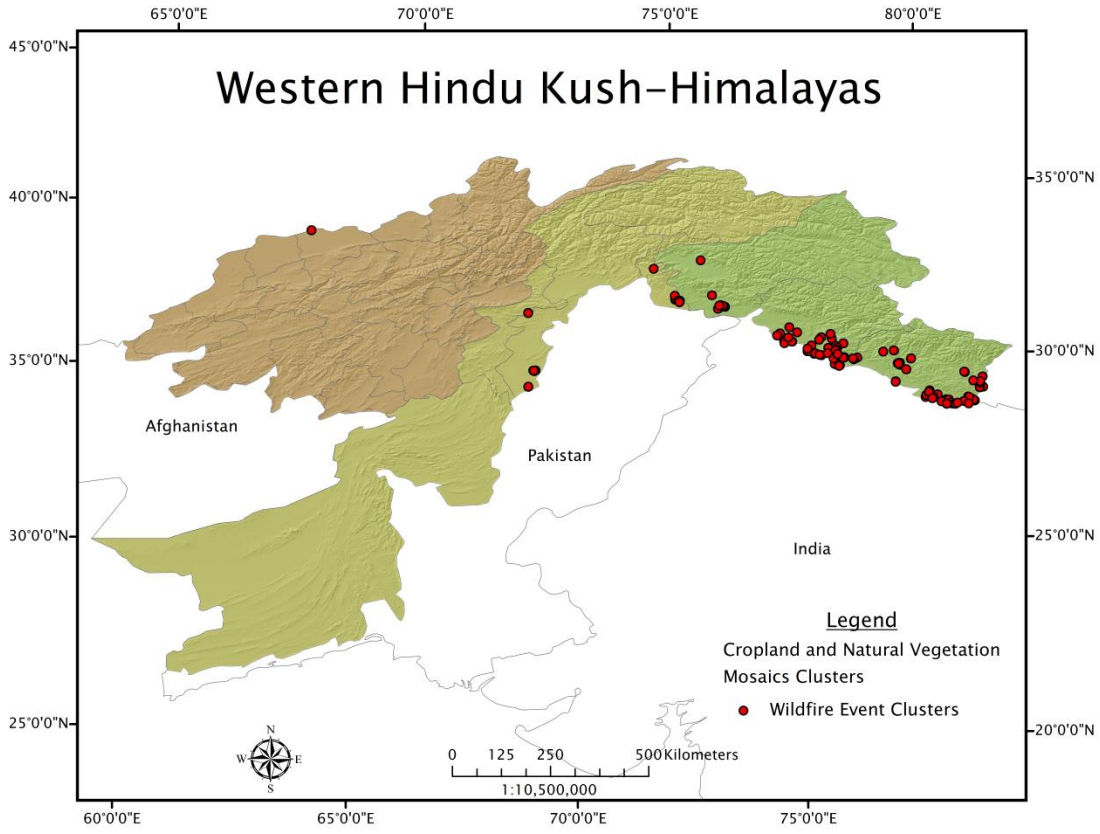

Figure 41: Wildfire Event Clusters in Cropland and Natural Vegetation Mosaics

Modeling of wildfire potential in the Western Hindu Kush-Himalayas was performed using multi-criteria evaluation with weighted

linear combination. The model output was classified into six classes of wildfire potential, including no wildfire potential, very low wildfire potential, low wildfire potential, moderate wildfire potential, high wildfire potential, and very high wildfire potential.

The wildfire potential model was compared to a holdout data set comprised of 869 wildfire events to determine the validity of the model output. Model validation was evaluated using a chi-square goodness of fit test to evaluate the statistical significance of wildfire events in the Western Hindu Kush-Himalayas to the modeled wildfire potential classes (Burt et al., 2009; O'Sullivan, & Unwin, 2003). The strength of the relationship between wildfire events in the Western Hindu Kush-Himalayas and the modeled wildfire potential classes was evaluated using a Spearman's rho correlation (Burt et al., 2009; O'Sullivan, & Unwin, 2003).

A chi-square goodness of fit test was calculated to compare the frequency of wildfire events in the Western Hindu Kush-Himalayas and the modeled wildfire potential classes. The chi-square goodness of fit

test was performed comparing the holdout wildfire events to the modeled wildfire potential classes. The null hypothesis was that the frequency of wildfire events in the Western Hindu Kush-Himalayas is not consistent with the modeled wildfire potential classes. The alternate hypothesis was that the frequency of wildfire events in the Western Hindu Kush-Himalayas is consistent with the modeled wildfire potential classes.

No significant deviation between wildfire events in the Western Hindu Kush-Himalayas and the modeled wildfire potential classes was found ($X^2(4) = .000$, $p > .05$). Wildfire events in the Western Hindu Kush-Himalayas significantly correspond with the modeled wildfire potential classes.

A Spearman's rho correlation was calculated to determine the strength of the relationship between wildfire events in the Western Hindu Kush-Himalayas and the modeled wildfire potential classes. The correlation was calculated comparing the holdout wildfire events and the wildfire potential classes. The null hypothesis was that no association exists between the modeled wildfire potential classes and wildfire events

in the Western Hindu Kush-Himalayas. The alternate hypothesis was that an association exists between the modeled wildfire potential classes and wildfire events in the Western Hindu Kush-Himalayas.

A strong positive correlation was found between the modeled wildfire potential classes and wildfire events in the Western Hindu Kush-Himalayas ($rho(3) = .900$, $p < .05$). There is a significant relationship between the wildfire potential classes and wildfire events in the Western Hindu Kush-Himalayas.

Observed and predicted wildfire potential was then compared in an error matrix to determine user's and producer's accuracy, errors of omission, errors of commission, and to determine the overall accuracy of the modeled wildfire potential zones (Table 12). The producer's accuracy of the model was 100% for no wildfire potential, 100% for very low wildfire potential, 33% for low wildfire potential, 80% for moderate wildfire potential, 80% for high wildfire potential, and 98% for very high wildfire potential. User's accuracy was 100% for no wildfire potential, 100% for very low wildfire potential, 100% for low wildfire potential, 80%

for moderate wildfire potential, 77% for high wildfire potential, and 98% for very high wildfire potential.

Errors of omission generated by the model were 0% for no wildfire potential, 0% for very low wildfire potential, 67% for low wildfire potential, 20% for moderate wildfire potential, 20% for high wildfire potential, and 2% for very high wildfire potential. Errors of commission were 0% for no wildfire potential, 0% for very low wildfire potential, 0% for low wildfire potential, 20% for moderate wildfire potential, 23% for high wildfire potential, and 2% for very high wildfire potential.

The overall accuracy of the wildfire potential model was 96%, with a mean accuracy of 82%. The Kappa Coefficient of Agreement, which measures the level of accuracy that exists between observed data and predicted data, was also calculated. The Kappa Coefficient (K_{hat}) produced a wildfire potential model accuracy of 79% representing a substantial agreement between observed and predicted wildfire potential.

Table 12: Error Matrix

	Observed								
Predicted	0	1	2	3	4	5	Total =	Producer's Accuracy	Errors of Omission
0	0	0	0	0	0	0	0	100%	0%
1	0	0	0	0	0	0	0	100%	0%
2	0	0	1	1	1	0	3	33%	67%
3	0	0	0	12	2	1	15	80%	20%
4	0	0	0	2	68	15	85	80%	20%
5	0	0	0	0	17	749	766	98%	2%
Total =	0	0	1	15	88	765	869		
User's Accuracy	100%	100%	100%	80%	77%	98%			
Errors of Commission	0%	0%	0%	20%	23%	2%			
Overall Accuracy =	0.95512	96%	Mean Accuracy =		0.8185	82%	K_{hat} =	0.7901	79%

In the Western Hindu Kush-Himalayas, low potential wildfire zones were the most prevalent wildfire potential class (Figure 42). Low potential wildfire zones accounted for 15.46% of the Western Hindu Kush-Himalayas total area. Moderate potential wildfire zones comprised 14.27% of the Western Hindu Kush-Himalayas, high potential wildfire zones accounted for 13.92%, and very high potential zones comprised 10.27% of the region. Very low potential wildfire zones accounted for 8.39% of the Western Hindu Kush-Himalayas, and zones of no wildfire potential comprised the remaining 37.69% of the region.

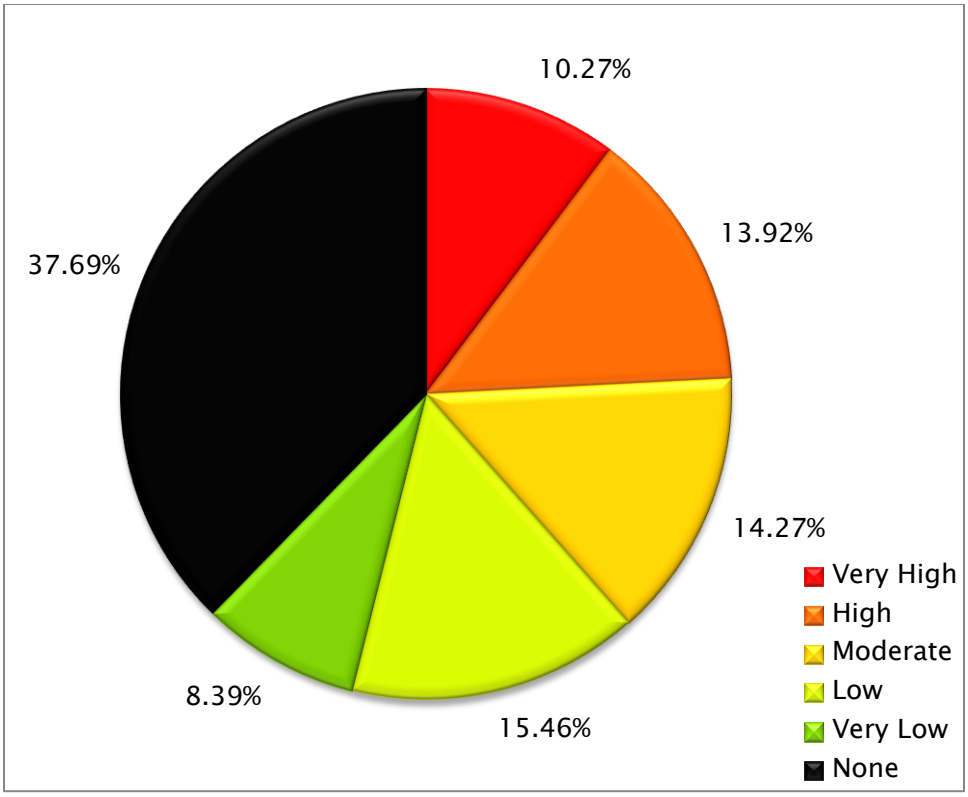

Figure 42: Percent Wildfire Potential
in the Western Hindu Kush-Himalayas

The geographic distribution of the wildfire potential zones in the Western Hindu Kush-Himalayas is shown in Figure 43. A total of 407,277 km^2 of area with no wildfire potential was found in the Western Hindu Kush-Himalayas, with a standard deviation of 3,252.146 km^2. No potential wildfire zones had a mean area of 80.062 km^2 with the smallest area in the region measuring 1 km^2 and the largest measuring 167,190 km^2.

Very low potential wildfire area in the Western Hindu Kush-Himalayas totaled 90,709 km^2 with a standard deviation of 12.613 km^2. The smallest area of very low wildfire potential measured 1 km^2 and the largest area measured 1,799 km^2. Mean very low wildfire potential area in the Western Hindu Kush-Himalayas measured 3.185 km^2.

Low potential wildfire area in the Western Hindu Kush-Himalayas totaled 166,931 km^2 with a standard deviation of 522.998 km^2. The smallest area of low wildfire potential in the region measured 1 km^2 and the largest area measured 64,179 km^2. Mean low wildfire potential area in the Western Hindu Kush-Himalayas measured 10.303 km^2.

Moderate potential wildfire area in the Western Hindu Kush-Himalayas totaled 154,128 km^2 with a standard deviation of 456.395 km^2. The smallest area of moderate wildfire potential in the region measured 1 km^2 and the largest area measured 42,907 km^2. Mean moderate wildfire potential area in the Western Hindu Kush-Himalayas measured 14.653 km^2.

High potential wildfire area in the Western Hindu Kush-Himalayas totaled 150,294 km^2 with a standard deviation of 409.681 km^2. The smallest area of high wildfire potential in the region measured 1 km^2 and the largest area measured 23,752 km^2. Mean high wildfire potential area in the Western Hindu Kush-Himalayas measured 17.994 km^2.

Very high potential wildfire area in the Western Hindu Kush-Himalayas totaled 111,030 km^2 with a standard deviation of 1,456.32 km^2. The smallest area of very high wildfire potential in the region measured 1 km^2 and the largest area measured 86,619 km^2. Mean very high wildfire potential area in the Western Hindu Kush-Himalayas measured 31.311 km^2.

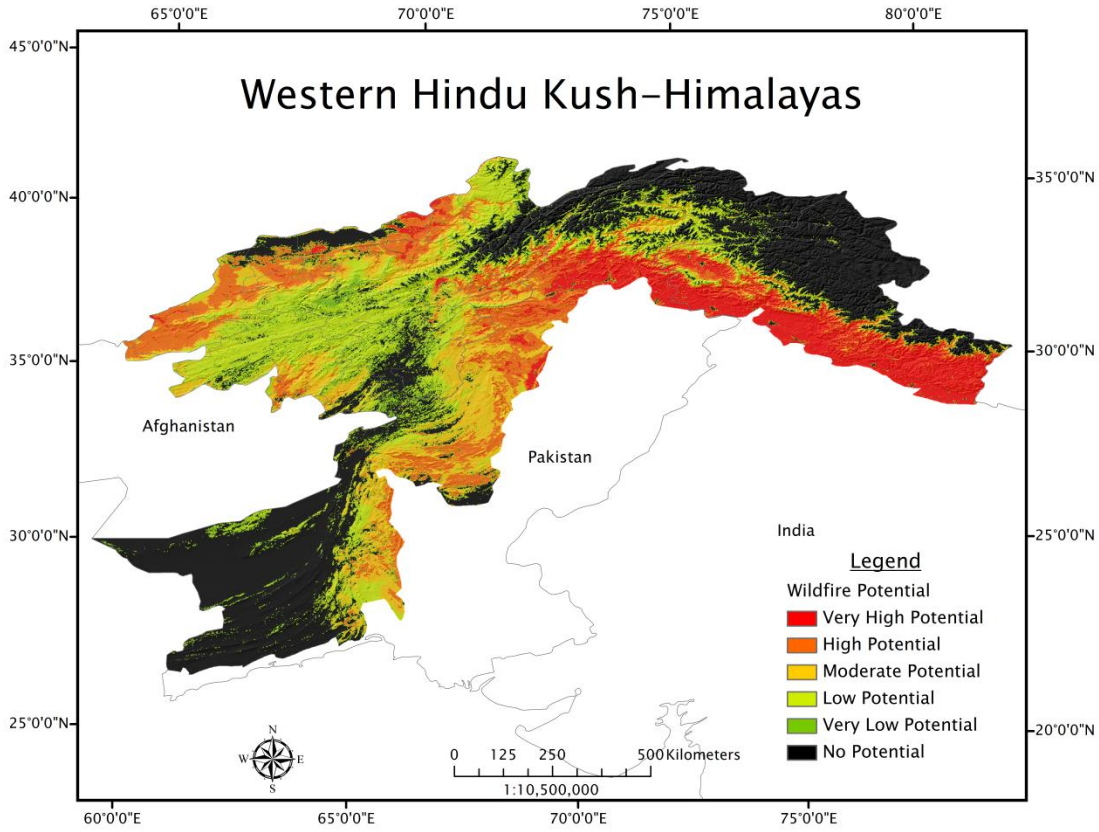

Figure 43: Western Hindu Kush-Himalayas Wildfire Potential Model

In the Afghanistan region of the Western Hindu Kush-Himalayas, low potential wildfire zones were the prevailing class of wildfire potential (Figure 44). The distributions of wildfire potential zones in the Western Hindu Kush-Himalayas of Afghanistan are mapped in Figure 45. Low potential wildfire zones accounted for 31.01% of the Afghanistan region of the Western Hindu Kush-Himalayas total area. Moderate potential

wildfire zones comprised 18.33% of the Afghanistan region, high potential wildfire zones accounted for 17.49%, and very low potential zones comprised 12.83% of the region. Very high potential wildfire zones accounted for only 2% of the Western Hindu Kush-Himalayas Afghanistan region, and zones of no wildfire potential comprised the region's remaining 18.34%.

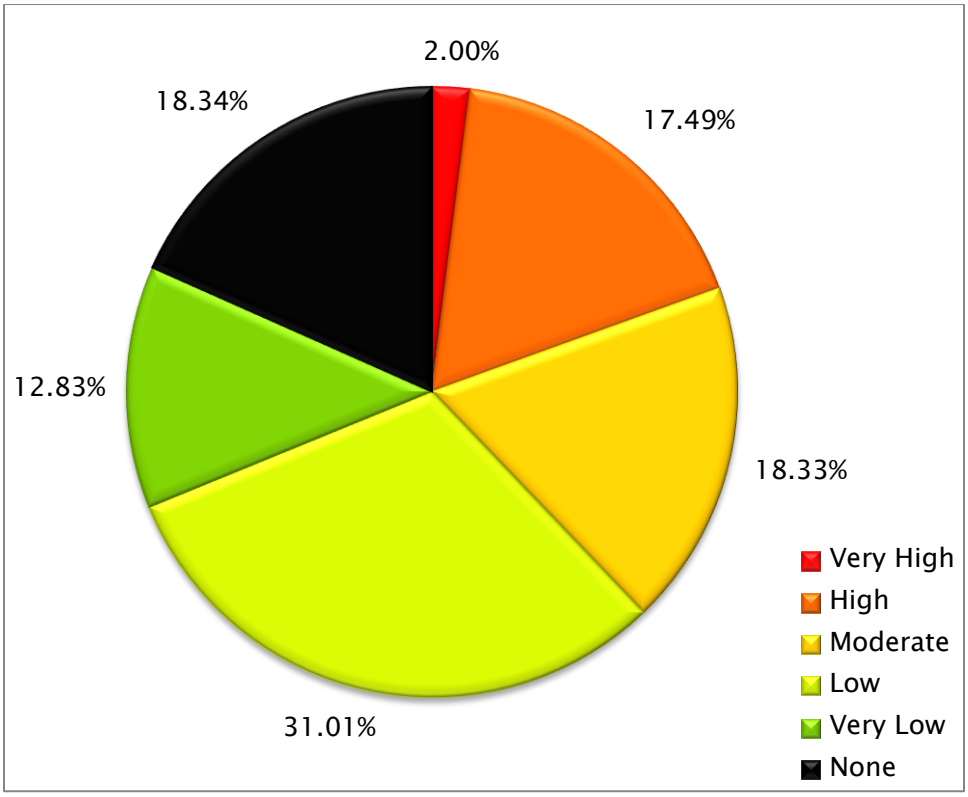

Figure 44: Percent Wildfire Potential in the Western Hindu Kush-Himalayas of Afghanistan

A total of 71,157.888 km^2 of no potential wildfire area was found in the Afghanistan region of the Western Hindu Kush-Himalayas with a standard deviation of 573.402 km^2. No potential wildfire zones had a mean area of 21.4 km^2, with the smallest area in the Afghanistan region measuring 66,382 m^2, and the largest area measuring 25,746.747 km^2. Very low potential wildfire area in the Afghanistan region of the Western Hindu Kush-Himalayas totaled 49,834.631 km^2 with a standard deviation of 16.999 km^2. The smallest area of very low wildfire potential in the Afghanistan region measured 1,104.370 m^2 and the largest area measured 1,799 km^2. Mean very low wildfire potential area in the Afghanistan region of the Western Hindu Kush-Himalayas measured 3.446 km^2.

Low potential wildfire area in the Afghanistan region of the Western Hindu Kush-Himalayas totaled 120,408.958 km^2 with a standard deviation of 781.394 km^2. The smallest area of low wildfire potential in the Afghanistan region measured 7,596.689 m^2 and the largest area measured 64,149.771 km^2. Mean low wildfire potential area in the

Afghanistan region of the Western Hindu Kush-Himalayas measured 16.744 km^2. Moderate potential wildfire area in the Afghanistan region totaled 71,259.868 km^2 with a standard deviation of 281.393 km^2. The smallest area of moderate wildfire potential in the Afghanistan region of the Western Hindu Kush-Himalayas measured 1,287.610 m^2 and the largest area measured 10,165.410 km^2. Mean moderate wildfire potential area in the Afghanistan region measured 16.158 km^2.

High potential wildfire area in the Afghanistan region of the Western Hindu Kush-Himalayas totaled 67,956.118 km^2 with a standard deviation of 691.833 km^2. The smallest area of high wildfire potential in the Afghanistan region measured 2,459.531 m^2 and the largest area measured 23,731.989 km^2. Mean high wildfire potential area in the Afghanistan region of the Western Hindu Kush-Himalayas measured 36.713 km^2. Very high potential wildfire area in the Afghanistan region totaled 7,784.324 km^2 with a standard deviation of 43.561 km^2. The smallest area of very high wildfire potential in the Afghanistan region of the Western Hindu Kush-Himalayas measured 97,279.593 m^2 and the

largest area measured 1,037 km^2. Mean very high wildfire potential area in the Afghanistan region measured 6.574 km^2.

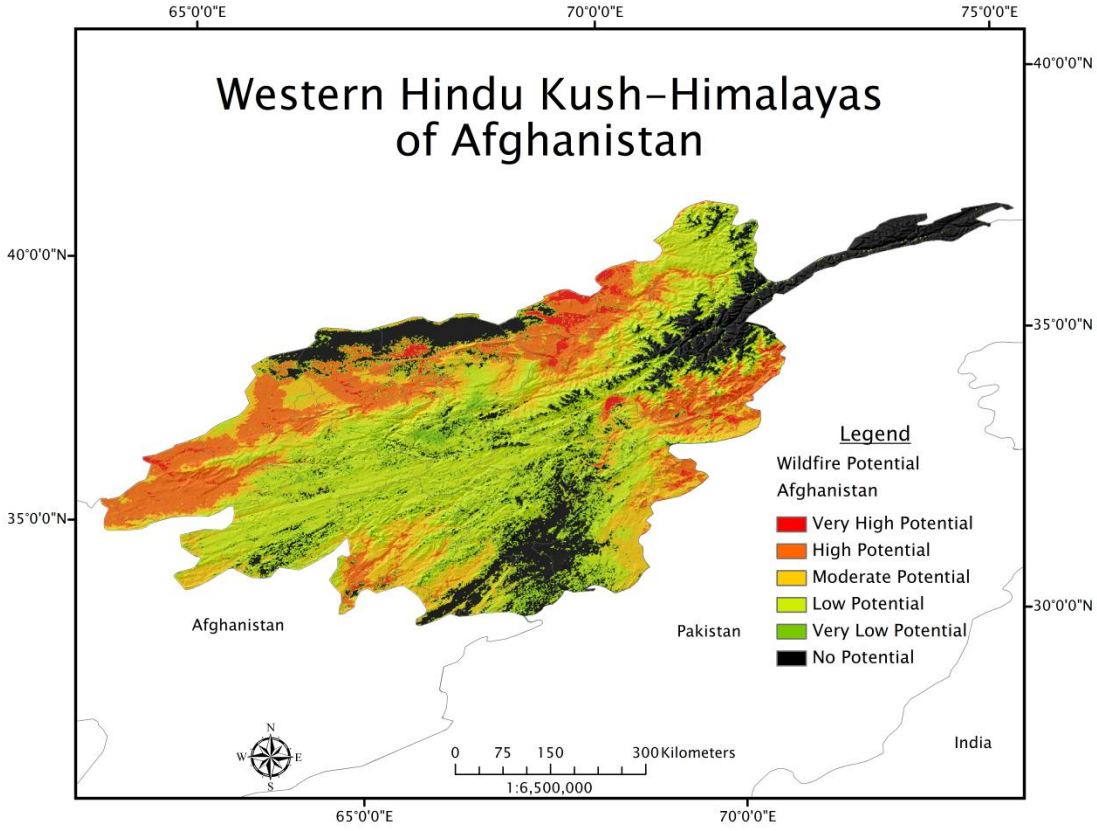

Figure 45: Western Hindu Kush-Himalayas Wildfire Potential Model for Afghanistan

In the Pakistan region of the Western Hindu Kush-Himalayas, moderate potential wildfire zones were the prevailing class of wildfire potential (Figure 46). The class distributions in the Western Hindu Kush-Himalayas of Pakistan are mapped in Figure 47. Moderate potential

wildfire zones accounted for 15.64% of the Pakistan region's total area. High potential wildfire zones comprised 13.44% of the Pakistan region of the Western Hindu Kush-Himalayas, low potential wildfire zones accounted for 7.85%, and very low potential zones comprised 7.17% of the region. Very high potential wildfire zones accounted for 6.03% of the Western Hindu Kush-Himalayas Pakistan region, and zones of no wildfire potential comprised the region's remaining 49.87%.

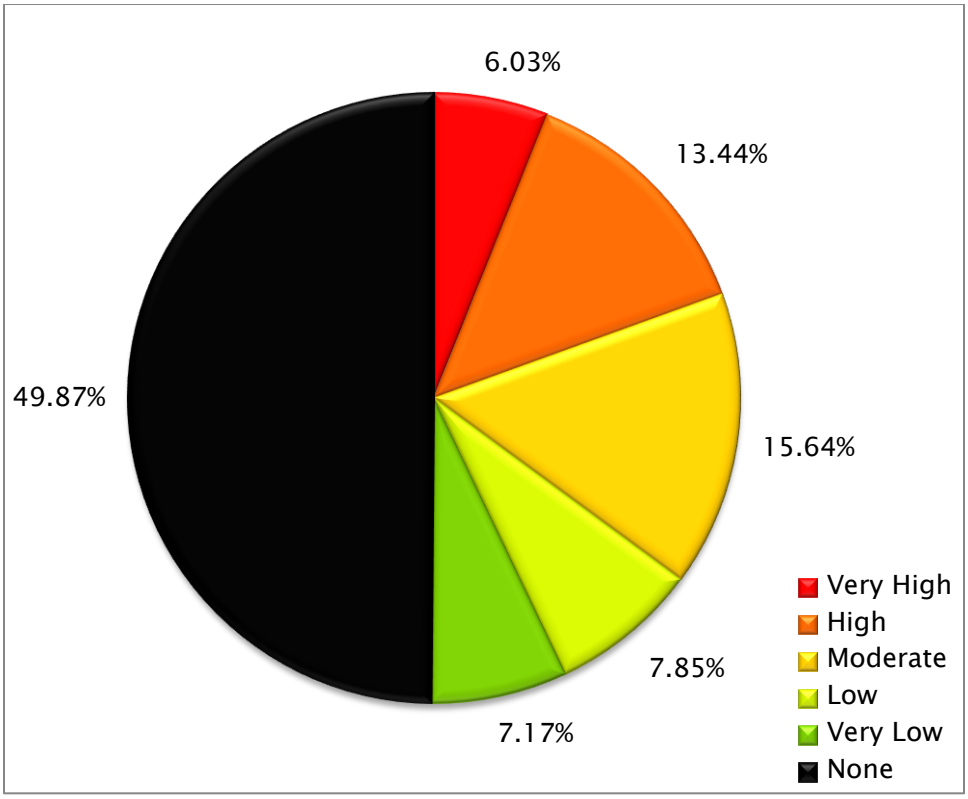

Figure 46: Percent Wildfire Potential
in the Western Hindu Kush-Himalayas of Pakistan

A total of 238,626.612 km^2 of no potential wildfire area was found in the Pakistan region of the Western Hindu Kush-Himalayas with a standard deviation of 4,259.748 km^2. No potential wildfire zones had a mean area of 150.648 km^2, with the smallest area in the Pakistan region measuring 50,237.211 m^2, and the largest area measuring 158,670.076 km^2. Very low potential wildfire area in the Pakistan region of the

Western Hindu Kush-Himalayas totaled 34,329.264 km^2 with a standard deviation of 5.072 km^2. The smallest area of very low wildfire potential in the Pakistan region measured 172.525 m^2 and the largest area measured 218 km^2. Mean very low wildfire potential area in the Pakistan region of the Western Hindu Kush-Himalayas measured 2.960 km^2.

Low potential wildfire area in the Pakistan region of the Western Hindu Kush-Himalayas totaled 120,408.958 km^2 with a standard deviation of 781.394 km^2. The smallest area of low wildfire potential in the Pakistan region measured 1,332.069 m^2 and the largest area measured 3,716.860 km^2. Mean low wildfire potential area in the Pakistan region of the Western Hindu Kush-Himalayas measured 4.981 km^2. Moderate potential wildfire area in the Pakistan region totaled 74,832.878 km^2 with a standard deviation of 535.083 km^2. The smallest area of moderate wildfire potential in the Pakistan region measured 367.253 m^2 and the largest area measured 34,299.363 km^2. Mean moderate wildfire potential area in the Pakistan region of the Western Hindu Kush-Himalayas measured 17.202 km^2.

High potential wildfire area in the Pakistan region of the Western Hindu Kush-Himalayas totaled 64,321.042 km^2 with a standard deviation of 368.416 km^2. The smallest area of high wildfire potential in the Pakistan region measured 4,630.820 m^2 and the largest area measured 15,484.573 km^2. Mean high wildfire potential area in the Pakistan region of the Western Hindu Kush-Himalayas measured 22.363 km^2. Very high potential wildfire area in the Pakistan region totaled 28,814.224 km^2 with a standard deviation of 568.585 km^2. The smallest area of very high wildfire potential in the Pakistan region measured 960.624 m^2 and the largest area measured 20,362.180 km^2. Mean very high wildfire potential area in the Pakistan region of the Western Hindu Kush-Himalayas measured 22.302 km^2.

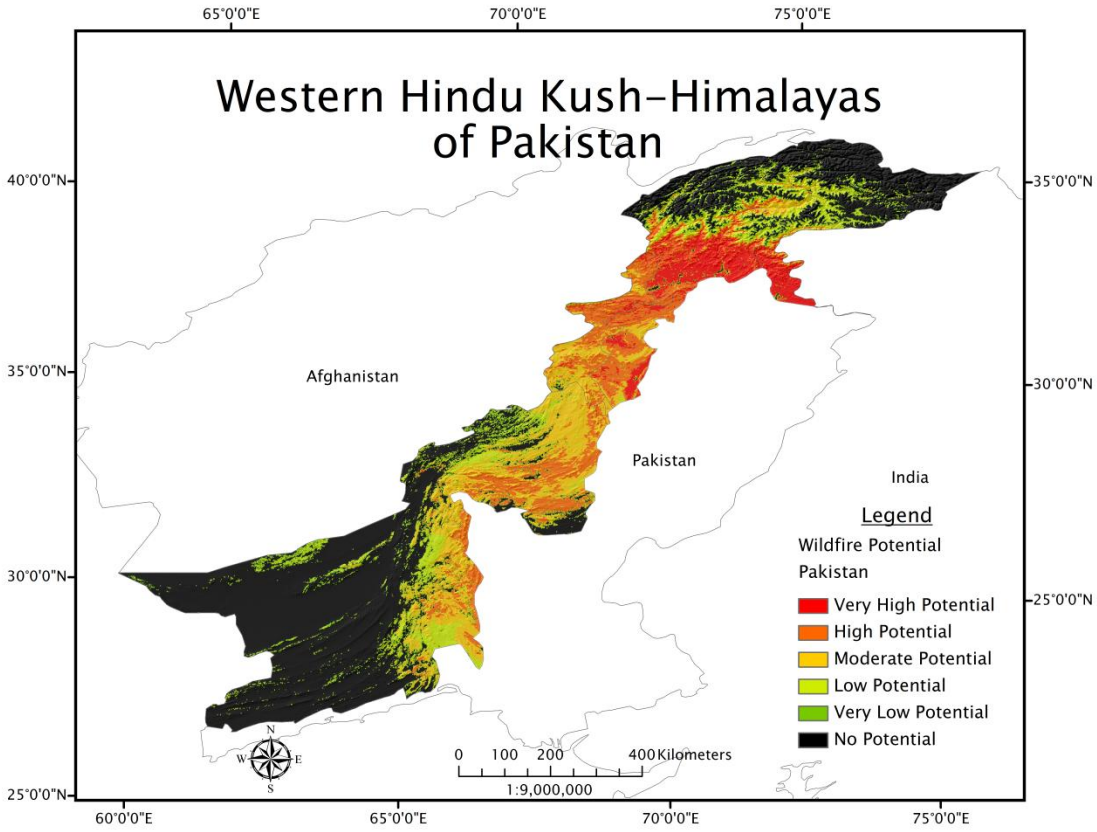

Figure 47: Western Hindu Kush-Himalayas
Wildfire Potential Model for Pakistan

In the India region of the Western Hindu Kush-Himalayas, very high potential wildfire zones were the prevailing class of wildfire potential (Figure 48). Class distributions in the Western Hindu Kush-Himalayas of India are mapped in Figure 49. Very high potential wildfire zones accounted for 34.91% of the India region's total area. High potential wildfire zones comprised 8.43% of the India region of the Western Hindu

Kush-Himalayas, low potential wildfire zones accounted for 4.15%, and moderate potential zones comprised 3.7% of the region. Very low potential wildfire zones accounted for 3.05% of the Western Hindu Kush-Himalayas India region, and zones of no wildfire potential comprised the region's remaining 45.76%.

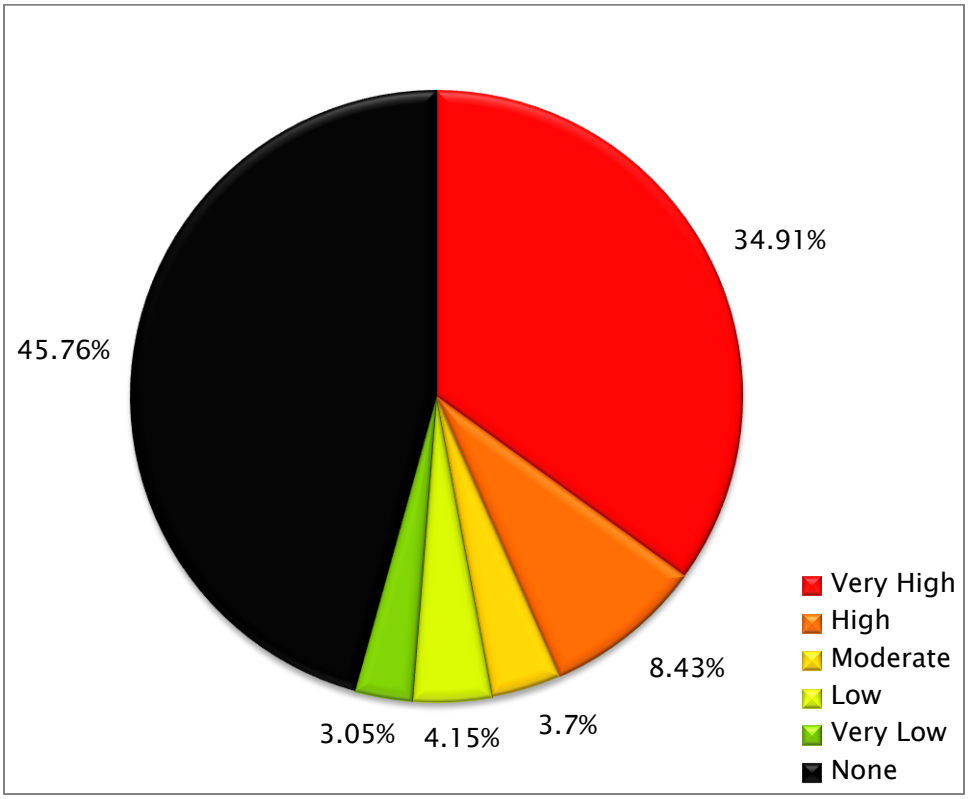

Figure 48: Percent Wildfire Potential
in the Western Hindu Kush-Himalayas of India

A total of 96,972.760 km^2 of no potential wildfire area was found in the India region of the Western Hindu Kush-Himalayas with a standard deviation of 5,829.822 km^2. No potential wildfire zones had a mean area of 484.863 km^2 with the smallest area in the India region measuring 402,417.025 m^2 and the largest area measuring 81,564.261 km^2. Very low potential wildfire area in the India region of the Western Hindu Kush-Himalayas totaled 6,476.581 km^2 with a standard deviation of 2.739 km^2. The smallest area of very low wildfire potential in the India region measured 29,334.729 m^2 and the largest area measured 32 km^2. Mean very low wildfire potential area in the India region of the Western Hindu Kush-Himalayas measured 2.597 km^2.

Low potential wildfire area in the India region of the Western Hindu Kush-Himalayas totaled 8,797.534 km^2 with a standard deviation of 46.789 km^2. The smallest area of low wildfire potential in the India region measured 6,273.170 m^2 and the largest area measured 1,289.943 km^2. Mean low wildfire potential area in the India region of the Western Hindu Kush-Himalayas measured 5.826 km^2. Moderate potential wildfire

area in the India region totaled 7,847.940 km^2 with a standard deviation of 10.122 km^2. The smallest area of moderate wildfire potential in the India region measured 53,133.556 m^2 and the largest area measured 194 km^2. Mean moderate wildfire potential area in the India region of the Western Hindu Kush-Himalayas measured 4.333 km^2.

High potential wildfire area in the India region of the Western Hindu Kush-Himalayas totaled 17,888.929 km^2 with a standard deviation of 23.251 km^2. The smallest area of high wildfire potential in the India region measured 6,327.487 m^2 and the largest area measured 945 km^2. Mean high wildfire potential area in the India region of the Western Hindu Kush-Himalayas measured 4.850 km^2. Very high potential wildfire area in the India region totaled 74,250.651 km^2 with a standard deviation of 1,997.013 km^2. The smallest area of very high wildfire potential in the India region measured 391,925.173 m^2 and the largest area measured 66,109.872 km^2. Mean very high wildfire potential area in the India region of the Western Hindu Kush-Himalayas measured 67.562 km^2.

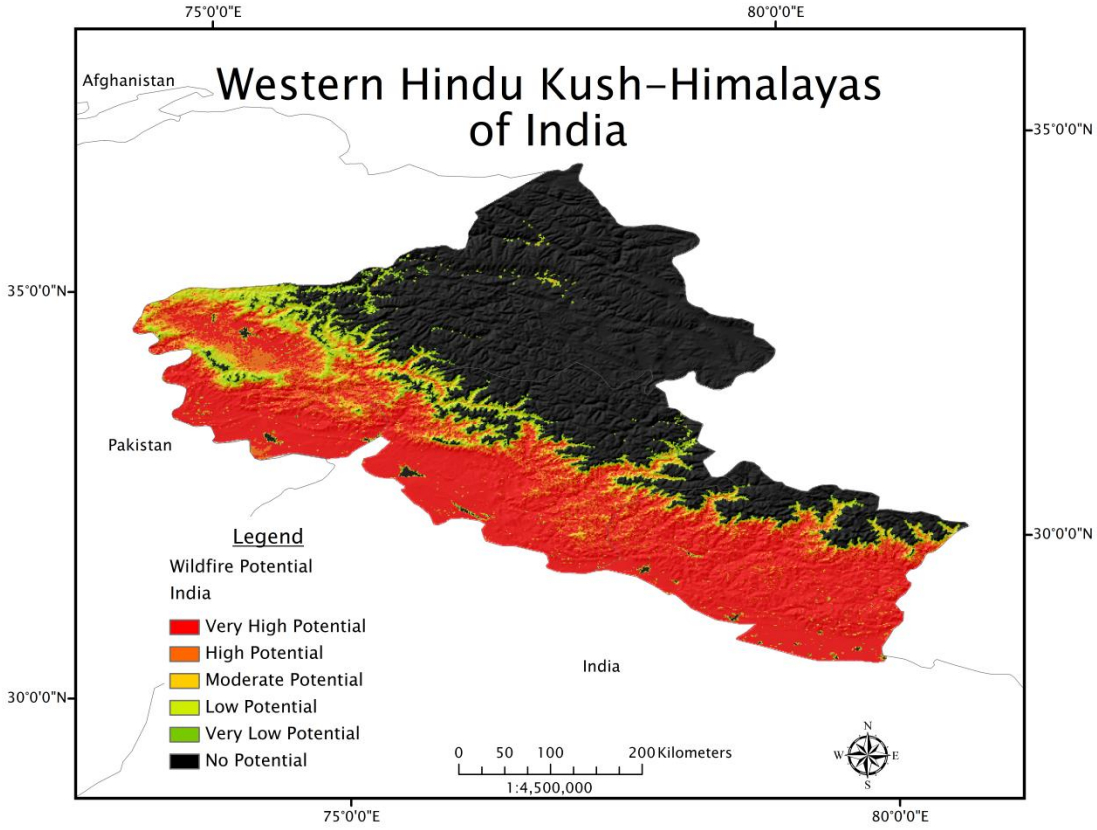

Figure 49: Western Hindu Kush-Himalayas
Wildfire Potential Model for India

The Western Hindu Kush-Himalayas wildfire potential model was then compared to the region's states and provinces, by country. Analysis of the wildfire potential model by state and province allowed for the identification of specific regional locations that were at the greatest risk of wildfire activity. This identified the location with the greatest potential for wildfire activity in the Western Hindu Kush-Himalayas as well as the

location of greatest wildfire potential in each regional country.

In the Western Hindu Kush-Himalayas, the location with the greatest potential for wildfire activity is Uttarakhand State in India. The state of Uttarakhand has a total of 32,615 km^2 of area with a standard deviation of 2,294.002 km^2 with very high potential for wildfire activity. This is equal to 64.266% of Uttarakhand States total land area, and comprises 15.367% of the Western Hindu Kush Himalayas of India.

The location with the greatest potential for wildfire in the Western Hindu Kush-Himalayas of Afghanistan is Kunduz Province. Kunduz Province has 1,872.623 km^2 of land area with a standard deviation of 141.384 km^2 with very high potential for wildfire activity. This comprises 23.336% of the total land area of Kunduz Province, and 0.482% of the Western Hindu Kush-Himalayas of Afghanistan.

The North-West Frontier Province in Pakistan has the greatest potential for wildfire activity in the Western Hindu Kush Himalayas of Pakistan. In the North-West Frontier Province a total of 20,522.642 km^2 of land area with a standard deviation of 523.083 km^2 has very high

potential for wildfire activity. This is equal to 27.485% of the North-West Frontier Province's total land area, and 4.288% of the Western Hindu Kush-Himalayas of Pakistan. Table 1 of Appendix B is a breakdown of wildfire potential in the states and provinces of the Western Hindu Kush-Himalayas.

Discussion

This study identified environmental, topological, and sociological factors that contribute to wildfire ignitions in the Western Hindu Kush-Himalayas, and modeled regional wildfire potential. Questions addressed by the research included:

1. Is there a relationship between land cover type and the locations of regional wildfire ignitions?
    a. Which land cover type has the greatest influence over regional wildfire ignitions?

A significant relationship was found between the locations of wildfires in the Western Hindu Kush-Himalayas and land cover type. The land cover type that had the greatest influence on the location of wildfire ignitions was mixed forest.

2. Is there a relationship between vegetation health and the locations of regional wildfire ignitions?

A significant relationship was found between the locations of wildfires in the Western Hindu Kush-Himalayas and vegetation

health. Wildfires in the Western Hindu Kush-Himalayas occurred predominantly in low health vegetation.

3. Is there a relationship between elevation and the locations of regional wildfire ignitions?

A significant relationship was found between the locations of wildfires in the Western Hindu Kush-Himalayas and elevation. Wildfires in the Western Hindu Kush-Himalayas occurred predominantly at very low elevations.

4. Does a relationship exist between aspect and the locations of regional wildfire ignitions?

A significant relationship was found between the locations of wildfires in the Western Hindu Kush-Himalayas and aspect. Wildfires in the Western Hindu Kush-Himalayas occurred predominantly on South facing aspects.

5. Is there a relationship between slope and the locations of regional wildfire ignitions?

A significant relationship was found between the locations of

wildfires in the Western Hindu Kush-Himalayas and slope. Wildfires in the Western Hindu Kush-Himalayas occurred predominantly on gentle slopes.

6. Is there a relationship between distance to road networks and the locations of regional wildfire ignitions?

   A significant relationship was found between the locations of wildfires in the Western Hindu Kush-Himalayas and distance to road features. Wildfires in the Western Hindu Kush-Himalayas occurred predominantly at very close distance to road features.

7. Does a relationship between distance to water features and the location of regional wildfire ignitions?

   A significant relationship was found between the locations of wildfires in the Western Hindu Kush-Himalayas and distance to water features. Wildfires in the Western Hindu Kush-Himalayas occurred predominantly at very close distance to water features.

8. Does a relationship exist between distance to settlements and the location of regional wildfire ignitions?

A significant relationship was not found between the locations of wildfires in the Western Hindu Kush-Himalayas and distance to settlements. Distance to settlements does not appear to be an effective indicator of wildfire locations in the Western Hindu Kush-Himalayas. Wildfires in the Western Hindu Kush-Himalayas occurred predominantly at distances far from settlements.

The study produced a model of wildfire potential in the Western Hindu Kush-Himalayas, and created thematic maps of regional wildfire potential. Multi-criteria evaluation with weighted linear combination successfully generated a significant model of wildfire potential.

The multi-criteria evaluation did an effective job of modeling wildfire potential in the Western Hindu Kush-Himalayas, although the presence of classification errors in the MODIS land cover data set may have lead to errors of omission in the wildfire potential model. The presence of topographic shadows resulted in misclassification of mountain shadows as water due to the similar spectral properties of the shadows and regional water features at moderate resolution. The

contrast of the topographic shadows against snow covered surfaces further intensified the effect resulting in misclassifications. For analyses performed in mountainous terrain, it is recommended that single pixel high elevation water be evaluated for correct classification, and any misclassifications of mountain shadows be appropriately corrected to improve model accuracy. MODIS data along with GIS data can be effectively integrated using multi-criteria evaluation with weighted linear combination to model wildfire potential with an acceptable level of error.

Additionally, model accuracy could have been enhanced through the inclusion of atmospheric factors including maximum surface temperature, mean wind speed and direction, and mean humidity. The use of data from multiple fire seasons in the analysis and modeling could have also enhanced the accuracy of the wildfire potential model. Validation of the model could have been enhanced through the use of in-situ data collection and analysis. Also, the wildfire potential model is based on satellite based wildfire detections and distributions, and could be improved through the inclusion of in-situ wildfire detections. The

inclusion of in-situ wildfire detections would allow the model to reflect wildfire potential based on true regional wildfire distributions.

Recommendations for further research include the building of a refined wildfire potential model that includes data derived from multiple peak wildfire seasons. An improved model that includes relevant environmental and atmospheric factors could also improve knowledge of wildfire potential in the Western Hindu Kush-Himalayas. The construction of a model at a finer resolution would allow for more precise identification of locations and environments that are prone to wildfire activity. A model constructed at a resolution of 30 m or less would provide additional spatial detail and more precise location information. In addition, the model could be extended to cover the entire Hindu Kush-Himalayas, providing the beneficial knowledge of the distribution of potential wildfire locations to the residents of the entire region. It would also be beneficial to use the model to forecast regional wildfire potential over consecutive wildfire seasons. This would allow regional wildfire

potential to be identified in both space and time, permitting more precise mitigation strategies and practices.

The model produced in this research allows the region's people, governments, and non-governmental organizations the opportunity to evaluate the potential for wildfires and create appropriate mitigation strategies. With knowledge of the locations of potential wildfires, the residents of the Western Hindu Kush-Himalayas can develop more sustainable agricultural and animal husbandry practices. It also allows the residents of the region to focus their economic activities in locations that are less susceptible to wildfires and their resulting loss of resources. The modeling of wildfire potential permits the residents of the Western Hindu Kush-Himalayas the opportunity to protect their livelihoods and precious resources, while minimizing degradation of a beautiful and strained environment.

References

Adil, A.W. (2001). The integration of biodiversity into national environmental assessment procedures: National case studies, Afghanistan. Retrieved March 25, 2011, from the United Nations via United Nations Environment Programme – Biodiversity Planning Support Programme: http://www.unep.org/bpsp/EIA/Case Studies/Afghanistan (EIA).pdf.

Agrawal, A.K. (1990). Floristic composition and phenology of temperate grasslands of Western Himalaya as affected by scraping, fire and heavy grazing. *Vegetatio, 88(2)*, 177-187.

Ahmad, A. (1993). Environmental impact assessment in the Himalayas: An ecosystem approach. *Ambio, 22(1)*, 4-9.

Anderson, R. (2008). Modern methods for robust regression. Thousand Oaks, CA: Sage Publications Inc.

Arno, S.F., & Allison-Bunnell, S. (2002). Flames in our forest: Disaster or renewal?. Washington, DC: Island Press.

Bagchi, S., Mishra, C., & Bhatnagar, Y.V. (2004). Conflicts between traditional pastoralism and conservation of Himalayan ibex (*Capra sibirica*) in the Trans-Himalayan mountains. *Animal Conservation, 7*, 121-128.

Barnes, W.L., Pagano, T.S., & Salomonson, V.V. (1998). Prelaunch characteristics of the Moderate Resolution Imaging Spectroradiometer (MODIS) on EOS-AM1. *IEEE Transactions on Geoscience and Remote Sensing, 36(4)*, 1088-1100.

Bartlett, J.E., Kotrlik, J.W., & Higgins, C.C. (2001). Organizational research: Determining appropriate sample size in survey research. *Information Technology, Learning, and Performance Journal, 19(1)*, 43-50.

Berk, R.A. (1990). A primer on robust regression. In J. Fox, & J.S. Long, *Modern methods of data analysis* (pp. 292-324). Newbury Park, CA: Sage Publications Inc.

Boles, S.H., & Verbyla, D.L. (2000). Comparison of three AVHRR-based fire detection algorithms for Interior Alaska. *Remote Sensing of Environment, 72(1)*, 1-16.

Breckle, S.W. (1971). Vegetation in alpine regions of Afghanistan. In P.H. Davis, P.C. Harper, & I.C. Hedge (Eds.), *Plant Life of South-West Asia* (pp. 106-115). Edinburgh, Scotland: Botanical Society of Edinburgh.

Burt, J.E., Barber, G.M., & Rigby, D.L. (2009). Elementary statistics for geographers (3rd ed.). New York, NY: The Guilford Press.

Chand, T.R.K., Badarinath, K.V.S., Murthy, M.S.R, Rajshekhar, G., Elvidge, C.D., & Tuttle, B.T. (2007). Active forest fire monitoring in Uttaranchal State, India using multi-temporal DMSP-OLS and MODIS data. *International Journal of Remote Sensing, 28(10)*, 2123-2132.

Chien, S., Cichy, B., Davies, A., Tran, D., Rabideau, G., & Castano, R. (2005). An autonomous earth-observing sensorweb. *IEEE Intelligent Systems*, *5*, 16-24.

Cochran, W.G. (1977). Sampling techniques (3rd ed.). New York, NY: John Wiley & Sons, Inc.

Cornelis, C., Deschrijver, G., & Kerre, E.E. (2004). Implication in intuitionistic fuzzy and interval-valued fuzzy set theory: Construction, classification, application. *International Journal of Approximate Reasoning, 35(1)*, 55-95.

Davis, K.P., Byram, G.M., & Krumm, W.R. (1959). Forest fire: Control and use. York, PA: The Maple Press Company.

Eastman, J.R. (2009). IDRISI Taiga (Version 16.05) [Computer Software]. Worcester, MA: Clark University.

ERDAS Inc. (2002). ERDAS ViewFinder (Version 2.1) [Computer Software]. Atlanta, GA: ERDAS Incorporated.

Esaias, W.E., Abbott, M.R., Barton, I., Brown, O.B., Campbell, J.W., Carder, K.L., Clark, D.K., Evans, R.H., Hoge, F.E., Gordon, H.R., Balch, W.M., Letelier, R., & Minnett, P.J. (1998). An overview of MODIS capabilities for ocean science observations. *IEEE Transactions on Geoscience and Remote Sensing, 36(4)*, 1250-1265.

ESRI Inc. (2010). ArcGIS Desktop (Version 10.0) [Computer Software]. Redlands, CA: Environmental Systems Research Institute.

ESRI Inc. (2004). ESRI Data and Maps: World, Europe, Canada, and Mexico [CD-ROM]. Redlands, CA: Environmental Systems Research Institute.

Flasse, S.P., & Ceccato, P. (1996). A contextual algorithm for AVHRR fire detection. *International Journal of Remote Sensing, 17*, 419-424.

Franz, B.A., Werdell, P.J., Meister, G., Kwiatkowska, E.J., Bailey, S.W., Ahmad, Z., & McClain, C.R. (2006). MODIS land bands for ocean remote sensing applications. *Proceedings of Ocean Optics XVIII*. Montreal, Quebec Canada.

Frost, P., & Vosloo, H. (2006). Providing satellite-based early warnings of fires to reduce fire flashovers on South Africa's transmission lines. *10th Biennial Australasian Bushfire Conference (Bushfire Conference 2006)*. Brisbane, Australia.

Fuller, M. (1991). Forest fires: An introduction to wildland fire behavior, management, firefighting, and prevention. New York, NY: John Wiley & Sons, Inc.

Giglio, L., Csiszar, I., & Justice, C.O. (2006). Global distribution and seasonality of active fires as observed with the Terra and Aqua Moderate Resolution Imaging Spectroradiometer (MODIS) sensors. *Journal of Geophysical Research, 111*, G02016.

Giglio, L., Descloitres, J., Justice, C.O., & Kaufman, Y.J. (2003). An enhanced contextual fire detection algorithm for MODIS. *Remote Sensing of Environment, 87(2-3)*, 273-282.

Guenther, B., Xiong, X., Salomonson, V.V., Barnes, W.L., & Young, J. (2002). On-orbit performance of the Earth Observing System Moderate Resolution Imaging Spectroradiometer: First year of data. *Remote Sensing of Environment, 83(1-2)*, 16-30.

Gupta, H.K., & Delany, F.M. (Eds.). (1981). Zagros, Hindu Kush, Himalaya, geodynamic evolution. Washington, DC: American Geophysical Union.

Gupta, R.K. (1978). Impact of human influences on the vegetation of the western Himalaya. *Vegetatio, 37(2)*, 111-117.

Gupta, R.K. (1972). Boreal and arcto-alpine elements in the flora of western Himalaya. *Vegetatio, 24(1-3)*, 159-175.

Hall, D.K., Riggs, G.A., Salomonson, V.V., DiGirolamo, N.E., & Bayr, K.J. (2002). MODIS snow-cover products. *Remote Sensing of Environment, 83(1-2)*, 181-194.

Hall, D.K., Riggs, G.A., & Salomonson, V.V. (2001). *Algorithm theoretical basis document (ATBD) for the MODIS snow and sea ice-mapping algorithms*. (NASA Publication No. ATBD-MOD-10). Greenbelt, MD: NASA Goddard Space Flight Center.

Hardy, C. (2005). Wildland fire hazard and risk: Problems, definitions, and context. *Forest Ecology and Management, 211*, 73-82.

Hawbaker, T.J., Radeloff, V.C., Syphard, A.D., Zhu, Z., & Stewart, S.I. (2008). Detection rates of the MODIS active fire product in the United States. *Remote Sensing of Environment, 112(5)*, 2656-2664.

Hefeeda, M., Bagheri, M. (2007). Wireless sensor networks for early detection of forest fires. *2007 IEEE International Conference on Mobile Adhoc and Sensor Systems*. Pisa, Italy.

Hewitt, K., Wake, C.P., Young, G.J., & David, C. (1989). Hydrological investigations at Biafo glacier, Karakoram Range, Himalaya; an important source of water for the Indus River. *Annals of Glaciology, 13*, 103-108.

Hussin, Y.A., Matakala, M., & Zagdaa, N. (2008). The applications of remote sensing and GIS in modeling forest fire hazard in Mongolia. *The International Archives of the Photogrammetry, Remote Sensing and Spatial Information Sciences, 37(B8)*, 289-294.

Ichoku, C., Giglio, L., Wooster, M.J., Remer, L.A. (2008). Global characterization of biomass-burning patterns using satellite measurements of fire radiative energy. *Remote Sensing of Environment, 112(6)*, 2950-2962.

ICIMOD. (2011). Mountain Peaks [Data file]. Kathmandu, Nepal: The International Centre for Integrated Mountain Development.

ICIMOD. (2010). HKH Outline [Data file]. Kathmandu, Nepal: The International Centre for Integrated Mountain Development.

Jaiswal, R.K., Mukherjee, S., Raju, K.D., & Saxena, R. (2002). Forest fire risk zone mapping from satellite imagery and GIS. *International Journal of Applied Earth Observation and Geoinformation, 4*, 1-10.

Jenks, G.F., & Caspall, F.C. (1971). Error on choropleth maps: Definition, measurement, and reduction. *Annals of the Association of American Geographers, 61(2)*, 217-244.

Joshi, S.C. (2003). Impact of forest fires on the regional climate. *Current Science, 85(1)*, 41-45.

Justice C.O., Townshend, J.R.G., Vermote, E.F., Masuoka, E., Wolfe, R.E., Saleous, N., Roy, D.P., & Morisette, J.T. (2002). An overview of MODIS land data processing and product status. *Remote Sensing of Environment, 83(1-2)*, 3-15.

Justice C.O., Vermote, E., Townshend, J.R.G., Defries, R., Roy, D.P., Hal, D.K., Salomonson, V.V., Privette, J.L., Riggs, G., Strahler, A., Lucht, W., Myneni, R.B., Knyazikhin, Y., Running, S.W., Nemani, R.R., Wan, Z., Huete, A.R., van Leeuwen, W., Wolfe, R.E., Giglio, L., Muller, J-P., Lewis, P., & Barnsley, M.J. (1998). The Moderate Resolution Imaging Spectroradiometer (MODIS): Land remote sensing for global change research. *IEEE Transactions on Geoscience and Remote Sensing, 36(4)*, 1228-1249.

King, M.D., Kaufman, Y.K., Menzel, W.P., & Tanré, D. (1992). Remote sensing of cloud, aerosol, and water vapor properties from the Moderate Resolution Imaging Spectroradiometer (MODIS). *IEEE Transactions on Geoscience and Remote Sensing, 30(1)*, 2-27.

Klimeš, L. (2003). Life-forms and clonality of vascular plants along an altitudinal gradient in E Ladakh (NW Himalayas). *Basic and Applied Ecology, 4(4)*, 317-328.

Kohavi, R. (1995). A study of cross-validation and bootstrap for accuracy estimation and model selection. *The International Joint Conference on Artificial Intelligence (IJCAI)*. Montreal, Quebec Canada.

Li, Z., Fraser, R., Jin, J., Abuelgasim, A.A., Csiszar, I., Gong, P., Pu, R., & Hao, W. (2003). Evaluation of algorithms for fire detection and mapping across North America from satellite. *Journal of Geophysical Research, 108*, D24076.

Li, Z., Kaufman, Y.J., Ichoku, C., Fraser, R., Trishchenko, A., Giglio, L., Jin, J., & Yu, X. (2001). A review of AVHRR-based active fire detection algorithms: Principles, limitations, and recommendations. In F.J. Ahern, J.G. Goldammer, & C.O. Justice (Eds.), *Global and regional vegetation fire monitoring from space: Planning a coordinated international effort* (pp. 199-225). The Hague, The Netherlands: SPB Academic Publishing BV.

Mayer, C., Lambrecht, A., Belò, M., Smiraglia, C., & Diolaiuti, G. (2006). Glaciological characteristics of the ablation zone of Baltoro glacier, Karakoram, Pakistan. *Annals of Glaciology, 43*, 123-131.

McNamara, D., Stephens, G., & Ruminiski, M. (2002). NOAA's multi-sensor fire detection program using environmental satellites. *Earth System Monitor, 13(1)*, 1-7.

Menon, A.G.K. (1954). Fish geography of the Himalayas. *Proceedings of the National Institute of Science of India, 20(4)*, 467-493.

Miehe, G., Miehe, S., & Schlütz, F. (2009). Early human impact in the forest ecotone of southern High Asia (Hindu Kush, Himalaya). *Quaternary Research, 71*, 255-265.

Molinaro, A.M., Simon, R., & Pfeiffer, R.M. (2005). Prediction error estimation: A comparison of resampling methods. *Bioinformatics, 21(15)*, 3301-3307.

Morisette, J.T., Giglio, L., Csiszar, I., Setzer, A., Schroeder, W., Morton, D., & Justice, C.O. (2005). Validation of MODIS active fire detection products derived from two algorithms. *Earth Interactions, 9*, 1-25.

Naithani, A.K., Nainwal, H.C., Sati, K.K., & Prasad, C. (2001). Geomorphological evidences of retreat of the Gangotri glacier and its characteristics. *Current Science, 80(1)*, 87-94.

NASA Land Process Distributed Active Archive Center (LPDAAC). (2011). MODIS products. Sioux Falls, SD: USGS/Earth Resources Observation and Science (EROS) Center. Retrieved September 15, 2011, from https://lpdaac.usgs.gov/products/

NASA MODIS Web, (2011). Data products. Greenbelt, MD: NASA Goddard Space Flight Center. Retrieved September 15, 2011, from http://modis.gsfc.nasa.gov/data/

Nishihama, M., Wolfe, R., Solomon, D., Patt, F., Blanchette, J., Fleig, A., & Masuoka, E. (1997). *MODIS level 1A earth location: Algorithm theoretical basis document version 3.0* (NASA Publication No. ATBD-MOD-28). Greenbelt, MD: NASA Goddard Space Flight Center.

Ohsawa, M., Shakya, P.R., & Numata, M. (1986). Distribution and succession of West Himalayan forest types in the eastern part of the Nepal Himalaya. *Mountain Research and Development, 6(2)*, 143-157.

O'Sullivan, D., & Unwin, D. (2003). Geographic information analysis. Hoboken, NJ: John Wiley & Sons, Inc.

Platnick, S., King, M.D., Ackerman, S.A., Menzel, W.P., Baum, B.A., Riedi, J.C., & Frey, R.A. (2003). The MODIS cloud products: Algorithms and examples from Terra. *IEEE Transactions on Geoscience and Remote Sensing, 41(2)*, 459-473.

Prestemon, J., Pye, J., Butry, D., Holmes, T., & Mercer, D. (2002). Understanding broadscale wildfire risks in a human-dominated landscape. *Forest Science, 48(4)*, 685-693.

Price, T., Zee, J., Jamdar, K., & Jamdar, J. (2003). Bird species diversity along the Himalayas: A comparison of Himachal Pradesh with Kashmir. *Journal of the Bombay Natural History Society, 100*, 394-409.

Princeton University. (2006). Wildfire. *WordNet 3.0*. Retrieved February 23, 2011, from http://wordnetweb.princeton.edu/perl/webwn.

Pyne, S.J. (1984). Introduction to wildland fire. New York, NY: John Wiley & Sons, Inc.

Quayle, B. (2002). Rapid mapping of active wildland fires: integrating satellite remote sensing, GIS, and internet technologies. (USFS Publication No. 0371-3805). Salt Lake City, UT: USFS Technology & Development Program.

R Development Core Team. (2008). R: A language and environment for statistical computing (Version 2.8.1) [Computer Software]. Vienna, Austria: R Foundation for Statistical Computing.

Read, S., Mitchell, K., Teague, M., Masuoka, E. (2004). *MODIS science data processing software version 4.0 system description* (NASA Publication No. SDST-119B). Greenbelt, MD: NASA Goddard Space Flight Center.

Refaeilzadeh, P., Tang, L., & Liu, H. (2009). Cross-validation. In L. Liu, & M.T. Özsu (Eds.), *Encyclopedia of database systems* (pp. 532-538). New York, NY: Springer.

Remer, L.A., Kaufman, Y.J., Tanré, D., Mattoo, S., Chu, D.A., Martins, J.V., Li, R.R., Ichoku, C., Levy, R.C., Kleidman, R.G., Eck, T.F., Vermote, E., & Holben, B.N. (2005). The MODIS aerosol algorithm, products, and validation. *Journal of the Atmospheric Sciences-Special Section, 62*, 947-973.

Rousseeuw, P.J., & Leroy, A.M. (1987). Robust regression and outlier detection. New York, NY: John Wiley & Sons, Inc.

Roy, P.S. (2004). Forest fire and degradation assessment using satellite remote sensing and geographic information systems. In M.V.K. Sivakumar, P.S. Roy, K. Harmesen, & S.K. Saha (Eds.), *Satellite remote sensing and GIS applications in agricultural meteorology* (pp. 361-400). Geneva, Switzerland: World Meteorological Organization.

Sastry, K.L.N., Jadhav, R., & Thakker, P.S. (2002). Forest fire risk area mapping of gir – P.A. Integrating remote sensing, meteorological and topographical data – a GIS approach. *Map India 2002*. New Delhi, India.

Savtchenko, A., Ouzounov, D., Ahmad, S., Acker, J., Leptoukh, G., Koziana, J., & Nickless, D. (2004). Terra and Aqua MODIS products available from NASA GES DAAC. *Advances in Space Research, 34*, 710-714.

Schweinfurth, U. (1992). Mapping mountains: Vegetation in the Himalaya. *GeoJournal, 27(1)*, 73-83.

Shrestha, B.B. (2003). *Quercus semecarpifolia* Sm. in the Himalayan region: Ecology, exploitation and threats. *Himalayan Journal of Sciences, 1(2)*, 126-128.

Singh, J.S., & Singh, S.P. (1987). Forest Vegetation of the Himalaya. *The Botanical Review, 53(1)*, 80-192.

Singpurwalla, N.D., & Booker, J.M. (2004). Membership functions and probability measures of fuzzy sets. *Journal of the American Statistical Association, 99(467)*, 867-877.

SPSS Inc. (2010). IBM SPSS Statistics (Version 19.0.0.1) [Computer Software]. Armonk, NY: IBM Corporation.

Stipanicev, D., Bodrozic, L., & Vuko, T. (2007). Location determination of automatic forest fire monitoring stations based on AHP and GIS data. *Proceedings of TIEMS (The International Emergency Management Society) 2007 International Conference*. Trogir, Croatia.

Tata Energy and Resources Institute, North America (TERI-NA). (2002). Background paper on Himalayan ecology: Main issues and concerns. Retrieved March 26, 2011, from the United Nations via United Nations Public Administration Network: http://unpan1.un.org/intradoc/groups/public/documents/apcity/unpan015817.pdf.

Tiwari, P.C. (2000). Land-use changes in Himalaya and their impact on the plains ecosystem: need for sustainable land use. *Land Use Policy, 17*, 101-111.

Tucker, R.P. (1982). The forests of the Western Himalayas: The legacy of British colonial administration. *Journal of Forest History, 26(3)*, 112-123.

Vadrevu, K.P., Badarinath, K.V.S., & Anuradha, E. (2008). Spatial patterns in vegetation fires in the Indian region. *Environmental Monitoring and Assessment, 147(1)*, 1-13.

Verma, D.D. (2002). Thematic report on mountain ecosystems. Retrieved May 1, 2011, from the United Nations Environment Programme via Convention on Biological Diversity: http://www.cbd.int/doc/world/in/in-nr-me-en.pdf.

Wilson, D.E., & Reeder, D.M. (Eds.). (2005). Mammal species of the world. A taxonomic and geographic reference (3rd ed.). Baltimore, MD: Johns Hopkins University Press.

Wolfe, R.E., Roy, D.P., & Vermote E. (1998). MODIS land data storage, gridding, and compositing methodology: Level 2 grid. *IEEE Transactions on Geoscience and Remote Sensing, 36(4)*, 1324-1338.

Woodcock, C.E., & Gopal, S. (2000). Fuzzy set theory and thematic maps: Accuracy assessment and area estimation. *International Journal of Geographical Information Science, 14(2)*, 153-172.

Xiong, J., Toller, G., Chiang, V., Sun, J., Esposito, J., & Barnes, W. (2005). *MODIS level 1B algorithm theoretical basis document* (NASA Publication No. ATBD-MOD-01). Greenbelt, MD: NASA Goddard Space Flight Center.

Appendix A: Western Hindu Kush-Himalayas Supplementary Maps

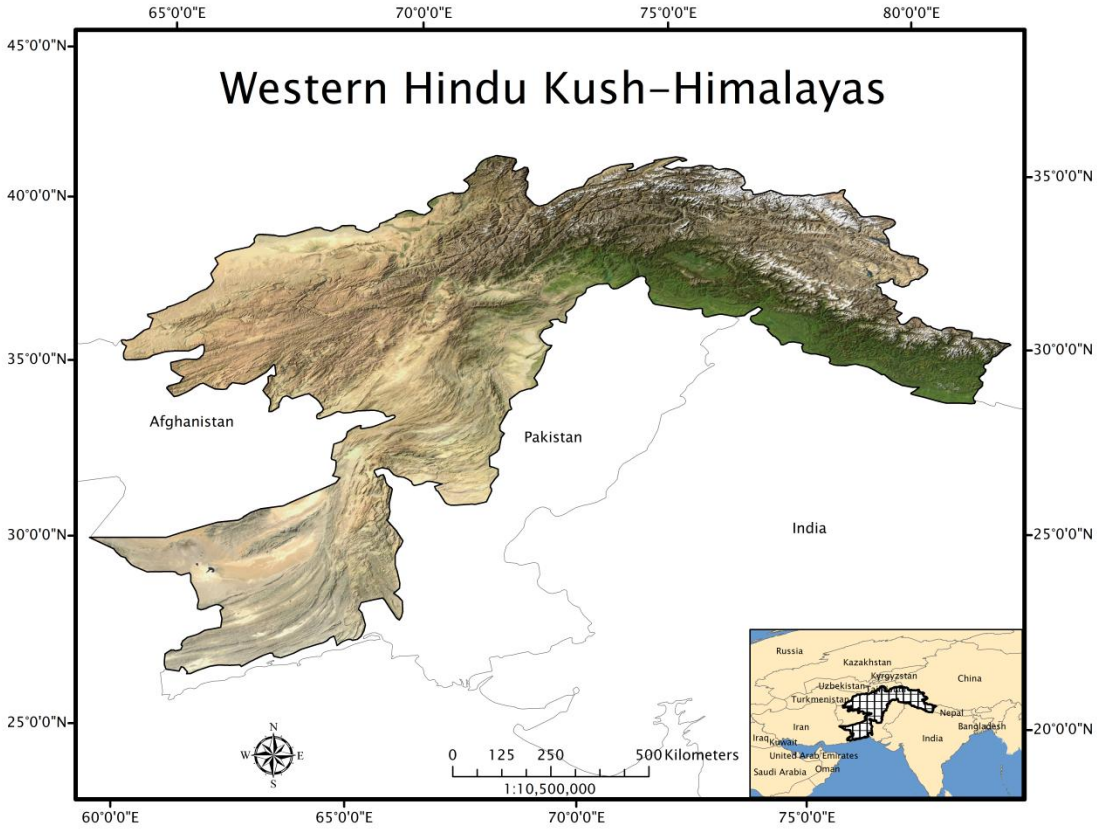

Figure A1: Regional MODIS visible.

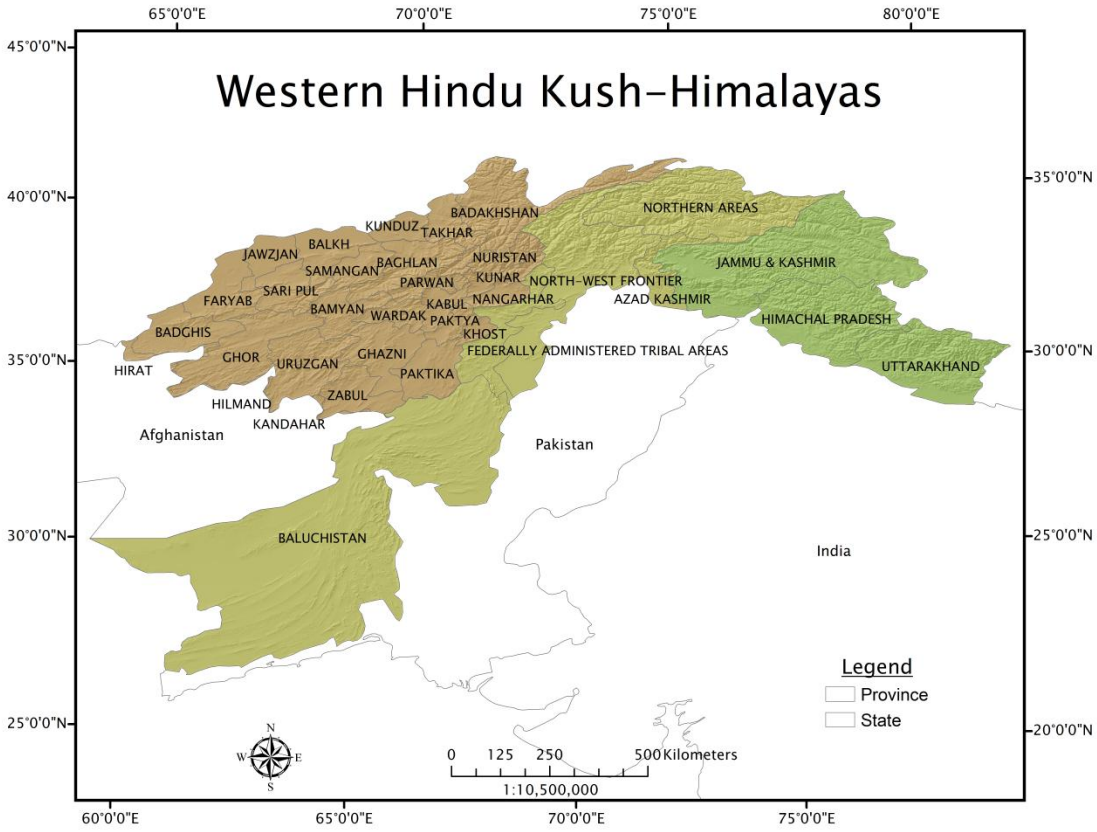

Figure A2: Regional States and Provinces.

Appendix B: Western Hindu Kush-Himalayas Wildfire Potential Area by State and Province

Country	State/Province	Wildfire Potential	Minimum Area (m)	Maximum Area (km)	Total Area (km)	% Total Area (km)	Total Area Standard Deviation (km)
Afghanistan	Badghis	No Potential	2,419.204	4.000	33.033	0.161	0.710
		Very Low	3,404.280	80.470	594.947	2.894	6.830
		Low	3,304.275	2,263.751	2,698.682	13.126	228.774
		Moderate	107,338.070	1,743.838	3,105.621	15.105	159.318
		High	564,929.391	13,355.379	13,498.761	65.657	1,619.322
		Very High	4,033.709	248.263	628.530	3.057	21.943
		Total =	685,428.929	17,695.702	20,559.574	100.000	2,036.896
	Hirat	No Potential	662,823.346	0.663	0.663	0.021	0.000
		Very Low	5,730.869	2.000	21.305	0.684	0.514
		Low	17,415.662	721.474	889.003	28.557	118.224
		Moderate	221,739.428	619.227	928.362	29.822	116.347
		High	345,786.791	1,238.105	1,264.450	40.618	466.359
		Very High	267,804.034	2.000	9.268	0.298	0.683
		Total =	1,521,300.130	2,583.469	3,113.050	100.000	702.127
	Bamyan	No Potential	26,587.327	89.903	1,107.708	7.815	9.441
		Very Low	979.120	1,644.025	4,634.093	32.695	61.796
		Low	124,717.017	7,403.421	8,402.002	59.280	502.489
		Moderate	2,239.789	9.000	29.725	0.210	2.169
		High	0.000	0.000	0.000	0.000	0.000
		Very High	0.000	0.000	0.000	0.000	0.000
		Total =	154,523.254	9,146.349	14,173.528	100.000	575.894
	Balkh	No Potential	135,971.278	6,310.677	7,102.255	41.354	468.840
		Very Low	755.529	17.000	1,787.923	10.410	1.643
		Low	25,807.119	296.284	1,259.337	7.333	11.776
		Moderate	710.195	929.553	2,652.940	15.447	41.901
		High	9,227.050	1,542.038	3,739.902	21.776	103.458
		Very High	142,688.209	420.000	632.037	3.680	44.449
		Total =	315,159.380	9,515.551	17,174.395	100.000	672.066

Country	State/Province	Wildfire Potential	Minimum Area (m)	Maximum Area (km)	Total Area (km)	% Total Area (km)	Total Area Standard Deviation (km)
	Faryab	No Potential	894,397.408	598.355	1,089.405	5.332	92.435
		Very Low	32,522.951	20.000	690.062	3.378	1.591
		Low	18,854.944	981.767	3,032.319	14.842	81.896
		Moderate	12,990.773	3,662.658	6,479.598	31.715	241.663
		High	376,994.392	8,373.676	8,967.875	43.894	845.981
		Very High	1,000,000.000	12.000	171.465	0.839	2.596
		Total =	2,335,760.469	13,648.455	20,430.725	100.000	1,266.161
	Ghor	No Potential	28,696.423	230.317	2,182.789	6.096	15.635
		Very Low	967.968	83.000	6,211.593	17.347	5.614
		Low	10.019	20,024.357	23,364.065	65.248	735.534
		Moderate	18,698.439	1,701.134	3,979.564	11.114	94.291
		High	1,000,000.000	38.000	68.822	0.192	10.252
		Very High	1,000,000.000	1.000	1.000	0.003	0.000
		Total =	2,048,372.849	22,077.807	35,807.833	100.000	861.326
	Jawzjan	No Potential	272.116	4,159.742	4,699.709	39.773	467.700
		Very Low	1,110.641	14.000	1,062.950	8.996	1.669
		Low	4,534.455	89.672	518.006	4.384	5.611
		Moderate	4,998.281	1,090.468	1,755.124	14.853	58.143
		High	8,047.947	2,510.835	3,673.949	31.092	241.496
		Very High	1,000,000.000	21.737	106.595	0.902	3.721
		Total =	1,018,963.439	7,886.454	11,816.333	100.000	778.341
	Farah	No Potential	100,227.693	5.683	18.732	6.849	2.077
		Very Low	15,481.724	7.998	54.559	19.948	1.730
		Low	19,509.256	16.546	70.836	25.899	3.336
		Moderate	465,359.157	55.951	129.381	47.304	18.837
		High	0.000	0.000	0.000	0.000	0.000
		Very High	0.000	0.000	0.000	0.000	0.000
		Total =	600,577.831	86.178	273.508	100.000	25.980

Country	State/Province	Wildfire Potential	Minimum Area (m)	Maximum Area (km)	Total Area (km)	% Total Area (km)	Total Area Standard Deviation (km)
	Hilmand	No Potential	2.733	1.585	2.774	0.703	0.715
		Very Low	4,882.938	3.800	36.861	9.349	1.013
		Low	5,923.427	240.648	328.372	83.281	77.055
		Moderate	617,408.565	5.084	17.404	4.414	1.574
		High	8,885,631.793	8.886	8.886	2.254	0.000
		Very High	0.000	0.000	0.000	0.000	0.000
		Total =	9,513,849.456	260.002	394.296	100.000	80.357
	Uruzgan	No Potential	59,851.095	82.000	612.639	2.142	6.088
		Very Low	4,842.381	53.000	3,293.969	11.517	4.008
		Low	1,254.857	9,767.709	11,919.837	41.678	470.745
		Moderate	64,177.751	7,753.998	9,292.888	32.493	485.566
		High	798,103.400	2,034.939	3,299.448	11.537	158.704
		Very High	1,000,000.000	37.000	181.000	0.633	6.078
		Total =	1,928,229.484	19,728.646	28,599.781	100.000	1,131.188
	Kandahar	No Potential	119,306.867	171.253	232.753	24.693	40.196
		Very Low	887.416	16.000	97.142	10.306	2.417
		Low	9,069.777	78.556	148.750	15.781	11.481
		Moderate	28,236.026	363.985	443.790	47.082	72.333
		High	68,302.775	8.996	20.160	2.139	2.671
		Very High	0.000	0.000	0.000	0.000	0.000
		Total =	225,802.862	638.790	942.595	100.000	129.098
	Zabul	No Potential	5,321.289	4,726.387	5,573.971	33.003	318.584
		Very Low	0.004	227.000	3,489.121	20.659	10.926
		Low	145.495	968.131	3,240.940	19.189	37.426
		Moderate	22,407.981	2,734.081	4,238.688	25.097	187.190
		High	1,000,000.000	87.000	345.625	2.046	13.812
		Very High	1,000,000.000	1.000	1.000	0.006	0.000
		Total =	2,027,874.769	8,743.599	16,889.345	100.000	567.938

Country	State/Province	Wildfire Potential	Minimum Area (m)	Maximum Area (km)	Total Area (km)	% Total Area (km)	Total Area Standard Deviation (km)
	Ghazni	No Potential	6,311.638	7,753.987	9,246.644	40.370	378.738
		Very Low	342.029	125.633	5,971.047	26.069	8.346
		Low	227.640	5,254.384	7,383.341	32.235	200.981
		Moderate	80,041.028	18.863	284.478	1.242	2.742
		High	1,000,000.000	5.000	19.000	0.083	1.272
		Very High	0.000	0.000	0.000	0.000	0.000
		Total =	1,086,922.336	13,157.868	22,904.510	100.000	592.080
	Paktya	No Potential	46,910.513	30.000	191.571	3.001	5.418
		Very Low	31.497	29.319	509.354	7.978	3.547
		Low	2,606.867	1,553.630	3,141.774	49.209	205.584
		Moderate	22,201.071	1,486.845	2,054.983	32.187	163.383
		High	999,676.142	259.827	454.917	7.125	37.553
		Very High	933,628.943	9.000	31.916	0.500	2.060
		Total =	2,005,055.034	3,368.621	6,384.515	100.000	417.546
	Paktika	No Potential	3,419.429	4,126.773	5,099.523	26.862	275.161
		Very Low	31.941	293.845	3,391.828	17.867	13.100
		Low	964.959	1,745.000	4,838.207	25.486	92.314
		Moderate	685,016.061	5,195.374	5,424.059	28.572	607.757
		High	1,703.463	50.496	229.419	1.208	13.798
		Very High	1,000,000.000	1.000	1.000	0.005	0.000
		Total =	1,691,135.853	11,412.489	18,984.035	100.000	1,002.129
	Baghlan	No Potential	65,897.447	427.015	1,601.586	7.583	43.997
		Very Low	2,009.714	96.170	2,357.168	11.161	6.358
		Low	57,434.159	4,040.451	6,934.755	32.835	214.848
		Moderate	5,473.037	4,465.040	5,325.210	25.214	291.884
		High	1,000,000.000	3,873.578	4,338.578	20.542	331.915
		Very High	1,000,000.000	286.000	562.946	2.665	47.330
		Total =	2,130,814.357	13,188.253	21,120.243	100.000	936.332

Country	State/Province	Wildfire Potential	Minimum Area (m)	Maximum Area (km)	Total Area (km)	% Total Area (km)	Total Area Standard Deviation (km)
	Kabul	No Potential	241,087.217	52.281	299.465	6.713	9.474
		Very Low	4,509.760	62.947	647.442	14.514	6.292
		Low	51,921.385	553.118	1,236.858	27.727	45.596
		Moderate	13,929.586	556.858	1,628.933	36.516	82.267
		High	2,488.042	312.717	605.539	13.575	54.928
		Very High	1,000,000.000	9.993	42.610	0.955	3.095
		Total =	1,313,935.990	1,547.914	4,460.848	100.000	201.653
	Kapisa	No Potential	596,771.510	3.518	15.547	0.844	1.011
		Very Low	32,465.545	19.196	120.214	6.526	3.236
		Low	278,072.470	309.671	405.898	22.036	62.970
		Moderate	617,968.753	268.265	641.586	34.831	65.839
		High	1,000,000.000	183.242	496.099	26.933	42.988
		Very High	1,000,000.000	110.661	162.661	8.831	33.685
		Total =	3,525,278.278	894.553	1,842.005	100.000	209.729
	Khost	No Potential	0.000	0.000	0.000	0.000	0.000
		Very Low	1,000,000.000	1.000	2.000	0.050	0.000
		Low	1,000,000.000	12.594	21.594	0.535	4.470
		Moderate	66,935.682	1,882.216	2,002.823	49.606	400.240
		High	323.858	1,076.353	1,794.070	44.436	141.420
		Very High	865,373.085	84.000	216.949	5.373	19.400
		Total =	2,932,632.624	3,056.163	4,037.436	100.000	565.531
	Laghman	No Potential	1,442.117	83.735	133.151	3.466	22.461
		Very Low	92,501.886	29.000	181.065	4.713	3.928
		Low	1,000,000.000	173.442	308.619	8.033	29.927
		Moderate	653,684.542	125.154	746.452	19.428	22.075
		High	27,198.679	2,147.389	2,208.598	57.484	343.602
		Very High	383,244.751	113.000	264.229	6.877	15.328
		Total =	2,158,071.975	2,671.720	3,842.113	100.000	437.322

Country	State/Province	Wildfire Potential	Minimum Area (m)	Maximum Area (km)	Total Area (km)	% Total Area (km)	Total Area Standard Deviation (km)
	Logar	No Potential	1,464.527	155.510	624.227	16.094	20.824
		Very Low	81,570.738	20.038	946.451	24.401	3.129
		Low	629.563	814.692	1,457.449	37.576	61.890
		Moderate	45,353.254	213.000	649.799	16.753	26.681
		High	759,263.851	43.000	158.786	4.094	11.151
		Very High	1,000,000.000	13.000	42.000	1.083	3.234
		Total =	1,888,281.933	1,259.240	3,878.711	100.000	126.909
	Parwan	No Potential	1.142	1,149.035	2,008.836	20.960	88.416
		Very Low	9,373.532	65.000	2,154.454	22.479	5.644
		Low	58,565.016	2,699.138	4,148.894	43.289	178.154
		Moderate	156,050.728	374.721	908.316	9.477	40.559
		High	997,511.958	79.140	151.280	1.578	13.569
		Very High	1,000,000.000	201.339	212.345	2.216	81.306
		Total =	2,221,502.376	4,568.373	9,584.127	100.000	407.648
	Samangan	No Potential	419,595.253	75.000	315.935	2.805	12.300
		Very Low	109,529.170	387.257	1,245.278	11.056	21.167
		Low	2,456.662	3,188.855	3,825.763	33.966	209.064
		Moderate	37,609.537	2,022.401	3,683.889	32.706	171.036
		High	7,556.139	1,340.203	2,154.501	19.128	187.294
		Very High	681,326.738	6.054	38.159	0.339	1.863
		Total =	1,258,073.499	7,019.771	11,263.525	100.000	602.725
	Sari Pul	No Potential	52,118.635	11.621	235.140	1.470	2.110
		Very Low	6,289.002	117.000	1,897.981	11.862	7.062
		Low	9,559.288	5,698.386	6,152.530	38.452	375.628
		Moderate	6,963.244	2,357.365	3,333.092	20.831	163.869
		High	718,571.798	3,620.735	4,211.671	26.322	430.275
		Very High	1,000,000.000	37.000	170.263	1.064	5.528
		Total =	1,793,501.967	11,842.107	16,000.676	100.000	984.472

Country	State/Province	Wildfire Potential	Minimum Area (m)	Maximum Area (km)	Total Area (km)	% Total Area (km)	Total Area Standard Deviation (km)
	Wardak	No Potential	6,544.747	188.672	1,251.925	14.010	17.990
		Very Low	34.350	69.466	2,162.056	24.194	5.278
		Low	124,715.568	3,738.584	5,277.118	59.053	251.601
		Moderate	95,734.711	37.000	226.828	2.538	4.943
		High	13,204.347	4.000	18.254	0.204	1.170
		Very High	0.000	0.000	0.000	0.000	0.000
		Total =	240,233.723	4,037.722	8,936.182	100.000	280.981
	Kunduz	No Potential	490,943.382	852.997	1,276.488	15.908	126.159
		Very Low	666.843	10.000	468.375	5.837	1.522
		Low	937.648	8.000	246.463	3.071	1.029
		Moderate	322.213	54.876	493.544	6.151	5.582
		High	28,035.937	3,167.898	3,666.933	45.697	301.996
		Very High	65,763.617	1,033.779	1,872.624	23.337	141.384
		Total =	586,669.640	5,127.550	8,024.426	100.000	577.672
	Takhar	No Potential	572,618.345	1,294.618	1,432.115	11.647	225.045
		Very Low	78,936.442	38.000	759.380	6.176	4.385
		Low	73,750.056	1,953.479	2,283.294	18.570	190.824
		Moderate	376,183.860	1,856.796	2,237.286	18.195	151.492
		High	498,580.782	4,163.781	4,436.900	36.084	438.610
		Very High	187,276.998	308.600	1,146.905	9.328	35.826
		Total =	1,787,346.483	9,615.275	12,295.879	100.000	1,046.183
	Badakhshan	No Potential	654,590.089	19,562.940	21,422.323	49.357	1,509.441
		Very Low	35,273.565	50.000	3,557.191	8.196	4.877
		Low	561,271.350	12,907.873	13,869.182	31.955	728.400
		Moderate	533,649.385	1,821.171	3,301.888	7.608	119.144
		High	510,493.513	675.608	1,200.910	2.767	76.796
		Very High	694,348.383	10.000	51.147	0.118	2.053
		Total =	2,989,626.284	35,027.592	43,402.640	100.000	2,440.712

Country	State/Province	Wildfire Potential	Minimum Area (m)	Maximum Area (km)	Total Area (km)	% Total Area (km)	Total Area Standard Deviation (km)
	Kunar	No Potential	473,964.267	5.083	14.304	0.306	2.003
		Very Low	5,639.789	7.000	37.354	0.799	1.666
		Low	104.818	124.300	256.614	5.490	34.972
		Moderate	26,733.409	219.242	857.006	18.335	34.410
		High	34,450.825	2,818.522	2,975.215	63.654	402.290
		Very High	2,710.824	38.000	533.560	11.415	6.315
		Total =	543,603.932	3,212.148	4,674.052	100.000	481.656
	Nangarhar	No Potential	685,282.835	19.430	50.590	0.677	5.274
		Very Low	71,233.871	14.000	130.151	1.742	2.468
		Low	220,394.442	651.890	711.410	9.521	96.981
		Moderate	4,770.423	2,547.816	3,383.550	45.281	308.042
		High	84,109.899	1,806.865	2,718.447	36.380	177.765
		Very High	186,271.990	158.000	478.116	6.399	20.324
		Total =	1,252,063.461	5,198.001	7,472.264	100.000	610.853
	Nuristan	No Potential	90,658.048	3,218.457	3,302.738	36.366	479.500
		Very Low	68.561	36.000	1,320.927	14.545	4.178
		Low	190,253.801	458.700	2,039.035	22.452	55.055
		Moderate	364,588.035	196.135	983.692	10.831	20.054
		High	276,709.358	942.246	1,210.523	13.329	111.480
		Very High	158,916.871	27.000	224.942	2.477	5.021
		Total =	1,081,194.675	4,878.539	9,081.857	100.000	675.289

Country	State/Province	Wildfire Potential	Minimum Area (m)	Maximum Area (km)	Total Area (km)	% Total Area (km)	Total Area Standard Deviation (km)
Pakistan	Baluchistan	No Potential	3,620.985	158,637.407	174,046.132	58.737	4,635.084
		Very Low	90,703.898	218.000	21,925.190	7.399	5.452
		Low	8,443.746	3,716.861	20,855.769	7.038	64.655
		Moderate	180,805.405	26,183.676	52,298.742	17.650	544.010
		High	572,727.130	6,455.161	27,017.990	9.118	310.367
		Very High	1,000,000.000	19.000	168.725	0.057	3.051
		Total =	1,856,301.164	195,230.105	296,312.546	100.000	5,562.619
	Federally Administered Tribal Areas	No Potential	347,768.085	82.000	145.805	0.551	18.105
		Very Low	4,260.254	9.000	210.403	0.796	1.468
		Low	1,178.093	128.913	355.400	1.344	11.035
		Moderate	51.789	7,572.937	10,244.063	38.742	465.864
		High	3,825.113	7,385.327	13,878.922	52.489	540.431
		Very High	70.464	212.391	1,607.006	6.078	16.637
		Total =	357,153.799	15,390.567	26,441.600	100.000	1,053.539
	North-West Frontier	No Potential	1,000,000.000	12,074.323	14,058.751	18.829	907.757
		Very Low	1,062.155	101.001	4,336.943	5.808	4.512
		Low	11,836.626	1,483.312	6,919.292	9.267	79.887
		Moderate	509.066	1,398.225	7,732.924	10.357	66.534
		High	781.240	8,101.283	21,095.895	28.254	266.361
		Very High	11,623.113	14,245.430	20,522.642	27.486	523.083
		Total =	1,025,812.200	37,403.573	74,666.447	100.000	1,848.134
	Azad Kashmir	No Potential	7,617.411	591.660	1,090.427	8.983	98.975
		Very Low	8,175.386	21.000	655.843	5.403	2.754
		Low	79,747.276	632.000	1,671.580	13.771	81.523
		Moderate	551.725	66.281	908.147	7.481	9.013
		High	1,618.794	167.000	1,441.061	11.871	11.502
		Very High	1,904.103	6,077.199	6,371.779	52.491	601.469
		Total =	99,614.695	7,555.140	12,138.837	100.000	805.236

Country	State/Province	Wildfire Potential	Minimum Area (m)	Maximum Area (km)	Total Area (km)	% Total Area (km)	Total Area Standard Deviation (km)
	Northern Areas	No Potential	627,349.505	47,417.401	49,251.121	71.384	3,440.458
		Very Low	4,383.345	56.000	7,202.235	10.439	4.216
		Low	9,304.744	1,226.834	7,796.597	11.300	50.417
		Moderate	30,846.065	1,802.549	3,689.410	5.347	82.354
		High	1,000,000.000	153.739	908.739	1.317	15.714
		Very High	1,000,000.000	17.000	146.232	0.212	2.673
		Total =	2,671,883.659	50,673.524	68,994.336	100.000	3,595.832

Country	State/Province	Wildfire Potential	Minimum Area (m)	Maximum Area (km)	Total Area (km)	% Total Area (km)	Total Area Standard Deviation (km)
India	Himachal Pradesh	No Potential	332,941.667	15,857.442	20,268.067	36.591	2,036.116
		Very Low	627.927	27.000	2,268.639	4.096	2.731
		Low	31,001.633	81.337	2,329.995	4.206	8.000
		Moderate	801.774	92.000	2,202.447	3.976	6.266
		High	13.288	234.000	5,366.956	9.689	12.401
		Very High	24,179.351	21,888.327	22,954.752	41.441	1,199.316
		Total =	389,565.640	38,180.106	55,390.855	100.000	3,264.829
	Jammu & Kashmir	No Potential	74,611.616	65,720.300	66,583.783	62.755	6,382.561
		Very Low	22,340.928	32.000	2,962.358	2.792	3.040
		Low	133.708	1,287.924	5,675.558	5.349	80.934
		Moderate	3,900.225	194.000	3,772.742	3.556	12.067
		High	1,132.061	945.000	8,426.593	7.942	38.736
		Very High	275,540.887	12,267.134	18,679.811	17.606	531.406
		Total =	377,659.427	80,446.359	106,100.844	100.000	7,048.745
	Uttarakhand	No Potential	29,943.506	9,979.912	10,133.779	19.968	1,618.298
		Very Low	26,750.555	13.000	1,244.719	2.453	1.984
		Low	363,421.940	17.000	790.412	1.557	1.558
		Moderate	321,732.909	92.000	1,871.855	3.688	10.679
		High	270.800	56.000	4,094.221	8.067	5.782
		Very High	7,661.004	31,954.716	32,615.527	64.266	2,294.002
		Total =	749,780.714	42,112.628	50,750.512	100.000	3,932.304